AD-A130 419 CONTRIBUTIONS TO THE THEORY OF THE PROPERTIES OF HYDROGENATED AMORPHOUS SILICON(U) NAVAL RESEARCH LAB WASHINGTON DC D A PAPACONSTANTOPOULOS ET AL. 21 JUL 83 1/1

UNCLASSIFIED NRL-MR-5129 F/G 20/12 NL

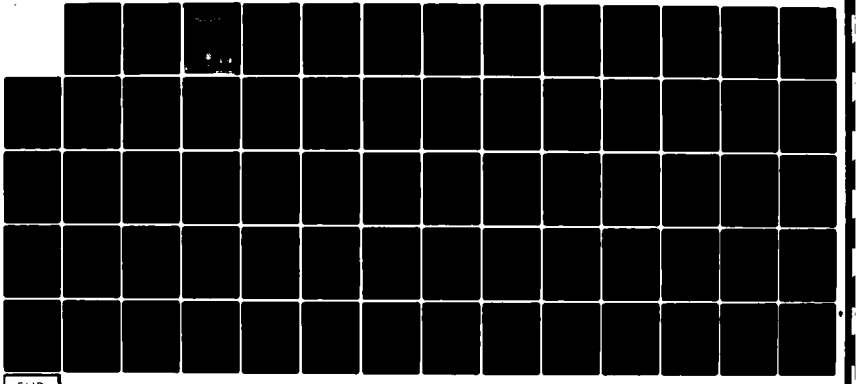

END
DATE FILMED
8-83
DTIC

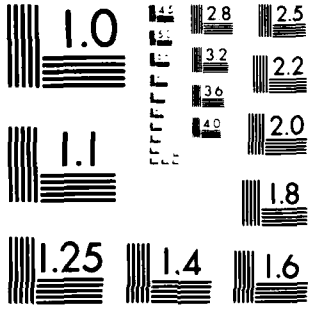

NRL Memorandum Report 5129

Contributions to the Theory of the Properties of Hydrogenated Amorphous Silicon

D. A. PAPACONSTANTOPOULOS

Metal Physics Branch
Condensed Matter and Radiation Sciences Division

W. E. PICKETT

Condensed Matter Physics Branch
Condensed Matter and Radiation Sciences Division

July 21, 1983

NAVAL RESEARCH LABORATORY
Washington, D.C.

[redacted]

[redacted]

[redacted]

[redacted]

[redacted]

[redacted]

[redacted]

July 21, 1983

SECURITY CLASSIFICATION OF THIS PAGE (When Data Entered)

REPORT DOCUMENTATION PAGE		READ INSTRUCTIONS BEFORE COMPLETING FORM
1. REPORT NUMBER NRL Memorandum Report 5129	2. GOVT ACCESSION NO. AD-A130419	3. RECIPIENT'S CATALOG NUMBER
4. TITLE (and Subtitle) CONTRIBUTIONS TO THE THEORY OF THE PROPERTIES OF HYDROGENATED AMORPHOUS SILICON		5. TYPE OF REPORT & PERIOD COVERED Final report 6. PERFORMING ORG. REPORT NUMBER
7. AUTHOR(s) D.A. Papaconstantopoulos and W.E. Pickett		8. CONTRACT OR GRANT NUMBER(s)
9. PERFORMING ORGANIZATION NAME AND ADDRESS Naval Research Laboratory Washington, DC 20375		10. PROGRAM ELEMENT, PROJECT, TASK AREA & WORK UNIT NUMBERS 61153N; RR0210201; 66-0428-0-0
11. CONTROLLING OFFICE NAME AND ADDRESS Office of Naval Research Arlington, VA 22217		12. REPORT DATE July 21, 1983 13. NUMBER OF PAGES 66
14. MONITORING AGENCY NAME & ADDRESS(if different from Controlling Office)		15. SECURITY CLASS. (of this report) UNCLASSIFIED 15a. DECLASSIFICATION/DOWNGRADING SCHEDULE

16. DISTRIBUTION STATEMENT (of this Report)

Approved for public release; distribution unlimited.

17. DISTRIBUTION STATEMENT (of the abstract entered in Block 20, if different from Report)

18. SUPPLEMENTARY NOTES

19. KEY WORDS (Continue on reverse side if necessary and identify by block number)

Amorphous silicon
Electronic structure
Transport properties
Coherent potential approximation
Optical absorption

20. ABSTRACT (Continue on reverse side if necessary and identify by block number)

This report presents a theoretical study of the electronic properties of hydrogenated amorphous silicon, a material which is now used in the manufacturing of solar cells as an alternative to crystalline silicon.

DD FORM 1 JAN 73 1473 EDITION OF 1 NOV 65 IS OBSOLETE
S/N 0102-014-6601

SECURITY CLASSIFICATION OF THIS PAGE (When Data Entered)

TABLE OF CONTENTS

REPRINTS

Contributions to the Theory of the Properties of Hydrogenated Amorphous Silicon

BACKGROUND

Knowledge of the electronic structure of crystalline and amorphous semiconductors has been of great assistance in the development of electronic devices. Such knowledge is derived from first principles calculations, the results of which can be tested against experiments and subsequently used in interpreting measurements or in guiding technological applications.

The problem of improving the efficiency of solar cells by using samples of hydrogenated amorphous silicon (a-Si:H) has received a lot of attention recently. Considerable progress has been made in this area by performing both experimental and theoretical studies of the role of hydrogen in amorphous silicon. Very recently a breakthrough was reported[1] in the manufacturing of thin films of a-Si:H which produced solar cells with an efficiency greater than 10%. This achievement suggests that the a-Si solar cell technology now presents a realistic alternative to the crystalline silicon technology.

In 1975 Spear and LeComber[2] succeeded in substitutionally doping amorphous Si (a-Si), produced by decomposition of silane, through the incorporation of phosphorous and boron impurities. This work became the starting point of the current intensive investigation of the electronic properties of a-Si. Paul et al.,[3] who also presented similar doping results in a-Si produced by sputtering in an Ar+H plasma, suggested that the origin of the doping effects as well as other good electronic properties of this material[4,5] is the passivation of dangling bonds by hydrogen. It has been shown recently[6] that the density of states (DOS) in the middle of the gap can be reduced through hydrogenation to values as low as 5×10^{14} cm^{-3} eV. However, the amount of hydrogen in these Si-H "alloys" was found to be as much as 100 times larger than the maximum number of dangling bonds. Therefore, hydrogen, in addition to saturating the dangling bonds, also resides elsewhere and perhaps introduces other changes in the electronic structure of a-Si. Hydrogenation not only eliminates the dangling bond states from the energy gap but also widens the gap as demonstrated by several workers[7-9] using different experimental techniques.

Manuscript approved April 29, 1983.

Away from the gap, photoemission measurements[10] revealed hydrogen associated states well within the valence band. In the conduction band, photoconductivity data[11] suggest the formation of Si-H antibonding states.

There have been several theoretical models and calculations in order to gain an understanding of these experiments. We mention the work of Allan and Joannopoulos[12] and coworkers who have studied Si-H molecules using the Bethe-lattice technique; the calculations of Ching et al.[13] using an orthogonalized linear-combination of atomic orbitals method based on a continuous-random-network, and the model defect method of Divincenzo et al.[14]

1. A.W. Catalano et al., IEEE Photovoltaic Specialists Conference, San Diego, Sept. 1982; and to be published.
2. W.E. Spear and P.G. LeComber, Solid State Colmun. 17, 1193 (1975).
3. W. Paul, A.J. Lewis, G.A.N. Connell, and T.D. Moustakas, Solid State Commun. 20, 969 (1976).
4. T.D. Moustakas, J. Electron. Mater. 8, 391 (1979).
5. H. Fritzsche, Sol. Energy Mater. 3, 447 (1980).
6. T. Tiedje, T.D. Moustakas, and J.M. Cebulka, Phys. Rev. B23, 5634 (1981).
7. E.C. Freeman and W. Paul, Phys. Rev. B20, 716 (1979).
8. G.D. Cody, C.R. Wronski, B. Abeles, R.B. Stephens, and B. Brooks, Sol. Cells 2, 227 (1980).
9. N.B. Goodman, H. Fritzsche, and H. Ozaki, J. Non-Cryst. Solids 35-36, 599 (1980).
10. B. von Roedern, L. Ley, and M. Cardona, Phys. Rev. Lett. 39, 1576 (1977).
11. T.D. Moustakas, D.A. Anderson, and W. Paul, Solid State Commun. 23, 155 (1977).
12. D.C. Allan and J.D. Joannopoulos, Phys. Rev. Lett. 44, 43 (1980).
13. W.Y. Ching, D.J. Lam, and C.C. Lin, Phys. Rev. Lett. 42, 805 (1980).
14. D.P. DiVincenzo, J. Bernholc, M.H. Brodsky, N.O. Lipari, and S.T. Pantelides, "Tetrahedrally Bonded Amorphous Semiconductors" eds. R.A. Street, D.K. Biegelsen and J.C. Knights (Am. Inst. Phys., New York 1981) p. 156.

MODEL OF THE DISORDER (P1-P4)

Our model[1] describes hydrogenated a-Si by constructing an effective lattice whose sites may have probability c of being vacant, and probability 1-c of having a Si atom. In addition, we have assumed that hydrogen atoms may be located along the lines connecting a vacant site with its nearest-neighbors. Thus, we have included in our model, at random, Si sites, vacancy sites, and sites surrounded by one, two, three, or four hydrogen atoms which saturate the Si dangling bonds. Using this

model of disorder, we have used the coherent-potential approximation (CPA) to perform calculations of the electronic density of states (DOS). The results (references 1-4 reprinted herein) may be summarized as follows:

a) We have demonstrated the existence of dangling bond states in the gap.
b) We have shown the restoration of the band gap upon hydrogenation.
c) We have shown that for a 20% hydrogen concentration the gap is wider by 0.4 eV due to a recession of the valence band.
d) We have identified H induced peaks in the DOS of the valence band.
e) We have concluded that Si-H antibonding states at the bottom of the conduction band have wavefunctions with very strong hydrogen component.

LOCAL Si-H BONDING (P5, P6)

We have carried out detailed self-consistent pseudopotential electronic structure calculations on the hydrogen saturated Si vacancy, (HSV) (i.e., a hydrogen atom attached to each of the four Si dangling bonds) to learn more about H-Si bonding in a bulk environment. The geometrical model consisted of a crystalline array of HSV "supercells". The local DOS confirmed the CPA results that valence band states within 0.6 eV of the gap are strongly depleted by hydrogenation and that conduction states just above the gap are strongly influenced by hydrogen. We have also studied relaxation (symmetric only) of the HSV by calculating forces (by the Hellman-Feynman theorem) and total energies. It was found that the DOS features discussed above are sensitive to H-Si bond length and possibly to H-H interactions. These studies suggest that the stable HSV assumes a low symmetry buckled form which is similar to the ideal (unrelaxed) HSV in local H-Si bonding features.

D.C. CONDUCTIVITY AND OPTICAL ABSORPTION (P7, P8)

In addition to our work summarized above, we have performed calculations of the transport properties of a-Si:H. We have evaluated the d.c. conductivity by the Kubo-Greenwood formulation using the Green's functions generated by our coherent potential approximation (CPA) calculations. Our results show that the mobility of electrons is greater than that of holes, apparently due to the strong hydrogen component of the density of states just above the gap.

Finally, we have been able to calculate the a.c. conductivity and thereby obtain the optical absorption coefficient. This is the first application of the CPA in the evaluation of the absorption and transport properties of a-Si:H using a realistic multi-band model. A comparison of our calculated optical absorption to the convoluted DOS shows that the optical gap is

larger than the DOS gap. This difference in calculated gaps is due to remanent wavevector conservation arising from short range order in a-Si:H.

Overall, the comparison of theoretical calculations with experimental data leads to the following important conclusion: for many properties of a-Si:H which do not intimately involve band tail states or gap states, knowledge of the precise atomic positions are not necessary for their calculation and comprehension.

ACKNOWLEDGEMENTS

This research was supported at various points by the U.S. Department of Energy (Contract #DE-AT-01-79ET-23078), by the Office of Naval Research (Contract #N0014-79-WR-90028) and by the Solar Energy Research Institute via an interagency agreement between the Naval Research Laboratory and the U.S. Department of Energy.

P1

PHYSICAL REVIEW B VOLUME 22, NUMBER 6 15 SEPTEMBER 1980

Slater-Koster parametrization for Si and the ideal-vacancy calculation

D. A. Papaconstantopoulos
Naval Research Laboratory, Washington, D.C. 20375

E. N. Economou
Department of Physics, McCormic Road, University of Virginia, Charlottesville, Virginia 22901

(Received 20 February 1980)

A Slater-Koster Hamiltonian for Si is constructed using four (one s and three p) orthogonal orbitals per site. This Hamiltonian reproduces reasonably accurately the empirical pseudopotential band structure not only for the valence but for the conduction band as well. It also determines correctly the position of the bound level of an unreconstructed vacancy demonstrating thus that the effects of electronic self-consistency are minor.

I. INTRODUCTION

Koster and Slater[1] proposed in 1954 a Green's-function method for the calculation of the changes in the electronic structure of perfect crystals caused by the presence of localized defects. The first numerical implementation of this method was made by Callaway and Hughes[2] on silicon. However, the first-principles numerical evaluation of the matrix elements in a Wannier representation made this approach too complicated.

Recently, due to the work of Bernholc *et al.*[3,4] and that of Baraff and Schlüter,[5,6] significant progress has been made in performing realistic defect calculations. These authors have presented similar formalisms and actual calculations which seem to indicate a level of accuracy approaching that of band-structure calculations for perfect crystals.

The purpose of the present work is to show that for Si an accurate orthogonal basis Slater-Koster[7] parametrization can be obtained, which when used in the Koster-Slater[1] impurity method gives results in close agreement to the self-consistent calculations of Refs. 4, 5, and 6. The orthogonality of the basis is a clear numerical advantage especially in attempts to treat disordered Si by an effective Slater-Koster (SK) Hamiltonian. On the other hand we recognize that the orthogonality assumption, which implies no atomiclike basis, makes it difficult to estimate modifications in the matrix elements resulting from structural changes.

Our SK Hamiltonian produces a very good fit to the pseudopotential band structure of silicon,[8] and reproduces fairly accurately not only the band gap but the conduction band as well, unlike all the previous attempts.

In Sec. II we describe our Slater-Koster interpolation scheme and in Sec. III we apply it to the ideal Si vacancy problem.

II. SLATER-KOSTER INTERPOLATION

Since Slater and Koster[7] proposed the use of the tight-binding method as an interpolation scheme there have been many attempts to apply this idea to the band structure of silicon.[9-15] Most of these calculations give a good description of the valence band but the band gap is too wide and the conduction band too narrow. For example, the calculation of Chadi and Cohen[12] and also that of Chadi[12] gives a gap of 3 eV and no reasonable representation of the conduction band. However, Chadi[16] has succeeded in obtaining the correct gap and conduction band by a different approach in which he used as adjustable parameters the exponential decay constants of Slater orbitals together with an empirical pseudopotential Hamiltonian. We consider this method as not falling into the same category as SK fits and, therefore, we will not compare with it except to say that our results are in close agreement.

The SK fit which has been repeatedly quoted in the literature as giving a realistic tight-binding Hamiltonian is that of Pandey and Phillips.[14] This calculation overestimates the gap to 1.4 eV and gives a very narrow conduction band. As stated by the authors, their calculations are not reliable for the conduction band. We will give a detailed comparison with Pandey and Phillips (PP) after we have given details about our own calculation.

Our SK fit uses an orthogonal basis set of s and p functions, thus our nonsymmetrized Hamiltonian is an 8×8. We have used, as adjustable parameters, 20 three-center interaction integrals which include first, second, and third neighbors. These parameters were determined by nonlinear least-squares fit to the local pseudopotential results of Pickett.[8] This step was done after reducing the 8×8 secular equation by symmetry following the original paper of Slater and Koster[7] and also that of Dresselhaus and Dresselhaus.[9] This block

TABLE I. Comparison of Slater-Koster parameters for Si expressed in eV.

	Present work	Pandey and Phillips[a]
$E_{s,s}(000)$	−3.953	−4.19
$E_{s,s}(110)$	0.001	0.0
$E_{s,x}(011)$	−0.196	0.0
$E_{s,x}(110)$	0.033	0.0
$E_{s,s}\left(\frac{111}{222}\right)$	−1.916	−2.08
$E_{s,x}\left(\frac{111}{222}\right)$	1.509	1.224
$E_{x,x}(000)$	1.512	0.20
$E_{x,x}(110)$	0.316	0.24
$E_{x,x}(011)$	−0.583	−0.10
$E_{x,y}(110)$	0.084	0.34
$E_{x,y}(011)$	−0.034	0.0
$E_{x,x}\left(\frac{111}{222}\right)$	0.276	0.43
$E_{x,y}\left(\frac{111}{222}\right)$	1.407	0.947
$E_{s,s}\left(\frac{311}{222}\right)$	−0.113	0.0
$E_{s,x}\left(\frac{311}{222}\right)$	−0.081	0.0
$E_{s,x}\left(\frac{113}{222}\right)$	0.101	0.0
$E_{x,x}\left(\frac{311}{222}\right)$	0.027	0.0
$E_{x,x}\left(\frac{113}{222}\right)$	0.062	0.0
$E_{x,y}\left(\frac{311}{222}\right)$	0.116	0.0
$E_{x,y}\left(\frac{113}{222}\right)$	−0.077	0.0

[a] Reference 14.

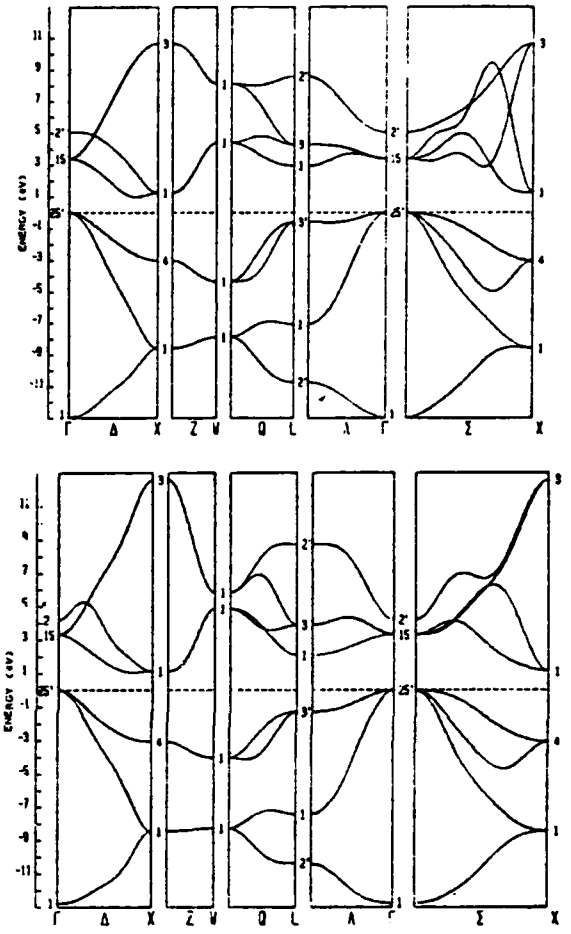

FIG. 1. (a) Energy bands for Si resulting from our Slater-Koster Hamiltonian. (b) Energy bands for Si from the pseudopotential calculation of Pickett.

diagonalization of the 8 × 8 matrix is essential for obtaining a reliable fit. We have fit in this way all eight bands of Pickett's calculation[8] for a grid of 20 k points in the irreducible Brillouin zone. The rms fitting error was less than 0.25 eV for the valence bands which is slightly better than the 0.30-eV value quoted by PP. For the conduction band our fitting errors were 0.36 eV (5th band), 0.50 eV (6th band), and 0.90 eV (7th and 8th bands). Pandey and Phillips[14] do not give rms errors for the conduction band; our own estimates using their parameters and the pseudopotential results of Pickett[8] are 0.7 eV (5th band), 1.5 eV (6th band), and 3.5 eV (7th and 8th bands). It is clear therefore that our own SK fit is of superior accuracy. We attribute this improvement to our inclusion, in contrast to PP, of the third-neighbor interactions. In Table I we list our SK parameters following the notation of the SK paper[7] and compare them with those of PP. The PP parameters have been converted from the two-center to the three-center notation in a straightforward manner.[7] Figure 1(a) shows our SK energy bands, and Fig. 1(b), for comparison, the bands from the empirical pseudopotential of Pickett.[8] One can see that we have even reproduced the plane-wave character of the conduction bands in contrast to the narrow conduction states given by Pandey and Phillips.[14] Our band gap from the SK bands is 1 eV wide, which is almost exactly the value from the pseudopotential results.[8]

In order to calculate the densities of states (DOS) we have generated from the SK Hamiltonian eigenvalues and eigenvectors for 89 k points. These results were then used in the tetrahedron method.[17] The resulting DOS are shown in Fig. 2 where one can note that the well-accepted three-peak structure of the valence bands is reproduced as well as a fairly accurate value for the gap and very reasonable shape for the conduction bands. Also, the angular momentum decomposition gives the

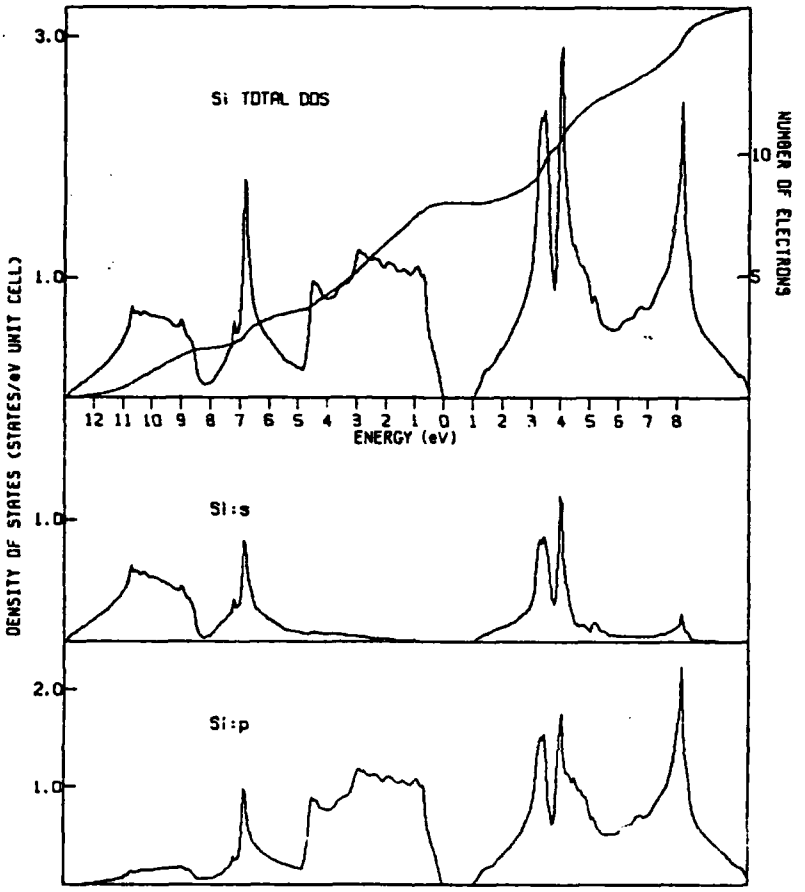

FIG. 2. Total and angular momentum-decomposed densities of states for Si derived from our Slater-Koster Hamiltonian.

expected strong s character at the bottom of the valence band and strong p character at the top of the valence band and the conduction band. In Fig. 3 we present, calculated in the same way, the DOS from the Pandey and Phillips[14] parameters. The similarity in tne valence band and the clear disagreement in the conduction band is evident.

III. IDEAL VACANCY IN SILICON

Bernholc and Pantelides[3] have given a clear summary of the Koster-Slater[1] theory, and performed calculations of the ideal vacancy in Si based on the SK parameters of PP.[14] We have done calculations along the same lines using the PP parameters, for the purpose of checking our computer codes, and also using our own SK parameters. We have reproduced the results of Bernholc and Pantelides[3] using the PP parameters. In particular, using the PP parameters we find a bound state of T_2 (p-like) symmetry at 0.27 eV above the top of the valence band.

However, using our own SK parameters we find the bound state of T_2 symmetry to be at 0.75 eV above the top of the valence band, i.e., much closer to the conduction band rather than the valence band. The bound levels are determined in general as solutions of the equation

$$\det \left\| \delta_{\alpha\alpha'} - \sum_{\alpha''} G^{\circ}_{\alpha\alpha''}(E) V_{\alpha''\alpha'} \right\| = 0 ,$$

where $G_{\alpha\alpha''}(E) \equiv \langle \alpha | (E - H^{\circ})^{-1} | \alpha'' \rangle$ is the unperturbed (crystalline) Green's function[18] and $V_{\alpha''\alpha'}$ are the matrix elements of the perturbing potential. In the present case $G_{\alpha\alpha''}(E)$ is diagonal when α, α'' refer to the four orbitals of the same site and $V_{\alpha''\alpha'}$ is diagonal and infinite when α'', α' refer to the four orbitals of the vacant site and zero otherwise. Thus the equations determining the bound levels become

$$G_p(E) = 0 , \tag{1}$$

$$G_s(E) = 0 , \tag{2}$$

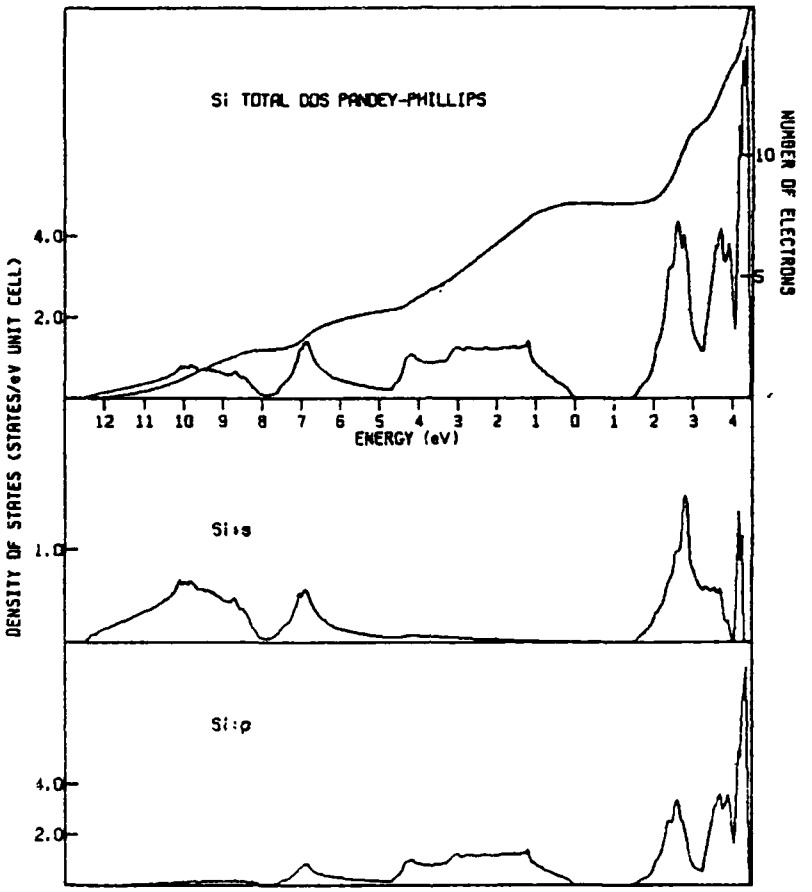

FIG. 3. Total and angular momentum-decomposed densities of states for Si derived using the Slater-Koster parameters of Pandey and Phillips.

where G_p, G_s are the p and s diagonal matrix elements of G°, respectively. In Fig. 4 we plot the real part of G_p ($\mathrm{Im}G_p$ is zero in the gap) vs E, showing thus the solution of Eq. (1) at $E = 0.75$ eV. On the other hand, the plot of the real part of G_s versus E in Fig. 5 shows that Eq. (2) has no solution, i.e., no s-like bound level exists.

The important point in this section is that the position of the bound state that we have calculated (0.75 eV) is in close agreement with the 0.8-eV value reported by Bernholc *et al.*[4] and obtained from electronically self-consistent calculations. Our value is also in good agreement with the 0.7-eV value given by Baraff and Schlüter[5,6] and also by an electronically self-consistent approach. This confirms the suspicion of Bernholc *et al.*[4] that the position of the bound level in the gap is determined mainly by the crystalline SK Hamiltonian. Indeed, the present calculation shows that the effect of electronic self-consistency on the position of the bound level is within the numerical uncertainties of the calculation and thus can be neglected. Hence, it appears to us that the question of carrying the calculation to self-consistency is of secondary importance. What is needed is a tight-binding Hamiltonian which gives the correct gap and a good representation of the valence as well as the conduction band. With such a Hamiltonian as a starting point the electronic self-consistency effects seem to be of minor importance. On the other hand, the effects of lattice relaxation due to the vacancy (i.e., the effects of ionic self-consistency) are quite important as suggested recently by White and Ngai[19] and demonstrated by elaborate first-principles calculations by Baraff *et al.*[20] and Lipari *et al.*[21]

In conclusion, we have succeeded in constructing an orthogonal s,p^3 basis Slater-Koster Hamiltonian for Si which reproduces reasonably accurately the crystalline band structure not only of the valence band but of the conduction band as well. This Hamiltonian was shown also to be

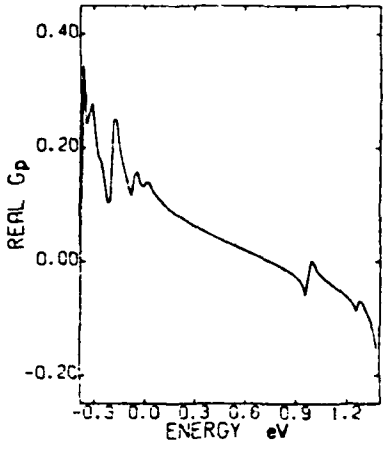

FIG. 4. The real part of the p-like Green function G_p plotted as a function of energy. Note that the gap is in the range $0 \leq E \leq 1.0$ eV.

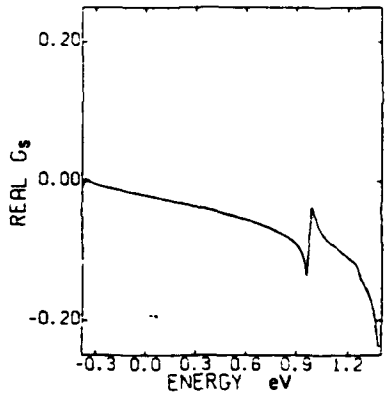

FIG. 5. The real part of the s-like Green functions G_s plotted as a function of energy. Note that the gap is in the range $0 \leq E \leq 1.0$ eV.

capable of calculating correctly the effects of unreconstructed vacancies. In forthcoming publications we employ this Hamiltonian together with a coherent potential approximation approach to study the electronic structure of amorphous and hydrogenated amorphous Si. In such a complicated calculation, the orthogonality and the small number (four orbitals per site) of the basis of the present SK scheme are very important advantages.

ACKNOWLEDGMENTS

We are indebted to Dr. W. E. Pickett for providing us with his unpublished pseudopotential calculation for silicon. We also wish to thank Dr. L. L. Boyer, Dr. B. M. Klein, Dr. W. E. Pickett, and Dr. C. T. White for many useful discussions. This work was supported in part by the U. S. Department of Energy Contract No. DE-AT-01-79ET-23078.

[1]G. F. Koster and J. C. Slater, Phys. Rev. 95, 1167 (1954).
[2]J. Callaway and A. J. Hughes, Phys. Rev. 156, 860 (1967).
[3]J. Bernholc and S. T. Pantelides, Phys. Rev. B 18, 1780 (1978).
[4]J. Bernholc, N. O. Lipari, and S. T. Pantelides, Phys. Rev. Lett. 41, 895 (1978).
[5]G. A. Baraff and M. Schlüter, Phys. Rev. Lett. 41, 892 (1978).
[6]G. A. Baraff and M. Schlüter, Phys. Rev. B 19, 4965 (1979).
[7]J. C. Slater and G. F. Koster, Phys. Rev. 94, 1498 (1954).
[8]W. E. Pickett (unpublished). This calculation utilized the local pseudopotential form factors of Chelikowsky and Cohen [Phys. Rev. B 10, 5095 (1974)].
[9]G. Dresselhaus and M. S. Dresselhaus, Phys. Rev. 160, 649 (1967).
[10]I. Alstrup and K. Johansen, Phys. Status Solidi 28, 555 (1968).
[11]V. Bortolani, C. Calandra, and M. J. Kelly, J. Phys. C 6, L349 (1973).
[12]D. J. Chadi and M. L. Cohen, Phys. Status Solidi B 68, 405 (1975); D. J. Chadi, Phys. Rev. B 16, 790 (1977).
[13]E. Kauffer, P. Pêcheur, and M. Gerl, J. Phys. C 9, 2319 (1976).
[14]K. C. Pandey and J. C. Phillips, Phys. Rev. B 13, 750 (1976).
[15]W. A. Harrison, *Electronic Structure and the Properties of Solids* (Freeman, San Francisco, 1980); S. Froyen and W. A. Harrison, Phys. Rev. B 20, 2420 (1979).
[16]D. J. Chadi, Phys. Rev. B 16, 3572 (1977).
[17]G. Lehmann and M. Taut, Phys. Status Solidi B 54, 469 (1972).
[18]E. N. Economou, *Green's Functions in Quantum Physics* (Springer, New York, 1979).
[19]C. T. White and K. L. Ngai, J. Vac. Sci. Technol. 16, 1412 (1979).
[20]G. A. Baraff, E. O. Kane, and M. Schlüter, Phys. Rev. Lett. 43, 956 (1979).
[21]N. O. Lipari, J. Bernholc, and S. T. Pantelides, Phys. Rev. Lett. 43, 1354 (1979).

P2

130

Electronic Densities of States in α-Si:H

D.A. Papaconstantopoulos
Naval Research Laboratory, Washington, DC 20375

E.N. Economou
Department of Physics, University of Athens, Greece

ABSTRACT

We have used the coherent potential approximation to calculate the electronic densities of states for a model of hydrogenated amorphous silicon. The results are in good agreement with photoemission, optical, photoconductivity and photoluminescence data.

Recent experimental work in α-Si:H has shown that hydrogen reduces the density of states (DOS) in the band gap by several *orders of magnitude*,[1] and also widens the optical gap.[2,3] In addition, other experiments have shown that hydrogen modifies both the valence[4] and conduction bands.[5]

For the purpose of understanding these experiments several theoretical models and calculations have been proposed.[6] We present here a brief account of our calculations[7] which we believe provide satisfactory explanations of the above mentioned measurements.

Our model assumes an effective lattice whose sites may have probability c of being vacant, and probability 1-c of having a Si atom. In addition, we have assumed that hydrogen atoms may be located along the lines connecting a vacant site with its nearest neighbors. Thus we have included in our model, at random, Si sites, vacancy sites, and sites that have one, two, three, or four hydrogen atoms. Using this model of disorder, we have used a tight-binding form of the coherent-potential approximation (CPA) to perform detailed calculations of the electronic DOS. Since we have not allowed for reconstruction, we believe that the most stable configuration to be compared with experiment is that in which a vacancy is replaced by a complex of four hydrogen atoms. This configuration is shown in two dimensions in Fig. 1.

The starting point of this calculation is a Slater-Koster (SK) Hamiltonian fit to the pseudopotential band structure of crystalline Si.[8] The basis is orthonormal with four orbitals (one s-like and three p-like) per atom. We have used 20 Si-Si matrix elements (three-center interactions) that include first, second, and

ISSN:0094-243X/81/730130-06$1.50

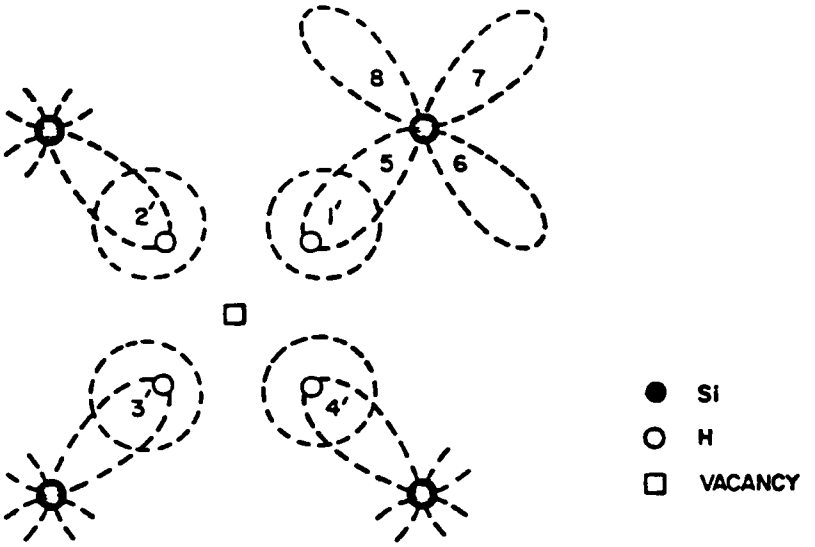

Figure 1. Two-dimensional view of the atom configuration used in the present calculations.

third nearest neighbors. We have determined the H-H, and H-Si matrix elements from the SiH_4 molecule on an sp^3 basis, and then converted them to our SK basis.

The CPA effective Hamiltonian H_e has off-diagonal matrix elements which for the first nearest neighbors are a virtual crystal average (VCA) of the Si-Si and H-Si values. The off-diagonal second and third nearest neighbor interactions were assumed to have the Si-Si values. The diagonal matrix elements Σ_s and Σ_p form a diagonal 4x4 matrix (since each site is associated with four orbitals):

$$\tilde{\Sigma} = \begin{pmatrix} \Sigma_s & 0 & 0 & 0 \\ 0 & \Sigma_p & 0 & 0 \\ 0 & 0 & \Sigma_p & 0 \\ 0 & 0 & 0 & \Sigma_p \end{pmatrix} \tag{1}$$

and they are determined from the CPA condition:

$$\sum_j P_j \tilde{t}_j = 0 \tag{2}$$

where P_j is the probability for each configuration j, and

$$\tilde{t}_j = \tilde{U}_j[1-\tilde{G}_e\tilde{U}_j]^{-1} \tag{3}$$

where $\tilde{G}_e$ is a 4x4 site diagonal Green's function corresponding to the effective Hamiltonian $\tilde{H}_e$, and

$$\tilde{U}_j = \tilde{E}_j(000) - \tilde{\Sigma} \tag{4}$$

where $\tilde{E}_j(000)$ is a 4x4, in general non-diagonal, matrix which contains the on-site SK parameters. Having determined Σ_s, Σ_p, and thus $\tilde{G}_e$ from the above equations we can calculate the DOS from the standard expression:

$$\rho(E) = -\frac{1}{\pi}\,\mathrm{Im}\mathrm{Tr}\tilde{G}_e \tag{5}$$

Our calculated DOS are shown in Fig. 2 for the case of 5% vacancies which are all saturated by hydrogen resulting in a hydrogen concentration of 20%. From Fig. 2 we note first a bandgap E_g=1.4eV that is wider by 0.4eV than the corresponding E_g=1.0eV which our tight-binding Hamiltonian gives for the non-hydrogenated case.[8] This widening of the gap is due to a narrowing of the third peak of the DOS at the top of the valence band which we have identified to be a result of a decrease of the $pp\pi$ interaction due to hydrogenation.[7] This recession of the valence band by 0.4eV is in excellent agreement with the photoemission measurements of von Roedern et al.[4] Figure 2 also shows a site decomposition of the DOS. Concentrating on the H site DOS, we have identified hydrogen induced peaks at approximately 5.2 eV, 7.6 eV, and 13.5 eV below the Fermi level. This is also in good agreement with the photoemission data.[4]

We have further demonstrated the widening of the band gap by performing a joint DOS calculation and presenting our results in the same manner as that followed in the analysis of the measurements of the optical absorption coefficient α.[9] The calculated square root of the joint DOS is assumed to be proportional to the quantity $(\alpha E)^{1/2}$, and has been normalized to the experimental value[3] at E=4eV. A comparison with the measurements of Cody et al[3] is shown in Fig. 3. Although the experimental graph corresponds to a smaller hydrogen content (16%) than the calculated one, the agreement is good with the only discrepancy being that the theory predicts a smaller gap.

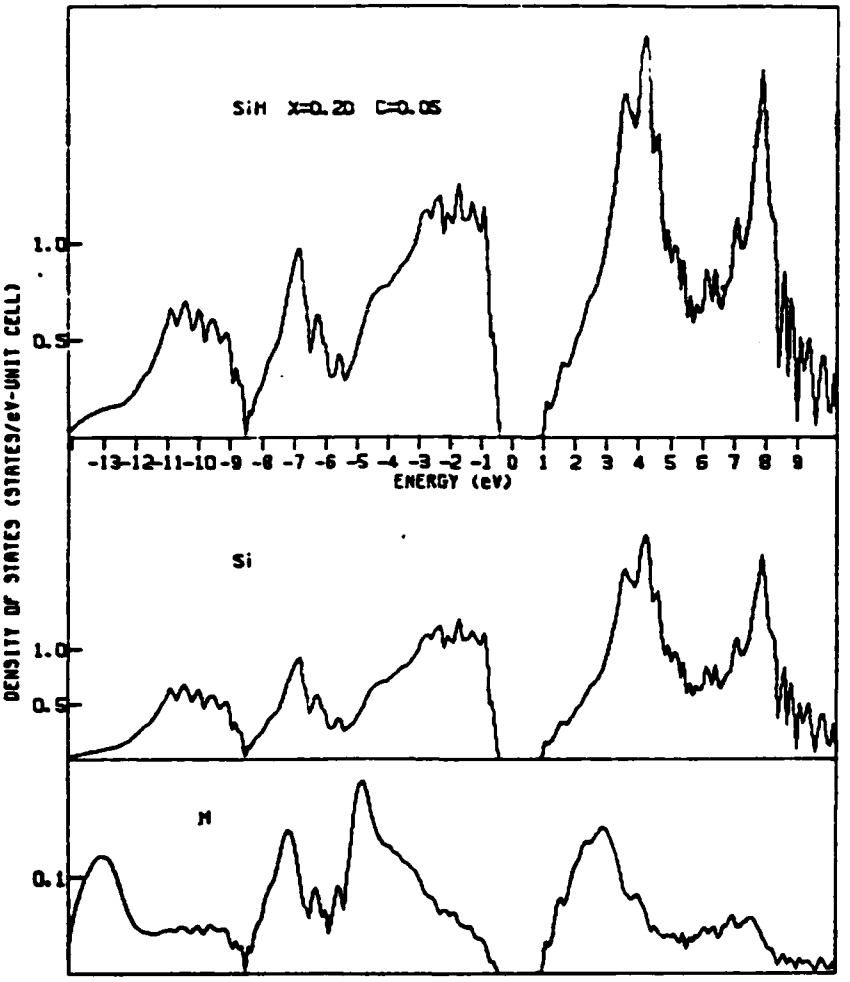

Figure 2. Total and site decomposed densities of states for SiH_x with x=0.20. Note that the Si and H DOS have been multiplied by 1-c and c respectively (c=0.05). The Fermi level is located in the middle of the gap.

Figure 4 shows the variation of the band gap as a function of the hydrogen content. In all cases shown in this graph we are dealing with vacancies fully saturated by hydrogen. We note a monotonic increase of the band gap with increasing hydrogen concentration. This is in qualitative agreement with the experiments of

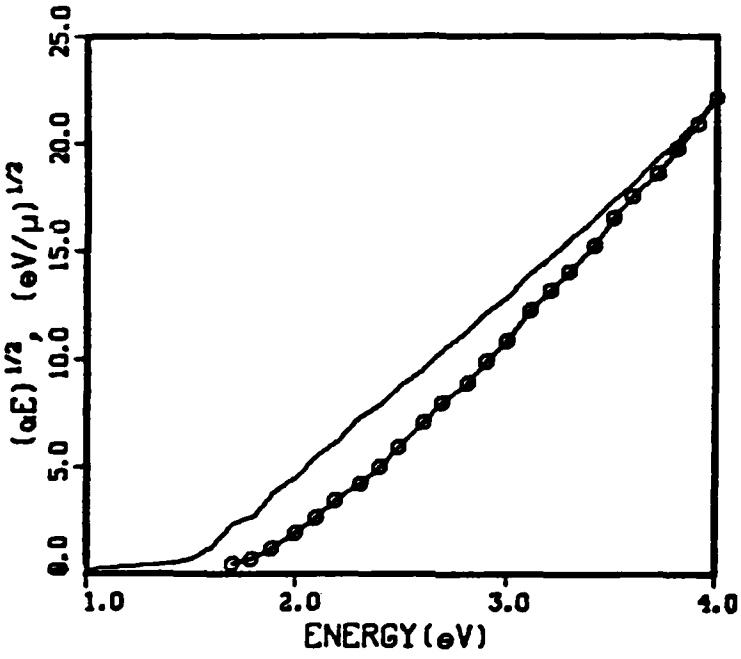

Figure 3. Plot of the square root of the joint density states versus energy. *The open circles are the experimental* values of the quantity $(\alpha E)^{1/2}$ (Ref. 3).

Moustakas et al[2] who have studied the dependence of the optical gap on hydrogen content for sputtered hydrogenated a-Si.

We should mention here that in addition to the hydrogen-saturated vacancy case we have also considered configurations where one, two, or three hydrogen atoms are present, leaving three, two, or one dangling bonds respectively. The results demonstrate the appearance of dangling bond states in the gap.[7]

Turning now to the conduction band, we have found from the site-decomposed DOS of Fig. 2 that the bottom of the conduction band has strong hydrogen character. This supports the notion that photoluminescence data[5] suggest the formation of Si-H antibonding states at the bottom of the conduction band.

We wish to acknowledge discussions with W.E. Pickett, T.D. Moustakas, L.L. Boyer, B.M. Klein, and G.D. Cody. We are also grateful to T.D. Moustakas for providing his unpublished data shown in Fig. 4. This work was supported in part by the Solar Energy Research Institute via an interagency agreement with the US Department of Energy.

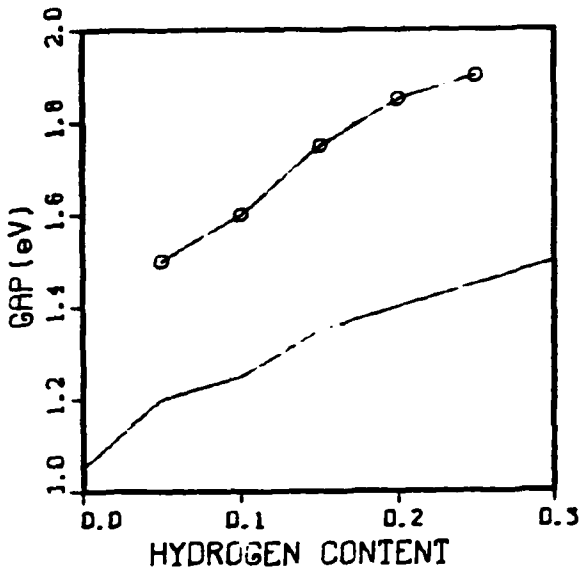

Figure 4.

Plot of band gap versus hydrogen content. The open circles are the measurements of Ref.2.

REFERENCES

1. W.E. Spear and P.G. LeComber, Solid State Commun. 17, 1193 (1975); D.E. Carlson and C.R. Wronski, Appl. Phys. Lett. 28, 671 (1976).
2. T.D. Moustakas, C.R. Wronski, and D.L. Morel, J. Non-Cryst. Solids 35 and 36, 719 (1980); T.D. Moustakas and W. Lanford, to be published.
3. G.D. Cody, C.R. Wronski, B. Abeles, R.B. Stephens, and B. Brooks, Solar Cells publ. by Elsevier Sequois-Lausanne (1981).
4. B. von Roedern, L. Ley, and M. Cardona, Phys. Rev. Lett. 39, 1576 (1977).
5. T.D. Moustakas, D.A. Anderson, and W. Paul, Solid State Commun. 23, 155 (1977).
6. W.Y. Ching, D.J. Lam, and C.C. Lin, Phys. Rev. Lett. 42, 805 (1979); D.C. Allan and J.D. Joannopoulos, Phys. Rev. Lett. 44, 43 (1980); K.J. Johnson, H.J. Kolari, J.P. deNeufville, and D.L. Morel, Phys. Rev. B21, 643 (1980); W.E. Pickett, Phys. Rev. (1981).
7. E.N. Economou and D.A. Papaconstantopoulos, Phys. Rev. B23, 2042 (1981).
8. D.A. Papaconstantopoulos and E.N. Economou, Phys. Rev. B22, 2903 (1980).
9. J. Tauc, R. Grigorovici, and A. Vancu, Phys. Stat. Sol. 15, 627 (1966).

P3

PHYSICAL REVIEW B VOLUME 23, NUMBER 4 15 FEBRUARY 1981

Theory of hydrogenated silicon

E. N. Economou
Department of Physics, University of Virginia, Charlottesville, Virginia

D. A. Papaconstantopoulos
Naval Research Laboratory, Washington, D.C. 20375

(Received 12 May 1980; revised manuscript received date 3 November 1980)

Using a coherent-potential approximation, we calculate the effects of hydrogenation on the density of states of silicon containing a finite concentration of ideal vacancies. The results reproduce the main features seen in the measurements including the restoration and the widening of the gap with increasing hydrogen content.

Hydrogenated α-Si has recently received a lot of attention partly because of the possibilities it offers as a device material.[1–4] In particular, emphasis has been given to the determination of the density of electronic states (DOS) by various experimental techniques[5–7] and to a lesser degree by theoretical calculations.[8–10] As a result of these efforts it is generally believed that the gap states in α-Si are associated with dangling bonds; hydrogen is attached to these dangling bonds thus pushing these states out of the gap. The model we consider in this work demonstrates, for the first time in a quantitative way, the appearance of dangling bond states and their passivation by hydrogen, and also shows the role of hydrogen in widening the gap. An alternate computational technique[9] using small Si-H molecules (terminated by Si Bethe lattices) has produced qualitatively similar conclusions to those presented here.

The starting point in our calculation is a Slater-Koster Hamiltonian H_0 including up to the third-nearest-neighbor interactions; the basis is orthonormal with four orbitals (one s-like and three p-like) per atom.[11] This Hamiltonian accurately reproduces[11] both the valence and the conduction bands of crystalline Si; we found that this level of accuracy is essential for our calculation. Randomness is introduced by assuming that there is a finite concentration c of ideal vacancies which means that the diagonal matrix elements of the Hamiltonian, $\langle n|H|n\rangle$, at a given site n have a probability c to be infinite and a probability $1-c$ to have the perfect-crystal values. This type of disorder produces the essential feature of dangling bonds at the atoms surrounding a vacancy. Topological disorder is simulated by changing the tight-binding parameters $E_{xy}(\frac{1}{2}\frac{1}{2}\frac{1}{2})$ and $E_{xx}(\frac{1}{2}\frac{1}{2}\frac{1}{2})$ from their crystalline Si values[11] to the values 1.39 and 0.31 eV, respectively, as a result of varying the dihedral angle in a range which spans the eclipsed and staggered configurations. We have omitted the reconstruction and relaxation of the Si lattice which tends to push the dangling bond states back into the bands as shown by explicit calculations in the one vacancy case.[12,13] Thus our model would overestimate the number of dangling bond states and consequently the hydrogen required for their passivation. The size of this overestimation depends on how much reconstruction has taken place, which in turn is affected by the method of preparation of the Si-H film.[3] For example reconstruction may be prohibited when the film is grown in the presence of a substantial amount of hydrogen.[2] Finally we point out that no correlation among the positions of the vacancies has been included in the present calculation. It has been shown elsewhere[14] that the main effect of the tendency to cluster the vacancies together to form divacancies, trivacancies, and internal voids, etc., is to replace c by a smaller effective c^*.

Hydrogens are assumed to be located along the lines connecting a vacant site with its nearest neighbors. Thus up to four hydrogens can be accomodated

around a Si vacancy. The H-Si distance is taken as in the SiH_4 molecule. Charge-density contours of a H saturated Si-vacancy calculation[15] suggest the existence of higher than s components of the hydrogen wave function; and show that this multiple l wave function can be approximated by a single s-wave function, $|S_H\rangle$, which is displaced towards Si by about 20%. Using this wave function $|S_H\rangle$, the matrix elements of SiH_4,[16] the results of Chadi[17] that Si wave functions decay as $\exp(-1.04r)$, and Mattheiss's values for hydrogenic matrix elements,[18] we have estimated matrix elements $\gamma_i (i = 1, \ldots, 6)$ analogous to those defined by Hirabayashi[19] with one or both of the Si sp^3 hybrids replaced by $|S_H\rangle$. When a hydrogen is missing the corresponding γ_i is taken as infinite. Knowing the matrix elements γ_i for each configuration, we can transform[19] to the original basis $|in\rangle$ and obtain $\langle ni|H|jn\rangle$. For the H-saturated Si vacancy the matrix elements in eV are $E_{ss}(000) = -8.72$, $E_{xx}(000) = -1.60$, $E_{ss}(\frac{1}{2}\frac{1}{2}\frac{1}{2}) = -3.05$, $E_{xx}(\frac{1}{2}\frac{1}{2}\frac{1}{2}) = 1.96$, $E_{xx}(\frac{1}{2}\frac{1}{2}\frac{1}{2}) = 0.64$, $E_{xy}(\frac{1}{2}\frac{1}{2}\frac{1}{2}) = 0.98$. The off-diagonal disorder in our model Hamiltonian was treated in the virtual-crystal approximation by averaging the above Si-H matrix elements with those of Si.[11] We then employ the coherent-potential approximation (CPA) to obtain the DOS. The CPA calculates the DOS from a periodic effective Hamiltonian H_e which is obtained by replacing $\langle ns|H|sn\rangle$ by $\Sigma_s(E)$ and $\langle np|H|pn\rangle$ by $\Sigma_p(E)$ where p stands for any of the three p orbitals. The unknown quantities (self-energies) Σ_s, Σ_p are determined from the self-consistency condition

$$\langle U(1 - G_e U)^{-1}\rangle = 0 \ , \tag{1}$$

where the parentheses denote average over the following 17 configurations at a given lattice site: the site occupied by Si (one configuration with probability $1-c$), the site being vacant with no H (one configuration with probability x_0), the site being vacant with one dangling bond occupied by H (four configurations each of probability $x_1/4$), the site being vacant with two dangling bonds occupied by H (six configurations each of probability $x_2/6$), the site being vacant with three dangling bonds occupied by H (four configurations each of probability $x_3/4$), and the site being vacant with all four dangling bonds occupied by H (one configuration of probability x_4); G_e is the diagonal 4×4 matrix $\langle ni|(E - H_e)^{-1}|in\rangle$ and U is the configuration-dependent 4×4 matrix $\langle ni|(H - H_e)|in\rangle$. As expected from symmetry considerations, the matrix $\langle U(1 - G_e U)^{-1}\rangle$ was found to be diagonal with the three p matrix elements equal to each other. Thus Eq. (1) is actually reduced to two equations which determine the unknown quantities Σ_s, Σ_p.

Explicit results were obtained by assuming that hydrogen occupies dangling bonds in an uncorrelated way. In this case the probabilities x_l, $(l = 0, \ldots, 4)$ are given by

$$x_l = \frac{4!}{(4-l)!l!} \frac{cx^l(4c - x)^{4-l}}{(4c)^4} \ , \tag{2}$$

where x is the ratio of hydrogen atoms to lattice sites. We found that the numerical work is significantly reduced if the following additional approximation is employed: Eq. (1) is solved for the limiting cases $x = 0$, $x = 4c$ obtaining thus $\Sigma_s(E;0)$, $\Sigma_p(E;0)$, $\Sigma_s(E;4c)$, and $\Sigma_p(E;4c)$. For intermediate values of x an average t-matrix approximation is used with

$$\Sigma_i(E;x) = \left(1 - \frac{x}{4c}\right)\Sigma_i(E;0) + \frac{x}{4c}\Sigma_i(E;4c); \quad i = s,p \ . \tag{3}$$

Using these Σ's we obtain the 4×4 matrix G_e and the configuration-dependent 4×4 matrices U. The Si and the H partial DOS are given explicitly by the equations

$$\rho_{Si}(E) = (1 - c)\left(-\frac{\mathrm{Im}}{\pi}\right)\mathrm{Tr}[(1 - G_e U_{Si})^{-1} G_e] \ , \tag{4}$$

$$\rho_H(E) = -c\frac{\mathrm{Im}}{\pi}\mathrm{Tr}\langle(1 - G_e U)^{-1} G_e\rangle_n \ , \tag{5}$$

where the symbol $\langle\ \rangle_n$ indicates average over only those configurations associated with no Si at the site n. The total DOS is of course:

$$\rho(E) = \rho_{Si}(E) + \rho_H(E) \ . \tag{6}$$

In Fig. 1 we plot the DOS in the gap where one sees that by increasing the hydrogen content x the states in the gap are reduced drastically in agreement with the experimental findings. It is our impression

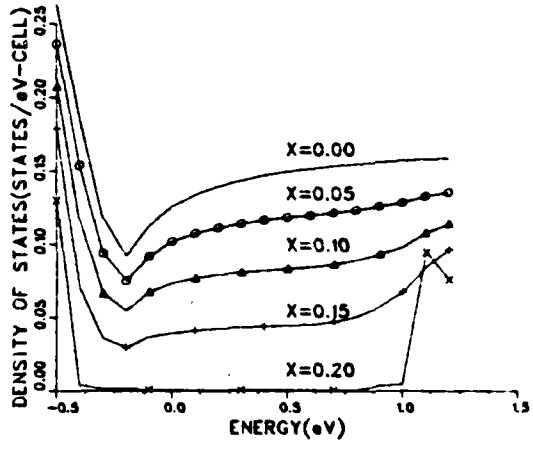

FIG. 1. Density of states in the gap for different hydrogen concentrations x. The Fermi level was found to be at $E = 0.4$ eV and was almost invariant with x.

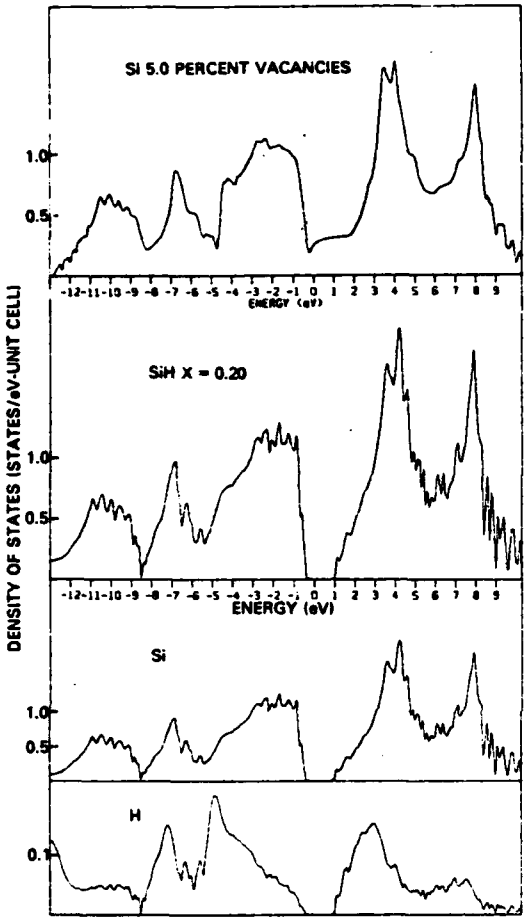

FIG. 2. Total and site decomposed densities of states. Top panel refers to 5% vacancies and no hydrogen, and the bottom panel shows the case with all dangling bonds terminated by hydrogen.

that the present calculation is the first one to show in a convincing quantitative manner, this restoration of the band gap upon hydrogenation.

In Fig. 2 we show the DOS for the whole spectrum including both the valence and conduction bands. Figure 2(a) shows the total DOS for the case of 5% vacancies, i.e., $c = 0.05$ and $x = 0.0$. This is compared to Fig. 2(b), where all ($x = 0.20$) of the dangling bonds are terminated by hydrogen. The H site DOS [in Fig. 2(b)] shows two peaks at approximately 5.2 and 7.6 eV below the Fermi level in good agreement with the photoemission data of von Roedern *et al.*[5] Furthermore our results show a recession of the valence band by about 0.4 eV in agreement with the above experiment.[5] By examining the site decomposition of the DOS and the limiting case of an isolated hydrogen impurity we have determined that

TABLE I. Band gap E_g (in eV) as a function of hydrogen content for cases where all dangling bonds are saturated (i.e., $x = 4c$). The estimated uncertainty is ±5%.

$x = 4c$	E_g
0.00	1.05
0.05	1.20
0.10	1.25
0.15	1.35
0.20	1.40
0.25	1.45
0.30	1.50

the eigenstates at the bottom of the conduction band of Si-H are resonance states exhibiting an enhanced probability to find the electron around the hydrogen atom. These states can be thought of as antibonding H-Si states mixed with regular conduction-band Si states. We would like to point out that the existence of this type of states has been suggested in order to interpret transport and photoluminescence[4] results in highly hydrogenated samples.

Finally, we wish to emphasize that the present work shows a substantial increase of the gap upon hydrogenation in agreement with experiment.[1,2] This is demonstrated in Table I which gives the size of the gap as a function of hydrogen content for cases where no dangling bonds are present. According to the present theory the widening of the gap is due to the following two effects: (a) The Si–H bond being stronger than the Si–Si bond tends to push the bottom of the conduction band towards higher energies, thus cancelling the opposite effect produced by the diagonal hydrogen matrix elements. (b) The difference $E_{xy}(\frac{1}{2}\frac{1}{2}\frac{1}{2}) - E_{xx}(\frac{1}{2}\frac{1}{2}\frac{1}{2})$, which is a measure of the $pp\pi$ interaction, effectively decreases upon hydrogenation; this causes a narrowing[20] of the third peak of the valence band (VB) which results in the recession of the top VB states.

In conclusion our calculations for Si-H reproduce with no adjustable parameters, the main features of the measurements of the DOS, including the widening of the gap.

ACKNOWLEDGMENTS

We should like to thank L. L. Boyer, B. M. Klein, T. D. Moustakas, and W. E. Pickett for many useful discussions and suggestions. This work was supported in part by the U.S. DOE and the University of Athens. Part of this work was done while one of us (E.N.E.) visited Exon Research Corporation.

[1]D. E. Carlson and C. R. Wronski, Appl. Phys. Lett. 28, 671 (1976).
[2]T. D. Moustakas, C. R. Wronski, and D. L. Morel, J. Non-Cryst. Solids 35 & 36, 719 (1980).
[3]W. E. Spear, Adv. Phys. 26, 811 (1977).
[4]T. D. Moustakas, J. Electron. Mater. 8, 391 (1979).
[5]B. von Roedern, L. Ley, and M. Cardona, Phys. Rev. Lett. 39, 1576 (1977).
[6]N. B. Goodman, H. Fritzsche, and H. Ozaki, J. Non-Cryst. Solids 35 & 36, 599 (1980).
[7]T. Tiedje, T. D. Moustakas, J. M. Cebulka, and C. R. Wronski, Bull. Am. Phys. Soc. 25, 329 (1980); and (unpublished).
[8]W. Y. Ching, D. J. Lam, and C. C. Lin, Phys. Rev. Lett. 42, 805 (1979).
[9]D. C. Allan and J. D. Joannopoulos, Phys. Rev. Lett. 44, 43 (1980).
[10]K. H. Johnson, H. J. Kolari, J. P. deNeufville, and D. L. Morel, Phys. Rev. B 21, 643 (1980).
[11]D. A. Papaconstantopoulos and E. N. Economou, Phys. Rev. B 22, 2903 (1980).
[12]N. O Lipari, J. Bernholc, and S. T. Pantelides, Phys. Rev. Lett. 43, 1354 (1979).
[13]G. A. Baraff, E. O. Kane, and M. Schlüter, Phys. Rev. Lett. 43, 956 (1979).
[14]D. A. Papaconstantopoulos, E. N. Economou, L. L. Boyer, and B. M. Klein (unpublished).
[15]W. E. Pickett (unpublished).
[16]M. L. Sink and G. E. Juras, Chem. Phys. Lett. 20, 474 (1973); K. C. Pandey, Phys. Rev. B 14, 1557 (1976).
[17]D. J. Chadi, Phys. Rev. B 16, 3572 (1977).
[18]L. F. Mattheiss, Phys. Rev. 123, 1209 (1961).
[19]K. Hirabayashi, J. Phys. Soc. Jpn. 27, 1475 (1969).
[20]V. T. Rajan and F. Yndurain, Solid State Commun. 20, 309 (1976).

P4

PHYSICAL REVIEW B VOLUME 24, NUMBER 12 15 DECEMBER 1981

Calculations of the electronic properties of hydrogenated silicon

D. A. Papaconstantopoulos
Naval Research Laboratory, Washington, D. C. 20375

E. N. Economou
University of Crete, Crete, Greece
(Received 16 July 1981)

We have used the coherent potential approximation to calculate the electronic densities of states for a model of hydrogenated amorphous silicon. The results demonstrate the restoration and widening of the band gap with increasing hydrogen content. In the valence band, excellent agreement with photoemission experiments is obtained. In the conduction band Si-H antibonding states are predicted that can be inferred from photoconductivity measurements.

I. INTRODUCTION

Basic experimental facts

The current intensive investigation of hydrogenated amorphous silicon originated in 1975 when Spear and LeComber[1] succeeded to substitutionally dope amorphous Si(*a*-Si), produced by decomposition of silane, through the incorporation of phosphorous and boron impurities. Soon after, it became apparent, as a result of work by Paul *et al.*[2] who also presented similar doping results in *a*-Si produced by sputtering in an Ar + H plasma, that the origin of the doping effects as well as other good electronic properties of this material[3,4] is the H passivation of dangling bonds. It has been shown recently,[5] for example, that the density of states in the middle of the gap can be reduced through hydrogenation to values as low as 5×10^{14} $cm^{-3}eV^{-1}$. However, the amounts of hydrogen in these Si-H "alloys" were found to be as much as 100 times larger than the maximum number of dangling bonds. Therefore hydrogen, in addition to saturating the dangling bonds, introduces other changes in the electronic structure of *a*-Si.

Hydrogenation not only eliminates the dangling-bond states from the energy gap, but also widens the gap as demonstrated by Freeman and Paul,[6] by Cody *et al.*,[7] and by Goodman *et al.*[8] using different experimental techniques.

Away from the gap, photoemission measurements by von Roedern *et al.*[9] revealed hydrogen associated states well within the valence band. In the conduction band the photoconductivity data of Moustakas *et al.*[10] suggest the formation of Si-H antibonding states. The role of hydrogen in modifying the network is investigated through a variety of experimental techniques, such as infrared and Raman spectroscopy,[11,12] nuclear magnetic resonance,[13] small-angle x-ray scattering,[14] H implantation in *c*-Si,[15] and neutron scattering measurements.[16] For review of experimental work the reader is referred to the articles by Spear,[17] Moustakas,[3] and Fritzsche.[4]

Present physical understanding

Unhydrogenated *a*-Si is thought of as a random network where the local tetrahedral arrangement, with bond lengths almost identical to those of the crystalline state, is retained to a high degree. An idealization of this concept is the so-called "ideal random network," where the tetrahedral coordination is satisfied throughout with very small fluctuations in the bond lengths and larger fluctuations in other longer range geometrical aspects such as ring sizes, dihedral angles, etc. This ideal random network defines the concept of topological disorder. In reality, there are important deviations from the ideal network, such as vacancies and other strong local distortions, which may even cluster together to form voids, internal surfaces, etc. Associated with this type of defect are dangling bonds (or, more generally, weakly bonded states). The number of these states is considerably smaller than

expected because the random lattice undergoes relaxation processes around a vacancy (or a cluster of vacancies) which result in a substantial bond reconstruction and, consequently, partial elimination of dangling-bond states. This "healing" process cannot be complete because of the high coordination[18,19] of Si which imposes severe geometrical restrictions on the reconstruction process.

Calculations for the ideal single-vacancy problem[20–22] show that dangling bonds are associated with local states whose eigenenergy lies in the gap (about 0.75 eV above the valence-band edge). Allowing the atoms around the ideal vacancy to relax pushes these states toward the valence and the conduction band. On the basis of these calculations, one can conclude that the dangling bonds, which have survived reconstruction, create states in the gap. These states are of the order of $10^{19}-10^{20}$ $cm^{-3}eV^{-1}$ as electron-spin-resonance experiments show.[11,12] It is generally believed that hydrogen passivates the dangling-bond states by forming Si—H bonds which are associated with states lying well within the valence band. Furthermore, if the material is grown in the presence of hydrogen, much of the reconstruction is prevented as a result of Si—H bond formation.[3] This explains why the highest amount of hydrogen in a-SiH_x is so much larger than the number of dangling bonds (which survived reconstruction) in the unhydrogenated specimens. One may view the abundant presence of hydrogen during the growth process as effectively reducing the coordination of the resulting structure and thus allowing the growth of an unstrained, chemically stable substance. The widening[6–8] of the gap upon hydrogenation has been attributed to the stronger Si—H bond as compared with the Si—Si bond. Here, as well as in a preliminary report[23,24] of this work, we argue that an equally important contribution comes from the effective reduction of the $pp\pi$ interaction upon hydrogenation.

Theoretical models

From the above discussion it follows that a complete theory of hydrogenated a-Si has to deal with the following aspects of the problem.

(*a*) *Topological disorder.* Models incorporating topological disorder (TD) using a continuous random network, have been used[25,26] in conjunction with the orthogonalized-linear-combination-of-atomic-orbitals method to perform calculations of the electronic structure of a-Si:H. These calculations are consistent with photoemission experiments,[9] but they do not seem capable of obtaining detailed information for the densities of states (DOS) in the gap region and in the conduction band. Recently, Cohen *et al.*[27] argued that TD widens the gap and creates a tail in the DOS which enters the gap. Using small Si-H molecules terminated by Si Bethe lattices, Allan and Joannopoulos[28] have examined the question of ring statistics and its influence on certain regions of the spectrum. We feel that increasing hydrogenation may reduce the importance of ring statistics. Finally, TD, introduced by allowing variation in the dihedral angle, seems to effectively reduce the size of the $pp\pi$ interaction[23] and thus contributes further to the widening of the gap.

(*b*) *Reconstruction.* Reconstruction is probably the most important aspect of unhydrogenated a-Si. A qualitative lattice distortion model has been proposed by Watkins.[29] This model has been used as the basis to address the problem of the single reconstructed vacancy in Si using elaborate Green's-function techniques.[30,31] Also, White and Ngai[32] have discussed reconstructing states at the Si-SiO_2 interface. However, it seems that the amount of reconstruction, and therefore its importance, is reduced when hydrogen is present during the growth process.[3] Thus, depending on the abundance of hydrogen, the method of preparation, and other details of the growth process, the importance of reconstruction may vary from a dominant role to an insignificant detail.

(*c*) *Chemical nature and statistics of the hydrogen incorporation.* By chemical nature we mean whether the hydrogen is always bonded to one of the four sp^3 hybrids of Si, or may participate in other bonding configurations. Even if hydrogen is only bonded to Si one still has to know statistical information such as the percentage of monohydrides versus polyhydrides, whether or not there are some hydrogen clustering tendencies, etc. Obviously, these questions affect the electronic structure of the material.

With the exception of the continuous-random-network work,[25,26] most attempts in the literature to study the above three aspects are based on considering small Si-H molecules. These Si-H clusters are either isolated or terminated by hydrogen[33] or by Si Bethe lattice[28] to avoid unphysical boundary effects. These approaches are very useful in revealing certain qualitative and even semiquantitative aspects of the subject; they are also necessary in some cases (*e.g.*, other hydrogen bonding config-

urations) given the difficulty of the problem. However, these approaches cannot be considered as a substitute for calculations dealing with macroscopic size systems. We should not lose sight of the fact that these calculations more properly apply to the study of Si-H molecules than to the Si-H solid. In addition, the Bethe-lattice calculations are based on a first-nearest-neighbor interaction Hamiltonian which, as has been shown,[22,34] is inadequate to reproduce the correct gap or a reasonable conduction band.

The work we report here is one of the first attempts to deal with the problem at the actual macroscopic scale which involves many particular local configurations. We found it necessary to omit aspects related to topological disorder and reconstruction, and concentrate our efforts on the third aspect which is the role of hydrogen in the electronic structure of a-SiH_x. We think that for fully hydrogenated samples with high hydrogen content, hydrogenation is the most important aspect and that TD and reconstruction will change our results only quantitatively. To treat the role of hydrogen, we have used a particular model of hydrogen incorporation which assumes that all hydrogens are bonded to Si. Although our model may not be quite realistic, we think that it incorporates the important features (which are independent of particular models) such as bonding and antibonding states made out of Si sp^3 and hydrogen orbitals, a stronger Si—H bond (as compared with Si—Si bond) which affects the states at the bottom of the conduction band, and an effective reduction, with hydrogenation, of the $pp\pi$ interaction which is very important for the states at the top of the valence band.

Thus we believe that the main conclusions of our work have a much wider validity than the particular model from which they were derived. Recently, a calculation complementary to ours was reported by Pickett.[35] Pickett has employed the self-consistent pseudopotential method with a supercell configuration to study the electronic states of the hydrogen-saturated vacancy in Si. His approach differs from ours in that he is using a periodic array of atoms, while we are using a random array. The results of the two calculations, however, have the same qualitative features. In the Appendix we utilize his conclusion of a strong Si—H bond and his charge-density contours to estimate certain H-Si matrix elements of our tight-binding Hamiltonian. Finally, we refer to a calculation along similar lines to ours reported by Divincenzo *et al.*[36] This calculation deals with a model defect which is an isolated monovacancy in an otherwise perfect crystal.

The rest of the paper is organized as follows. Section II describes our model configuration of hydrogenated a-Si; Sec. III gives the theory of the coherent-potential approximation as applied in the present work; Sec. IV discusses the results and compares with experiment, and the Appendix deals with the estimation of the H-H and H-Si matrix elements.

II. THE PRESENT MODEL

Our model describes hydrogenated Si by constructing an effective lattice whose sites may have probability c of being vacant and probability $1-c$ of having a Si atom. In addition, we have assumed that hydrogen atoms may be located along the lines connecting a vacant site with its nearest neighbors, as shown in Fig. 1(b). Thus we have included in our model, at random, Si sites, vacancy sites, and sites that have one, two, three, or four hydrogen atoms. Using this model of disorder, we have used a tight-binding form of the coherent-potential approximation[37,38] (CPA) to perform detailed calculations of the electronic DOS.

The starting point of the present calculations is a Slater-Koster (SK) Hamiltonian H; the bases are four Si orbitals (one $|s\rangle$ and three $|p\rangle$) which have been taken as orthonormal. The matrix elements in this basis have been chosen in such a way as to reproduce the band structure of crystalline Si (both valence and conduction band) rather accurately.[22] Such an accuracy is necessary in order to study dangling-bond states. As we have discussed in the Introduction, we have neglected the TD except for the following point: Because the dihedral angle (i.e., the angle which determines the orientation of the three bonds which are attached to one end of a given bond with respect to the other three bonds which are attached to the other end of this given bond) varies in a disordered structure in a range which starts from the eclipsed configuration all the way to the staggered configuration, the $pp\pi$ interaction fluctuates. As we have mentioned before, the $pp\pi$ interaction is very important because it controls the position of the top of the valence band. In the periodic case, the $pp\pi$ interaction is equal to the difference $\Delta = E_{x,y}(\frac{1}{2}\frac{1}{2}\frac{1}{2}) - E_{x,x}(\frac{1}{2}\frac{1}{2}\frac{1}{2}) = \gamma_6 - \gamma_5$, where $\gamma_6 = \langle 6|H|2\rangle$ and $\gamma_5 = \langle 6|H|3\rangle = \langle 6|H|4\rangle$ and $|2\rangle$, $|3\rangle$,

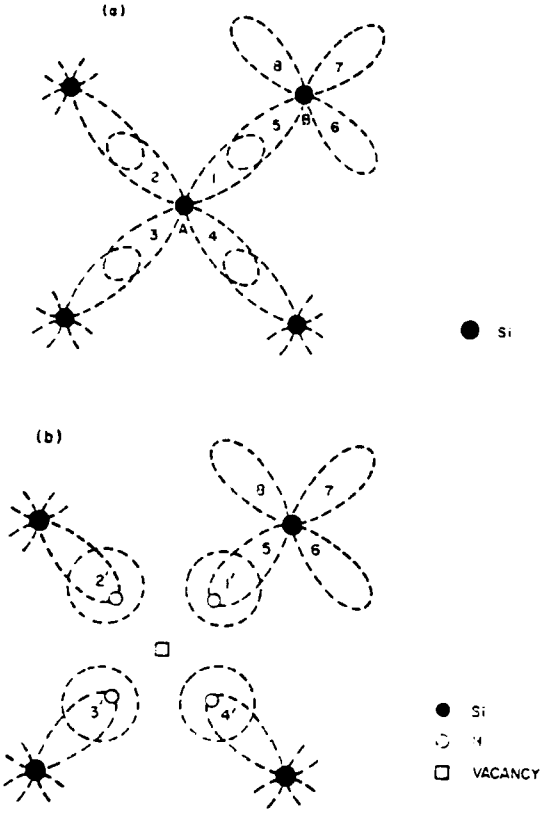

FIG. 1. (a) Two-dimensional view of the atom configuration for Si showing the sp^3 orbitals. (b) Two-dimensional view of the atom configuration for Si-H showing the replacement of one Si atom by four H atoms.

$|4\rangle$, and $|6\rangle$ are the sp^3 hybrids shown in Fig. 1(a). In the random structure $\langle 6|H|3\rangle \neq \langle 6|H|4\rangle$ so that, in general, there are three different matrix elements $\langle 6|H|2\rangle$, $\langle 6|H|3\rangle$, and $\langle 6|H|4\rangle$. We have found how these matrix elements vary with the dihedral angle and we have taken, as a measure of the $pp\pi$ interaction, the average of the maximum of the three differences of one of them from the mean value of the other two. To perform the average, we have assumed that the dihedral angle has a uniform (constant) probability distribution. The effect of this is to change the matrix elements $E_{x,y}(\frac{1}{2}\frac{1}{2}\frac{1}{2})$ and $E_{x,x}(\frac{1}{2}\frac{1}{2}\frac{1}{2})$ from their crystalline values[22] 1.407 and 0.276 eV, respectively, to the values 1.39 and 0.31 eV. This reduces the $pp\pi$ interaction Δ from the value 1.131 eV to the value 1.08 eV. This leads to a recession of the top of the valence band and, hence, a widening of the gap from $E_g = 1.0$ eV in the crystalline case to 1.05 in the "amorphous" state. We believe that if TD were taken into account in a more rigorous way, it would lead to a more substantial widening of the gap and to a tailing of the states into the gap.

Our model also omits reconstruction; this is a very serious omission in the cases where the dangling bonds have not been passivated by hydrogen. For those cases, our results should not be taken seriously except to say that if all these dangling bonds were present there would be substantial DOS in the gap. On the other hand, in the fully hydrogenated cases we expect that reconstruction is minimal and thus its omission in our model is not a serious shortcoming.

The way hydrogen is incorporated in our model is shown in Fig. 1(b), where an ideal vacancy has been created, resulting in four sp^3 Si dangling bonds. Such vacancies can accommodate up to four hydrogen atoms as shown in Fig. 1(b). The result of replacing a Si by four hydrogens as shown in Fig. 1(b) is to replace the Si-Si matrix elements [given in Table I of Ref. 22 with $E_{x,y}(\frac{1}{2}\frac{1}{2}\frac{1}{2})$ and $E_{x,x}(\frac{1}{2}\frac{1}{2}\frac{1}{2})$ changed as discussed above] by H-H or H-Si matrix elements. In the Appendix we explicitly estimate the effective matrix elements associated with the configuration of Fig. 1(b). They are the following:

$$E'_{s,s}(000) = -8.72 \text{ eV}, \quad E'_{x,x}(000) = -1.6 \text{ eV},$$

$$E'_{s,s}(\tfrac{1}{2}\tfrac{1}{2}\tfrac{1}{2}) = [illegible] \text{ eV},$$

$$E'_{s,x}(\tfrac{1}{2}\tfrac{1}{2}\tfrac{1}{2}) = 1.96 \text{ eV}, \quad E'_{x,x}(\tfrac{1}{2}\tfrac{1}{2}\tfrac{1}{2}) = 0.64 \text{ eV},$$

$$E'_{x,y}(\tfrac{1}{2}\tfrac{1}{2}\tfrac{1}{2}) = 0.98 \text{ eV}.$$

Actually, the second- and third-nearest-neighbor matrix elements will be affected by the replacement of a Si by four hydrogens. We assumed that this additional modification is much less significant than the diagonal and first-nearest-neighbor changes and thus we have omitted it. It must be pointed out that the $E'(000)$'s given above are matrix elements between fictitious s and p orbitals associated with the four hydrogens shown in Fig. 1(b) (they are the same linear combinations of the hydrogen orbitals $|1'\rangle$, $|2'\rangle$, $|3'\rangle$, and $|4'\rangle$ as the actual Si, s, and p are of the corresponding four sp^3 hybrids; see Appendix) and the $E'(\frac{1}{2}\frac{1}{2}\frac{1}{2})$'s are matrix elements between the fictitious four hydrogen s and p's and the s and p's of the nearest Si's.

III. COHERENT-POTENTIAL APPROXIMATION

As we have mentioned in the previous section, we have used the tight-binding (TB) CPA (Refs. 37 and 38) to obtain the DOS. Since, in addition to the configuration shown in Fig. 1(b), we have also considered cases where one or more of the hydrogens shown are missing, we had to generalize the TB-CPA to handle these additional configurations. The CPA condition of zero scattering on the average leads, in our case to the following equation:

$$(1-c)\tilde{U}_{\mathrm{Si}}(1-\tilde{G}_e\tilde{U}_{\mathrm{Si}})^{-1}+x_v\tilde{U}_v(1-\tilde{G}_e\tilde{U}_v)^{-1}+\frac{x_1}{4}\sum_{i=1}^{4}\tilde{U}_{1i}(1-\tilde{G}_e\tilde{U}_{1i})^{-1}+\frac{x_2}{6}\sum_{i=1}^{6}\tilde{U}_{2i}(1-\tilde{G}_e\tilde{U}_{2i})^{-1}$$
$$+\frac{x_3}{4}\sum_{i=1}^{4}\tilde{U}_{3i}(1-\tilde{G}_e\tilde{U}_{3i})^{-1}+x_4\tilde{U}_4(1-\tilde{G}_e\tilde{U}_4)^{-1}=0\ , \tag{1}$$

where $\tilde{G}_e$ is an effective Green's function obtained from the corresponding crystalline Si Green's function $\tilde{G}$ by replacing ϵ_s and ϵ_p with the CPA self-energies Σ_s and Σ_p, respectively. From Ref. 22 we have that $\epsilon_s \equiv E_{s,s}(000) = -3.953$ eV and $\epsilon_p \equiv E_{x,x}(000) = 1.512$ eV. $\tilde{G}(E)$ is a 4×4 diagonal matrix with matrix elements $G_{11}, G_{22}, G_{22}, G_{22}$, and where $G_{11} = \langle 0s \,|\, (E-H)^{-1} \,|\, 0s \rangle$ and $G_{22} = \langle 0x \,|\, (E-H)^{-1} \,|\, 0x \rangle$, where $|\,0s\,\rangle$ and $|\,0x\,\rangle$ are the s and p_x Si orbitals at the site 0, and where $\tilde{U}_{\mathrm{Si}}$, the Si scattering matrix, is

$$\tilde{U}_{\mathrm{Si}} = \begin{vmatrix} \epsilon_s-\Sigma_s & 0 & 0 & 0 \\ 0 & \epsilon_p-\Sigma_p & 0 & 0 \\ 0 & 0 & \epsilon_p-\Sigma_p & 0 \\ 0 & 0 & 0 & \epsilon_p-\Sigma_p \end{vmatrix} . \tag{2}$$

$\tilde{U}_v$, the vacancy scattering matrix is

$$\tilde{U}_v = \begin{vmatrix} \infty & 0 & 0 & 0 \\ 0 & \infty & 0 & 0 \\ 0 & 0 & \infty & 0 \\ 0 & 0 & 0 & \infty \end{vmatrix} . \tag{3}$$

$\tilde{U}_{1i}$ is a matrix corresponding to the four equivalent configurations where only one hydrogen atom is present with probability of occurrence $x_1/4$,

$$\tilde{U}_{11} = \tilde{S}\begin{vmatrix} \gamma_1' & 0 & 0 & 0 \\ 0 & \infty & 0 & 0 \\ 0 & 0 & \infty & 0 \\ 0 & 0 & 0 & \infty \end{vmatrix}\tilde{S}-\tilde{\Sigma}\ , \tag{4}$$

and, similarly, for $\tilde{U}_{12}$, $\tilde{U}_{13}$, and $\tilde{U}_{14}$. $\tilde{S}$ is the matrix which accomplished the orbital transformation (Appendix). The hydrogen matrix element γ_1' is taken equal to -3.38 eV which is its value for silane (Appendix). The matrix $-\tilde{\Sigma}$ is a diagonal matrix like (2) but without the ϵ_s and ϵ_p. $\tilde{U}_{2i}$ is a matrix corresponding to the six equivalent configurations where two hydrogen atoms are present with probability $x_2/6$,

$$\tilde{U}_{21} = \tilde{S}\begin{vmatrix} \gamma_1' & \gamma_2' & 0 & 0 \\ \gamma_2' & \gamma_1' & 0 & 0 \\ 0 & 0 & \infty & 0 \\ 0 & 0 & 0 & \infty \end{vmatrix}\tilde{S}-\tilde{\Sigma}\ , \tag{5}$$

and similarly for $\tilde{U}_{22}$, $\tilde{U}_{23}$, $\tilde{U}_{24}$, $\tilde{U}_{25}$, and $\tilde{U}_{26}$. The matrix element $\gamma_2' = -1.78$ eV is estimated in the Appendix. $\tilde{U}_{3i}$ is a matrix corresponding to the four equivalent configurations where three hydrogen atoms are present with probability $x_3/4$,

$$\tilde{U}_{31} = \tilde{S}\begin{vmatrix} \gamma_1' & \gamma_2' & \gamma_2' & 0 \\ \gamma_2' & \gamma_1' & \gamma_2' & 0 \\ \gamma_2' & \gamma_2' & \gamma_1' & 0 \\ 0 & 0 & 0 & \infty \end{vmatrix}\tilde{S}-\tilde{\Sigma}\ , \tag{6}$$

and similarly for $\tilde{U}_{32}$, $\tilde{U}_{33}$, and $\tilde{U}_{34}$. $\tilde{U}_4$ is a matrix corresponding to the case of four hydrogen atoms present with probability x_4:

$$\tilde{U}_4 = \tilde{S}\begin{vmatrix} \gamma_1' & \gamma_2' & \gamma_2' & \gamma_2' \\ \gamma_2' & \gamma_1' & \gamma_2' & \gamma_2' \\ \gamma_2' & \gamma_2' & \gamma_1' & \gamma_2' \\ \gamma_2' & \gamma_2' & \gamma_2' & \gamma_1' \end{vmatrix}\tilde{S}-\tilde{\Sigma}\ . \tag{7}$$

The probability of occurrence of the configuration shown in Fig. 1(a) is denoted by $1-c$; the probability of the configuration of Fig. 1(b) is denoted by x_4. Obviously,

$$c = x_0 + x_1 + x_2 + x_3 + x_4\ . \tag{8}$$

In the case where there is no statistical correlation among hydrogens the probabilities x_l $(l=0,\ldots,4)$ can be expressed in terms of the quantity x, which is the ratio of the total number of hydrogens over the total number of lattice sites, and the quantity c:

$$x_l = c\frac{4!}{(4-l)!l!}\frac{x^l(4c-x)^{4-l}}{(4c)^4},\quad l=0,\ldots,4\ . \tag{9}$$

The case $x=4c$ represents the fully hydrogenated case where $x_4=c$ and $x_l=0$, $l=0,\ldots,3$; this is the case where the reconstruction effects are expected to be minimal and, consequently, our model to be more realistic.

Since the Green's function $\tilde{G}_e$ is a function of the self-energy $\tilde{\Sigma}$, the CPA condition [Eq. (1)] is very complicated to solve, even numerically. For this reason we have solved Eq. (1) for the limiting cases $x=0$ (no hydrogen) and $x=4c$ (all vacancies saturated by hydrogen). For $x=0$, Eq. (1) combined with Eq. (3) reduces to

$$(1-c)\tilde{U}_{\mathrm{Si}}(1-\tilde{G}_e\tilde{U}_{\mathrm{Si}})^{-1}-c\tilde{G}_e^{-1}=0\ . \tag{10}$$

Utilizing symmetry Eq. (10) results in the following two scalar equations:

$$\Sigma_s=\epsilon_s-c/G_{11}(E,\Sigma_s,\Sigma_p)\ ,$$
$$\Sigma_p=\epsilon_p-c/G_{22}(E,\Sigma_s,\Sigma_p)\ . \tag{11}$$

Equations (11) are solved simultaneously for Σ_s and Σ_p using a Newton-Raphson iterative procedure. The Brillouin-zone summation necessary in evaluating G_{11},G_{22} was done for 240 k points in the irreducible zone.

For $x=4c$, Eq. (1) reduces to the following expressions:

$$G_{11}\Sigma_s^2+(1-\epsilon_sG_{11}-\epsilon_s'G_{11})\Sigma_s-c(\epsilon_s'-\epsilon_s)-\epsilon_s+\epsilon_s\epsilon_s'G_{11}=0\ , \tag{12}$$
$$G_{22}\Sigma_p^2+(1-\epsilon_pG_{22}-\epsilon_p'G_{22})\Sigma_p-c(\epsilon_p'-\epsilon_p)-\epsilon_p+\epsilon_p\epsilon_p'G_{22}=0\ ,$$

where $\epsilon_s'=E_{s,s}'(000)=-8.72$ eV and $\epsilon_p'=E_{x,x}'(000)=-1.6$ eV are the effective H-H matrix elements (Appendix). Equations (12) are also solved for Σ_s and Σ_p by iteration. Since both sets of Eqs. (11) and (12) are complex, we found it computationally efficient to separate them into their real and imaginary parts and do the computer code in real arithmetic.

For the intermediate values of x, we have employed an average t-matrix approximation (ATA) instead of the CPA. We have done this to simplify the computational effort since the additional errors are small, and because the cases with $x<4c$ are not very realistic due to the reconstruction that takes place. The ATA-like approximation used for $0<x<4c$ is the following. We define $\Sigma_i(E;x)$ $i=s,p$ by the relation

$$\Sigma_i(E;x)=\left(1-\frac{x}{4c}\right)\Sigma_i(E;0)+\frac{x}{4c}\Sigma_i(E;4c)\ , \tag{13}$$

where $\Sigma_i(E;0)$ and $\Sigma_i(E;4c)$ have been obtained from the CPA described above.

Having determined Σ_s and Σ_p [using the CPA condition (1) for the cases $x=0,4c$ and Eq. (13) for $x\neq 0,4c$] we can obtian $\tilde{G}_e(E)$; then in all cases the DOS is given from the following expressions:

$$N_{\mathrm{Si}}=\frac{(1-c)}{\pi}\{-\mathrm{Im\ Tr}[(1-\tilde{G}_e\tilde{U}_{\mathrm{Si}})^{-1}\tilde{G}_e]\}\ ,$$
$$N_{\mathrm{H}}=\frac{x_1}{4\pi}\sum_{i=1}^{4}\{-\mathrm{Im\ Tr}[(1-\tilde{G}_e\tilde{U}_{1i})^{-1}\tilde{G}_e]\}+\frac{x_2}{6\pi}\sum_{i=1}^{6}\{-\mathrm{Im\ Tr}[(1-\tilde{G}_e\tilde{U}_{2i})^{-1}\tilde{G}_e]\}$$
$$+\frac{x_3}{4\pi}\sum_{i=1}^{4}\{-\mathrm{Im\ Tr}[(1-\tilde{G}_e\tilde{U}_{3i})^{-1}\tilde{G}_e]\}+\frac{x_4}{\pi}\{-\mathrm{Im\ Tr}[(1-\tilde{G}_e\tilde{U}_4)^{-1}\tilde{G}_e]\}\ , \tag{14}$$

where the notation is the same as that of Eq. (1).

In the special case of the fully saturated vacancy, i.e., $x=4c$, $x_4=c$, and $x_1=x_2=x_3=x_v=0$, the above Eqs. (14) become

$$N_{\mathrm{Si}}=-\frac{1}{\pi}\mathrm{Im\ Tr}\left[(\tilde{\Sigma}-\tilde{\epsilon}_{\mathrm{H}})\frac{1}{\epsilon_{\mathrm{Si}}-\tilde{\epsilon}_{\mathrm{H}}}\tilde{G}_e\right]\ , \tag{15}$$

$$N_{\mathrm{H}}=-\frac{1}{\pi}\mathrm{Im\ Tr}\left[(\tilde{\Sigma}-\tilde{\epsilon}_{\mathrm{Si}})\frac{1}{\epsilon_{\mathrm{H}}-\tilde{\epsilon}_{\mathrm{Si}}}\tilde{G}_e\right]\ .$$

These equations can be further reduced to give the s- and p-like components of the DOS. The total DOS is of course the sum of N_{Si} and N_{H}. The CPA, as described above, treats the diagonal disorder. The inclusion of off-diagonal disorder in the

TB-CPA is computationally very complicated and at present there is no established "best" technique.

In our calculations, the off-diagonal disorder was treated within the virtual crystal approximation (VCA), i.e., the nearest-neighbor matrix elements were replaced by their averaged values:

$$E_{i,j}(\tfrac{1}{2}\tfrac{1}{2}\tfrac{1}{2}) = \left[1-\frac{x}{2}\right] E_{i,j}^{\text{Si-Si}}(\tfrac{1}{2}\tfrac{1}{2}\tfrac{1}{2}) + \frac{x}{2} E_{i,j}^{\text{Si-H}}(\tfrac{1}{2}\tfrac{1}{2}\tfrac{1}{2})$$

$$i,j = s,x,y,z \ . \quad (16)$$

The VCA is a good approximation if the difference between the Si-Si and the Si-H matrix elements is small in comparison to their average value. This condition is not satisfied for all matrix elements and so there is a need here for improving our present calculational techniques. Given, however, the complexity of introducing off-diagonal disorder in the CPA and that there are already other uncertainties in our model, we decided in the present stage to work with the VCA for the off-diagonal disorder. We have used the simple CPA (no cluster extensions) and have assumed that there is no statistical correlation among the various configurations discussed before. At this point we must note that it has been proposed that vacancies [see Fig. 1(b)] tend to cluster together as to form microvoids and internal surfaces.[13,39] We have found that this clustering effect effectively reduces the value of c and tends to create some internal surface states which make a small contribution to the total DOS. Thus the vacancy clustering effects can easily be incorporated in our model by appropriately reducing the value of c. Let us add that in the presence of adequate hydrogen during the growth process this clustering effect may not occur.

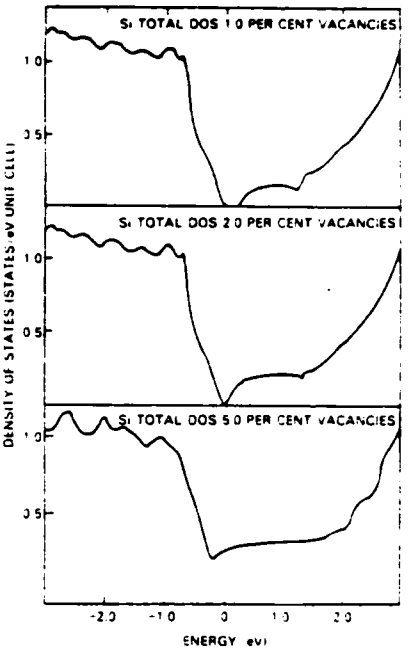

FIG. 2. CPA densities of states in the gap region for the Si vacancy case for different vacancy concentrations.

IV. RESULTS AND DISCUSSION

In Fig. 2 we show the DOS in the gap region for the configuration Si and vacancies with no hydrogen introduced yet. We note the appearance of dangling-bond states in the gap. The density of these states increases with vacancy concentration c. Also the gap becomes smaller with increasing c until it is completely filled. It is also interesting to note that the gap states have as their center of gravity the position of the bound state (0.75 eV) of the ideal single vacancy.[20–22] It should be stressed here that the results of Fig. 2 are useful in demonstrating qualitatively the existence of dangling-bond states in the gap. However, due to the omission of the effects of reconstruction, we certainly overestimate the number of these states and, therefore, we don't attempt any quantitative comparison with experiment.

Figure 3 deals with the restoration of the band gap upon hydrogenation. Figure 3 corresponds to $c = 0.05$ and $0 \le x \le 4c$. It is evident that by in-

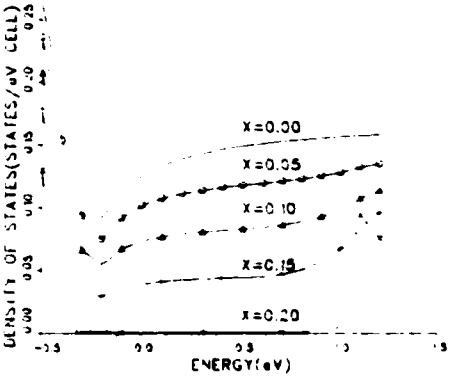

FIG. 3. Densities of states of SiH_x in the gap region for different hydrogen concentrations (x, $c = 0.05$).

creasing the hydrogen content x, the states in the gap are reduced until they are completely eliminated for the fully hydrogen-saturated-vacancy case ($x=0.20$). This is, of course, what the experimental situation is and the reason why a-Si:H has semiconducting properties similar to those of crystalline Si.

In Fig. 4 we show the DOS of Si-H (with $c=0.05$ and $x=0.20$) for the whole spectrum, including both the valence and conduction bands. We note first a band gap $E_g=1.4$ eV that is wider by 0.4 eV than the corresponding $E_g=1.0$ eV which our tight-binding Hamiltonian gives for the nonhydrogenated case. This widening of the gap is due to a narrowing of the third DOS peak at the top of the valence band. We have identified this to be the result of a decrease of the difference: $E_{x,y}(\frac{1}{2}\frac{1}{2}\frac{1}{2})-E_{x,x}(\frac{1}{2}\frac{1}{2}\frac{1}{2})$, which is a measure of the $pp\pi$ interaction. This recession of the valence band by 0.4 eV is in excellent agreement with the photoemission experiments of von Roedern *et al.*[9] Figure 4 also shows the DOS decomposed by site. The hydrogen-site DOS shows pronounced peaks at 5.2, 7.6, and 13.5 eV below the Fermi level. Comparison with photoemission data is more appropriately done after smoothing the H-site DOS

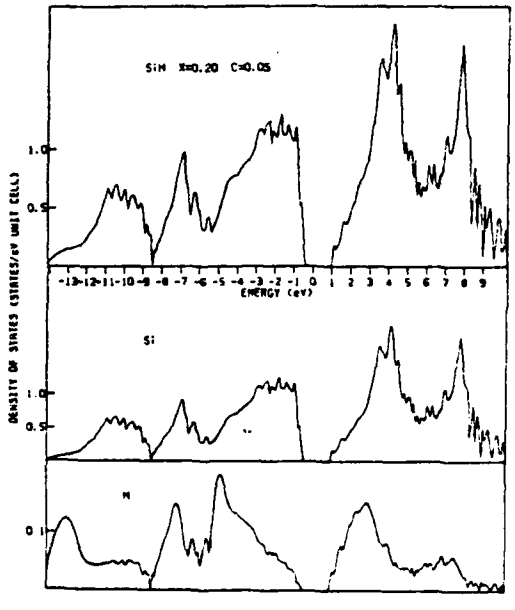

FIG. 4. Total and site-decomposed densities of states for SiH_x with $x=0.2$. Note that the Si and H DOS are multipled by $(1-c)$ and c, respectively ($c=0.05$). The Fermi level is located in the middle of the gap.

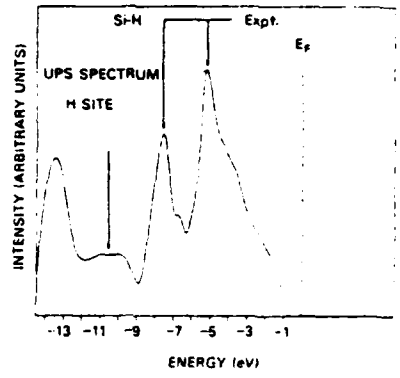

FIG. 5. Broadened H-site density of states. The arrows indicate the peak positions from the photoemission measurements (Ref. 9).

by applying a Lorentzian broadening. This is plotted in Fig. 5 which shows that the 5.2 and 7.6 eV peaks are predicted in almost exactly the same position found in the measurements.[9] The 13.5 eV peak is not seen experimentally for reasons we do not understand.

The widening of the band gap has been demonstrated experimentally by a variety of experimental techniques.[6-8] To compare with these experiments, we have performed a calculation of the joint DOS $N^J(E)$. The calculated $[N^J(E)]^{1/2}$ is assumed to be proportional to the measured quantity $(\alpha E)^{1/2}$, where α is the absorption coefficient. A comparison with the measurements of Cody *et al.*[7] is shown in Fig. 6, where $[N^J(E)]^{1/2}$ has been normalized to the value of $(\alpha E)^{1/2}$ at $E=4$ eV. The experimental graph was obtained at approximately

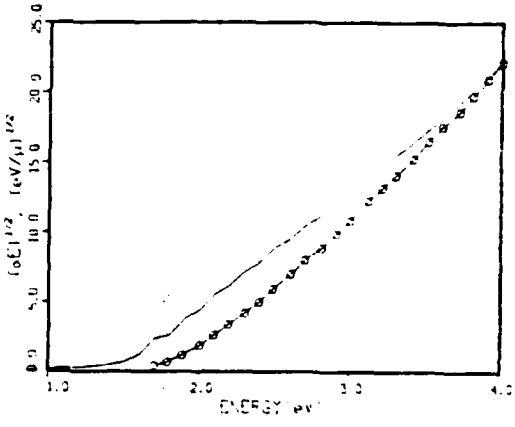

FIG. 6. Plot of the square root of the joint density of states versus energy. The line joining the open circles represents the measured quantity $(\alpha E)^{1/2}$ (Ref. 7).

16% hydrogen content, while the theoretical graph corresponds to 20%. Despite this and the fact that the theory predicts a smaller gap the overall agreement is rather good.

Our calculations can also be used to compare with Auger and soft-x-ray-emission measurements.[40] We present in Fig. 7 a decomposition of the Si-site DOS of SiH in its s and p components. The s-like and p-like DOS are proportional to the K and L spectra, respectively.

We now turn to a discussion of hydrogen-induced antibonding states at the bottom of the conduction band. Let us first examine the case of a single configuration of the kind shown in Fig. 1(b) embedded in a Si lattice.

The bound states around this four-hydrogen cluster will be given by

$$G_{11}(E)=\frac{1}{E'_{ss}(000)-E_{ss}(000)}\ , \tag{17a}$$

$$G_{22}(E)=\frac{1}{E'_{xx}(000)-E_{xx}(000)}\ . \tag{17b}$$

The graphical solution of Eq. (17a) is shown in Fig. 8. As we see from Fig. 8, there is no real solution of Eq. (17a) because the intersection of $\mathrm{Re}G$ with $1/E'-E$ occurs within the band where $\mathrm{Im}G\neq 0$. On the other hand, this intersection occurs near the bottom of the conduction band (CB). The physical meaning of no real intersection is that there are no true bound states associated with the four-hydrogen cluster embedded in a Si lattice. The fact that the intersection occurs near the bottom of the CB where $\mathrm{Im}G$ is very small means, physically, that the four-hydrogen cluster creates resonance s states i.e., states where the wave function has a peak around the cluster. These resonance states can be viewed as a hybridization of the Si-H s-antibonding states with the regular Si states at the bottom of the conduction band. Such resonance states are associated with a lower than the regular CB mobility (because the electron is almost trapped around the hydrogen). Evaluation of Eq. (17b) showed neither bound states of p character nor any resonance states below 3 eV.

The suggestion of Moustakas *et al.*,[10] born out of their photoconductivity measurements that Si-H antibonding states form at the bottom of the conduction band, is strongly supported by the present calculations. This is shown in Fig. 9 where we have plotted the ratio N_H/N_t as a function of E. Indeed, this graph, in addition to the peaks in the valence band that we have already discussed, shows a pronounced maximum at the bottom of the CB indicating strong H participation in the formation of these states.

Finally, we will discuss the variation of the gap size E_g with hydrogen content x. We define the Fermi level $E_F=(E_c+E_v)/2$ where E_v is the top of the valence band and E_c the bottom of the con-

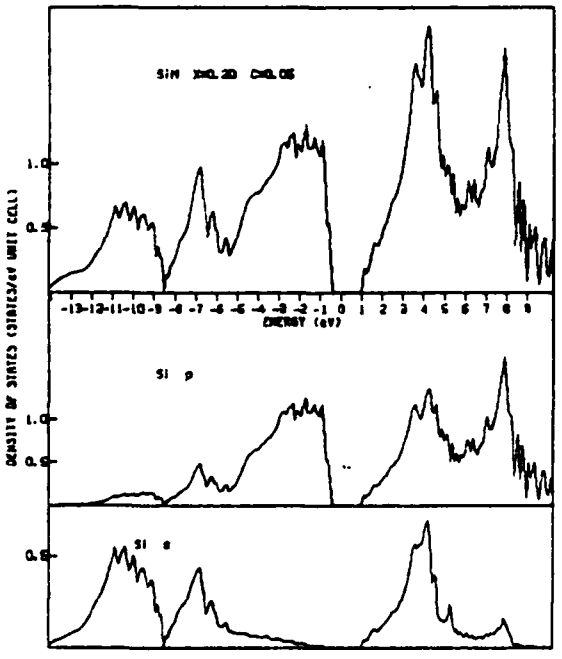

FIG. 7. Si-site density of states and its s- and p-like components.

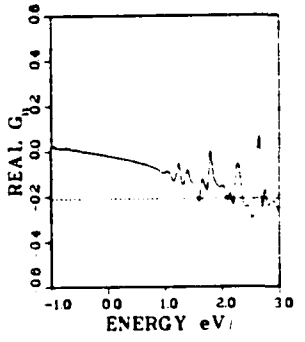

FIG. 8. The real part of the s-like Green's function plotted as a function of energy for the case of the single impurity that consists of four hydrogen atoms. The dotted line indicates the value of the right-hand side of Eq. (17a).

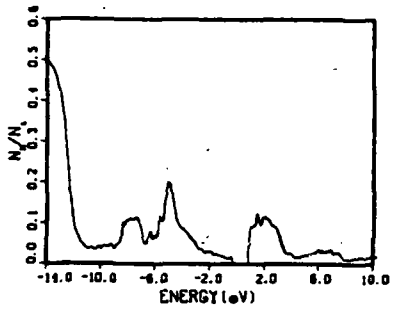

FIG. 9. Ratio of H-site density of states N_H to the total density of states N_t for SiH ($x=0.2$).

duction band. The variation of E_v, E_c, and E_F with x is shown in Fig. 10, where in all cases we are dealing with vacancies fully saturated by hydrogen, i.e., $x=4c$. We note first that E_c is essentially constant. This is due to a cancellation of the effects of disorder (tends to push E_c down) by the effect of a stronger Si—H bond (tends to push E_c up) as manifested by the larger value of the parameter γ_3 (see Appendix) in SiH_x. E_v depends mainly on the matrix element difference $\gamma_6-\gamma_5$ or equivalently $E_{x,y}(\frac{1}{2}\frac{1}{2}\frac{1}{2})-E_{z,z}(\frac{1}{2}\frac{1}{2}\frac{1}{2})$ which is a measure of the $pp\pi$ interaction. Hydrogen decreases $\gamma_6-\gamma_5$ and so pushes E_v down and widens the gap. As a result E_F is also pushed down.

Our work shows that the size of the gap depends essentially on two parameters: the bond strength γ_3 and the $pp\pi$ interaction $\gamma_6-\gamma_5$. Hydrogen incorporation effectively increases γ_3 and decreases $\gamma_6-\gamma_5$ thus producing a wider gap. This effect of hydrogenation on γ_3 and $\gamma_6-\gamma_5$, being essentially a local chemical effect, is expected to transcend the validity of our present model and thus constitutes a general feature of hydrogen incorporation in a Si tetrahedral structure.

In conclusion many important properties of fully hydrogenated a-Si (such as widening of the gap, Si-H bonding states, Si-H antibonding resonance states) depend mainly on the local chemical environment. Thus these properties are largely independent of the particular model, provided that it satisfactorily treats the limiting case of nonhydrogenated Si. Our present model satisfies these requirements (with the exception of the omission of topological disorder) and as a result we expect our main conclusions to have a much wider validity than the model itself.

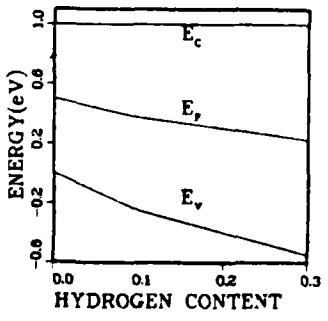

FIG. 10. Variation of the bottom of the conduction band E_c of the Fermi level E_F and the top of the valence band E_v versus hydrogen content for fully hydrogenated samples.

ACKNOWLEDGMENTS

We wish to thank Dr. W. E. Pickett, Dr. L. L Boyer, and Dr. B. M. Klein for many useful discussions and suggestions regarding the calculations. We also thank Dr. T. D. Moustakas, Dr. P. C. Taylor, and Professor W. Paul for discussions regarding the experimental situation. Technical assistance from Mrs. L. Blohm and Mr. A. Koppenhaver is gratefully acknowledged. This work was supported in part by the Solar Energy Research Institute via an interagency agreement between the U. S. Naval Research Laboratory and the U. S. Department of Energy.

APPENDIX: ESTIMATE OF HYDROGEN-HYDROGEN AND HYDROGEN-SILICON MATRIX ELEMENTS

For each Si we have the four orbitals $|s\rangle$, $|x\rangle$, $|y\rangle$, $|z\rangle$ or equivalently the four sp^3 hybridized orbitals shown in Fig. 1(a). The transformations from the one set to the other are the following:

$$\begin{pmatrix}|1\rangle\\|2\rangle\\|3\rangle\\|4\rangle\end{pmatrix}=S\begin{pmatrix}|s\rangle\\|x\rangle\\|y\rangle\\|z\rangle\end{pmatrix}, \tag{A1}$$

$$\begin{pmatrix}|s\rangle\\|x\rangle\\|y\rangle\\|z\rangle\end{pmatrix}=S\begin{pmatrix}|1\rangle\\|2\rangle\\|3\rangle\\|4\rangle\end{pmatrix}, \tag{A2}$$

for the Si at A. For the Si at B assuming that AB is along the 111 direction, we have

$$\begin{pmatrix} |5\rangle \\ |6\rangle \\ |7\rangle \\ |8\rangle \end{pmatrix} = \bar{S} \begin{pmatrix} |\bar{s}\rangle \\ |\bar{x}\rangle \\ |\bar{y}\rangle \\ |\bar{z}\rangle \end{pmatrix}, \tag{A3}$$

$$\begin{pmatrix} |\bar{s}\rangle \\ |\bar{x}\rangle \\ |\bar{y}\rangle \\ |\bar{z}\rangle \end{pmatrix} = \bar{S}^T \begin{pmatrix} |5\rangle \\ |6\rangle \\ |7\rangle \\ |8\rangle \end{pmatrix}, \tag{A4}$$

where $\bar{S}^T$ is the transposed matrix of $\bar{S}$. The 4×4 matrices S and $\bar{S}$ are given by

$$S = \frac{1}{2} \begin{pmatrix} 1 & 1 & 1 & 1 \\ 1 & 1 & -1 & -1 \\ 1 & -1 & 1 & -1 \\ 1 & -1 & -1 & 1 \end{pmatrix}, \tag{A5}$$

$$\bar{S} = \frac{1}{2} \begin{pmatrix} 1 & -1 & -1 & -1 \\ 1 & -1 & 1 & 1 \\ 1 & 1 & -1 & 1 \\ 1 & 1 & 1 & -1 \end{pmatrix}. \tag{A6}$$

Following the SK notation, the diagonal and nearest-neighbor matrix elements of the Hamiltonian in the $|s\rangle, |x\rangle, |y\rangle, |z\rangle$ representation are denoted as follows:

$$E_{s,s}(000) = \langle s | H | s \rangle , \tag{A7}$$

$$E_{x,x}(000) = \langle x | H | x \rangle = \langle y | H | y \rangle = \langle z | H | z \rangle , \tag{A8}$$

$$E_{s,s}(\tfrac{1}{2}\tfrac{1}{2}\tfrac{1}{2}) = \langle s | H | \bar{s} \rangle , \tag{A9}$$

$$E_{s,x}(\tfrac{1}{2}\tfrac{1}{2}\tfrac{1}{2}) = \langle \bar{x} | H | s \rangle = -\langle \bar{s} | H | x \rangle = \langle \bar{y} | H | s \rangle = \cdots , \tag{A10}$$

$$E_{x,x}(\tfrac{1}{2}\tfrac{1}{2}\tfrac{1}{2}) = \langle \bar{x} | H | x \rangle = \langle \bar{y} | H | y \rangle = \langle \bar{z} | H | z \rangle , \tag{A11}$$

$$E_{x,y}(\tfrac{1}{2}\tfrac{1}{2}\tfrac{1}{2}) = \langle \bar{x} | H | y \rangle = \langle \bar{x} | H | z \rangle = \langle \bar{y} | H | x \rangle = \langle \bar{y} | H | z \rangle = \cdots . \tag{A12}$$

Hirabayashi[41] has written the matrix elements of H in the hybrid representation as follows:

$$\gamma_1 = \langle 1 | H | 1 \rangle , \tag{A13}$$

$$\gamma_2 = \langle 1 | H | 2 \rangle , \tag{A14}$$

$$\gamma_3 = \langle 5 | H | 1 \rangle , \tag{A15}$$

$$\gamma_4 = \langle 6 | H | 1 \rangle , \tag{A16}$$

$$\gamma_5 = \langle 6 | H | 3 \rangle , \tag{A17}$$

$$\gamma_6 = \langle 6 | H | 2 \rangle , \tag{A18}$$

where the orbitals $|6\rangle$ and $|2\rangle$ are along antiparallel directions.

Using Eqs. (A1) and (A2) one easily expresses the γ's in terms of the E's and vice versa. We have

$$\gamma_1 = \tfrac{1}{4}[E_{s,s}(000) + 3E_{x,x}(000)] , \tag{A19}$$

$$\gamma_2 = \tfrac{1}{4}[E_{s,s}(000) - E_{x,x}(000)] , \tag{A20}$$

$$\gamma_3 = \tfrac{1}{4}[E_{s,s}(\tfrac{1}{2}\tfrac{1}{2}\tfrac{1}{2}) - 6E_{s,x}(\tfrac{1}{2}\tfrac{1}{2}\tfrac{1}{2}) - 3E_{x,x}(\tfrac{1}{2}\tfrac{1}{2}\tfrac{1}{2}) - 6E_{x,y}(\tfrac{1}{2}\tfrac{1}{2}\tfrac{1}{2})] , \tag{A21}$$

$$\gamma_4 = \tfrac{1}{4}[E_{s,s}(\tfrac{1}{2}\tfrac{1}{2}\tfrac{1}{2}) - 2E_{s,x}(\tfrac{1}{2}\tfrac{1}{2}\tfrac{1}{2}) + E_{x,x}(\tfrac{1}{2}\tfrac{1}{2}\tfrac{1}{2}) + 2E_{x,y}(\tfrac{1}{2}\tfrac{1}{2}\tfrac{1}{2})] , \tag{A22}$$

$$\gamma_5 = \tfrac{1}{4}[E_{s,s}(\tfrac{1}{2}\tfrac{1}{2}\tfrac{1}{2}) + 2E_{s,x}(\tfrac{1}{2}\tfrac{1}{2}\tfrac{1}{2}) + E_{x,x}(\tfrac{1}{2}\tfrac{1}{2}\tfrac{1}{2}) - 2E_{x,y}(\tfrac{1}{2}\tfrac{1}{2}\tfrac{1}{2})] , \tag{A23}$$

$$\gamma_6 = \tfrac{1}{4}[E_{s,s}(\tfrac{1}{2}\tfrac{1}{2}\tfrac{1}{2}) + 2E_{s,x}(\tfrac{1}{2}\tfrac{1}{2}\tfrac{1}{2}) - 3E_{x,x}(\tfrac{1}{2}\tfrac{1}{2}\tfrac{1}{2}) + 2E_{x,y}(\tfrac{1}{2}\tfrac{1}{2}\tfrac{1}{2})] , \tag{A24}$$

$$E_{s,s}(000) = \gamma_1 + 3\gamma_2 , \tag{A25}$$

$$E_{x,x}(000) = \gamma_1 - \gamma_2 , \tag{A26}$$

$$E_{s,s}(\tfrac{1}{2}\tfrac{1}{2}\tfrac{1}{2}) = \tfrac{1}{4}(\gamma_3 + 6\gamma_4 + 6\gamma_5 + 3\gamma_6) , \tag{A27}$$

$$E_{s,x}(\tfrac{1}{2}\tfrac{1}{2}\tfrac{1}{2}) = \tfrac{1}{4}(-\gamma_3 - 2\gamma_4 + 2\gamma_5 + \gamma_6) . \tag{A28}$$

$$E_{x,x}(\tfrac{1}{2}\tfrac{1}{2}\tfrac{1}{2}) = \tfrac{1}{4}(-\gamma_3 + 2\gamma_4 + 2\gamma_5 - 3\gamma_6) , \tag{A29}$$

$$E_{x,y}(\tfrac{1}{2}\tfrac{1}{2}\tfrac{1}{2}) = \tfrac{1}{4}(-\gamma_3 + 2\gamma_4 - 2\gamma_5 + \gamma_6) . \tag{A30}$$

In Fig. 1(b) the Si at A has been removed and four hydrogens have been placed as shown, in order to passivate the Si dangling bonds. Charge-density contours resulting from the pseudopotential supercell calculation of Pickett[35] involving the configuration shown in Fig. 1(b), demonstrate that there are hydrogen p and even d components in the eigenfunction. Furthermore, these charge-density contours strongly suggest that this multiple l hydrogen state can be approximated by an s-only or-

bital which is displaced towards the Si site by about 20% as shown in Fig. 1(b). If $0_{1'}$, $0_{2'}$, $0_{3'}$, and $0_{4'}$ are the positions of the centers of the displaced hydrogen s orbitals $|1'\rangle$, $|2'\rangle$, $|3'\rangle$, and $|4'\rangle$, respectively, the distances are as follows: $B0_{1'}=2.30$ a.u., $B0_{2'}=5.18$ a.u., $0_{1'}0_{2'}=3.50$ a.u.

Comparing Figs. 1(a) and 1(b) we can see that the role of the four sp^3 hybrids $|1\rangle$ to $|4\rangle$ is played by the four orbitals $|1'\rangle$ to $|4'\rangle$. The result of this replacement is to change the $\gamma_1,\gamma_2,\ldots,\gamma_6$ to $\gamma'_1,\ldots,\gamma'_6$ given by

$$\gamma'_1=\langle 1'|H|1'\rangle\ , \tag{A31}$$

$$\gamma'_2=\langle 1'|H|2'\rangle\ , \tag{A32}$$

$$\gamma'_3=\langle 5|H|1'\rangle\ , \tag{A33}$$

$$\gamma'_{4(1)}=\langle 6|H|1'\rangle\ , \tag{A34}$$

$$\gamma'_{4(2)}=\langle 5|H|2'\rangle\ , \tag{A35}$$

$$\gamma'_5=\langle 6|H|3'\rangle\ , \tag{A36}$$

$$\gamma'_6=\langle 6|H|2'\rangle\ . \tag{A37}$$

A complication associated with the configuration of Fig. 1(b) is that $\gamma'_{4(1)}$ and $\gamma'_{4(2)}$ are not necessarily equal as in the configuration of Fig. 1(a). However, as we shall see below the difference between $\gamma'_{4(1)}$ and $\gamma'_{4(2)}$ turns out to be small, thus we can replace these matrix elements by their mean value, i.e.,

$$\gamma'_4=\frac{\gamma'_{4(1)}+\gamma'_{4(2)}}{2}\ . \tag{A38}$$

Before we proceed with the estimation of the values of the γ''s we mention that we can introduce fictitious s and p orbitals $|s'\rangle,|x'\rangle,|y'\rangle,|z'\rangle$ associated with four hydrogens of Fig. 1(b) through the relation

$$\begin{pmatrix}|s'\rangle\\|x'\rangle\\|y'\rangle\\|z'\rangle\end{pmatrix}=S\begin{pmatrix}|1'\rangle\\|2'\rangle\\|3'\rangle\\|4'\rangle\end{pmatrix}\ . \tag{A39}$$

These orbitals allow us to define hydrogen associated E''s by replacing in Eqs. (A7)–(A12) the $|s\rangle,|x\rangle,|y\rangle,|z\rangle$ by $|s'\rangle,|x'\rangle,|y'\rangle,|z'\rangle$. Because the transformation in Eq. (A39) is identical to that in Eq. (A2), it follows that the E''s are given in terms of γ''s as in Eqs. (A25) and (A30). Thus the removal of a Si and the placement of four hydrogens as shown in Fig. 1(b) is equivalent to changing the six matrix elements E's to the new values E''s. Actually, the second- and third-nearest-neighbor matrix elements should be modified as well. These modifications are difficult to estimate and are not expected to be as important as the changes in the diagonal and nearest-neighbor matrix elements. For these reasons we have omitted these modifications.

We now proceed to estimate the γ''s. The quantity γ'_1 is taken equal to its value in the SiH_4 molecule[42]

$$\gamma'_1=-3.38\ \text{eV}\ . \tag{A40}$$

To estimate γ'_2 we need to obtain the off-diagonal matrix element between the orthogonalized hydrogenic wave functions associated with the configuration shown in Fig. 1(b). Mattheiss[43] has examined this problem in detail for a system of six hydrogens placed in the corners of a canonical hexagon. We think that the nearest-neighbor matrix elements do not depend so sensitively on the geometry and consequently Mattheiss's results can be used to obtain a fair estimate of γ. We have fitted Mattheiss's results for separations $R=2$, 3, 5 a.u. with a quadratic function times the exponential function $[\exp(-R)]$. We found from this fitting that

$$\gamma'_2=-27.07(1.491-0.072R+0.077R^2)e^{-R} \tag{A41}$$

in units of eV which for $R=3.5$ a.u. gives

$$\gamma'_2=-1.78\ \text{eV}\ . \tag{A42}$$

To obtain γ'_3 we shall write it by employing Eq. (A3) as follows:

$$\gamma'_3=\tfrac{1}{7}(\langle\bar{s}|H|1'\rangle-3\langle\bar{x}|H|1'\rangle)\ . \tag{A43}$$

Chadi[44] has found that the nonorthogonalized orbital $|\bar{s}_n\rangle$ to which $|\bar{s}\rangle$ reduces as the overlap goes goes to zero is proportional to $R\exp(-1.04R)$. The fact that this s Si decays almost exactly like a hydrogen s orbital suggests that Eq. (A41) may be used to obtain $\langle\bar{s}|H|1'\rangle$. However, the extra factor of R in $|\bar{s}_n\rangle$ would cause the matrix element to decay more slowly than the right-hand side of Eq. (A41). To take this into account we write, in eV

$$\langle\bar{s}|H|1'\rangle=-\frac{V_{\text{Si-H}}}{V_{\text{H-H}}}27.07(1.491-0.072R+0.077R^2)e^{-R}\ , \tag{A44}$$

where

$$V_{\text{Si-H}} = -\left[(\sqrt{3}/4+1\sqrt{3})(1+R) + \frac{R^2}{3\sqrt{3}}(2+R/4)\right]\exp(-R)$$

is the off-diagonal matrix element between $\exp(-R)$ and $R\exp(-R)$ and

$$V_{\text{H-H}} = -(1.5+1.5R+R^2/6)\exp(-R)$$

is the same matrix element between two hydrogenic wave functions. To check the accuracy of Eq. (A44) we substitute for R the Si—H distance in SiH_4 ($R=2.8$ a.u.) and we obtain -3.58 eV. This is in surprisingly good agreement with the established[42] value of -3.57 eV. To obtain $\langle \bar{x} \mid H \mid 1' \rangle$ we take into account that the nonorthogonalized $\mid \bar{x}_n \rangle$ is proportional to $x \mid \bar{s}_n \rangle$. Hence it is plausible to write

$$\langle \bar{x} \mid H \mid 1' \rangle = -cR_x \langle \bar{s} \mid H \mid 1' \rangle , \tag{A45}$$

where R_x is the x component of the vector $0_1 \cdot B$, and the constant c can be determined from the known values of $\langle \bar{x} \mid H \mid 1' \rangle$ and $\langle \bar{s} \mid H \mid 1' \rangle$ for the SiH_4 molecule.[42] We found $c \approx \frac{1}{3}$. Substituting in Eqs. (A44) and (A45) the values $R = 0_1 \cdot B = 2.3$ a.u. and $R_x = 1.33$ a.u., we obtain $\langle \bar{s} \mid H \mid 1' \rangle = -4.85$ eV and $\langle \bar{x} \mid H \mid 1' \rangle = 2.15$ eV. Thus,

$$\gamma'_3 = -5.65 \text{ eV} . \tag{A46}$$

The quantity $\gamma'_{4(1)}$ can be written, by employing Eq. (A3), as

$$\gamma'_{4(1)} = \tfrac{1}{2}(\langle \bar{s} \mid H \mid 1' \rangle + \langle \bar{x} \mid H \mid 1' \rangle) = -1.35 \text{ eV} . \tag{A47}$$

By employing Eq. (A3) we can rewrite the rest of the γ''s as follows:

$$\gamma'_{4(2)} = \tfrac{1}{2}(\langle \bar{s} \mid H \mid 2' \rangle - \langle \bar{x} \mid H \mid 2' \rangle - \langle \bar{y} \mid H \mid 2' \rangle - \langle \bar{z} \mid H \mid 2' \rangle) , \tag{A48}$$

$$\gamma'_5 = \tfrac{1}{2}(\langle \bar{s} \mid H \mid 3' \rangle - \langle \bar{x} \mid H \mid 3' \rangle + \langle \bar{y} \mid H \mid 3' \rangle + \langle \bar{z} \mid H \mid 3' \rangle) , \tag{A49}$$

$$\gamma'_6 = \tfrac{1}{2}(\langle \bar{s} \mid H \mid 2' \rangle - \langle \bar{x} \mid H \mid 2' \rangle + \langle \bar{y} \mid H \mid 2' \rangle + \langle \bar{z} \mid H \mid 2' \rangle) . \tag{A50}$$

One may attempt to calculate the matrix elements in the right-hand side of Eqs. (A48)—(A50) by using Eqs. (A44) and (A45). However, Eq. (A44) will overestimate the size of the $(\langle \bar{s} \mid H \mid 2' \rangle)$ matrix element because of the presence of the hydrogen at 1′ which represents an effective repulsive potential. In Mattheiss's[43] calculation this reduction of the next-nearest-neighbor transfer matrix element is so large that the matrix element becomes almost zero (actually it changes sign and is positive). In the present case, due to the fact that the hydrogen 1′ is closer to Si and that there is the extra R factor in the Si wave function, one expects a smaller reduction of about 50% assuming that only half the space, i.e., the region around the hydrogen at 2′ would contribute to the integral. This crude reasoning suggests that $\langle \bar{s} \mid H \mid 2' \rangle$ is roughly half the value given by Eq. (A44), i.e.,

$$\langle \bar{s} \mid H \mid 2' \rangle = -0.42 \text{ eV} . \tag{A51}$$

The other matrix elements entering Eqs. (A48)—(A50) can be estimated by employing Eq. (A45) and the fact that the vector $2'B$ and $3'B$ are (1.327, 3.799, 3.799) and (3.799, 1.327, 3.799), respectively. We obtain thus

$$\langle \bar{y} \mid H \mid 3' \rangle = \langle \bar{x} \mid H \mid 2' \rangle = 0.19 \text{ eV} , \tag{A52}$$

$$\langle \bar{x} \mid H \mid 3' \rangle = \langle \bar{z} \mid H \mid 3' \rangle = \langle \bar{y} \mid H \mid 2' \rangle = \langle \bar{z} \mid H \mid 2' \rangle = 0.53 \text{ ev} , \tag{A53}$$

which give

$$\gamma'_{4(2)} = -0.84 \text{ eV} , \tag{A54}$$

$$\gamma'_5 = -0.11 \text{ eV} , \tag{A55}$$

$$\gamma'_6 = 0.23 \text{ eV} . \tag{A56}$$

Using Eq. (A38) we obtain for γ'_4

$$\gamma'_4 = -1.10 \text{ eV} . \tag{A57}$$

The corresponding E''s are obtained from Eqs. (A25)—(A30),

$$E'_{s,s}(000) = -8.72 \text{ eV} ,$$

$$E'_{x,x}(000) = -1.60 \text{ eV} ,$$

$$E'_{s,s}(\tfrac{1}{2}\tfrac{1}{2}\tfrac{1}{2}) = -3.05 \text{ eV} ,$$

$$E'_{s,x}(\tfrac{1}{2}\tfrac{1}{2}\tfrac{1}{2}) = 1.96 \text{ eV} ,$$

$$E'_{x,x}(\tfrac{1}{2}\tfrac{1}{2}\tfrac{1}{2}) = 0.64 \text{ eV} ,$$

$$E'_{x,y}(\tfrac{1}{2}\tfrac{1}{2}\tfrac{1}{2}) = 0.98 \text{ eV} .$$

[1]W. E. Spear and P. G. LeComber, Solid State Commun. 17, 1193 (1975).
[2]W. Paul, A. J. Lewis, G. A. N. Connell, and T. D. Moustakas, Solid State Commun. 20, 969 (1976).
[3]T. D. Moustakas, J. Electron. Mater. 8, 391 (1979).
[4]H. Fritzsche, Sol. Energy Mater. 3, 447 (1980).
[5]T. Tiedje, T. D. Moustakas, and J. M. Cebulka, Phys. Rev. B 23, 5634 (1981).
[6]E. C. Freeman and W. Paul, Phys. Rev. B 20, 716 (1979).
[7]G. D. Cody, C. R. Wronski, B. Abeles, R. B. Stephens, and B. Brooks, Sol. Cells 2, 227 (1980).
[8]N. B. Goodman, H. Fritzsche, and H. Ozaki, J. Non-Cryst. Solids 35–36, 599 (1980).
[9]B. von Roedern, L. Ley, and M. Cardona, Phys. Rev. Lett. 39, 1576 (1977); B. von Roedern, L. Ley, M. Cardona, and F. W. Smith, Philos. Mag. B40, 433 (1970).
[10]T. D. Moustakas, D. A. Anderson, W. Paul, Solid State Commun. 23, 155 (1977).
[11]M. H. Brodsky, M. Cardona, and J. J. Cuomo, Phys. Rev. B 16, 3556 (1977).
[12]J. C. Knights, G. Lucovsky, and R. J. Nemanich, Philos. Mag. B37, 467 (1978).
[13]W. E. Carlos and P. C. Taylor, Phys. Rev. Lett. 45, 358 (1980).
[14]P. D'Antonio and J. H. Konnert, Phys. Rev. Lett. 43, 1161 (1979).
[15]H. J. Stein, Phys. Rev. Lett. 43, 1030 (1979).
[16]T. A. Postol, C. M. Falco, R. T. Kampwirth, I. K. Schuller, and W. B. Yelon, Phys. Rev. Lett. 45, 648 (1980).
[17]W. E. Spear, Adv. Phys. 26, 811 (1977).
[18]J. C. Phillips, Phys. Rev. Lett. 42, 1151 (1979).
[19]D. Alder, Phys. Rev. Lett. 41, 1755 (1978).
[20]G. A. Baraff and M. Schlüter, Phys. Rev. Lett. 41 892 (1978); Phys. Rev. B 19, 4965 (1978).
[21]J. Bernholc, N. O. Lipari, and S. T. Pantelides, Phys. Rev. Lett. 41, 895 (1978); Phys. Rev. B 21, 3545 (1980).
[22]D. A. Papaconstantopoulos and E. N. Economou, Phys. Rev. B 22, 2903 (1980).
[23]E. N. Economou and D. A. Papaconstantopoulos, Phys. Rev. B 23, 2042 (1981).
[24]D. A. Papaconstantopoulos and E. N. Economou, *Tetrahedrally Bonded Amorphous Semiconductors*, edited by R. A. Street, D. K. Biegelsen, and J. C. Knights (American Institute of Physics, New York, 1981), p. 130.
[25]W. Y. Ching, D. J. Lam, and C. C. Lin, Phys. Rev. Lett. 42, 805 (1979); Phys. Rev. B 21, 2378 (1980).
[26]L. Guttman, W. Y. Ching, and J. Rath, Phys. Rev. Lett. 44, 1513 (1980).
[27]M. H. Cohen, J. Singh, and F. Yonezawa, J. Non-Cryst. Solids 35–36, 55 (1980).
[28]D. C. Allan and J. D. Joannopoulos, Phys. Rev. Lett. 44, 43 (1980); J. D. Joannopoulos, J. Non-Cryst. Solids 35–36, 781 (1980).
[29]G. D. Watkins, *International Conference on Lattice Defects in Semiconductors, Frieburg, Germany, 1974* (Institute of Physics, London, 1975), p. 1.
[30]G. A. Baraff, E. O. Kane, and M. Schlüter, Phys. Rev. Lett. 43, 956 (1979).
[31]N. O. Lipari, J. Bernholc, and S. T. Pantelides, Phys. Rev. Lett. 43, 1354 (1979).
[32]C. T. White and K. L. Ngai, J. Vac. Sci. Technol. 16, 1412 (1979).
[33]K. H. Johnson, H. J. Kolari, J. P. de Neufville, and D. L. Morel, Phys. Rev. B 21, 643 (1980).
[34]L. F. Mattheiss and J. R. Patel, Phys. Rev. B 23, 5384 (1981).
[35]W. E. Pickett, Phys. Rev. B 23, 6603 (1981).
[36]D. P. DiVincenzo, J. Bernholc, M. H. Brodsky, N. O. Lipari, and S. T. Pantelides, *Tetrahedrally Bonded Amorphous Semiconductors*, edited by R. A. Street, D. K. Biegelsen, and J. C. Knights (American Institute of Physics, New York, 1981), p. 156.
[37]P. Soven, Phys. Rev. 156, 809 (1967); S. Kirkpatrick, B. Velicky, and H. Ehrenreich, Phys. Rev. B 1, 3250 (1970).
[38]J. S. Faulkner, Phys. Rev. B 13, 2391 (1976); D. A. Papaconstantopoulos, B. M. Klein, J. S. Faulkner, and L. L. Boyer, *ibid.* 18, 2784 91978).
[39]J. A. Reimer, R. W. Vaughan, and J. C. Knights, Phys. Rev. Lett. 44, 193 (1980).
[40]H. H. Madden, Bull. Am. Phys. Soc. 26, 453 (1981); G. Wiech and E. Zöpf, in *Band Structure Spectroscopy of Metals and Alloys*, edited by D. J. Fabian and L. M. Watson (Academic, New York, 1973), pp. 629–640.
[41]K. Hirabayashi, J. Phys. Soc. Jpn. 27, 1475 (1969).
[42]M. L. Sink and G. E. Juras, Chem. Phys. Lett. 20, 474 (1973); K. C. Pandey, Phys. Rev. B 14, 1557 (1976).
[43]L. F. Mattheiss, Phys. Rev. 123, 1209 (1961).
[44]D. J. Chadi, Phys. Rev. B 16, 3572 (1977).

PHYSICAL REVIEW B VOLUME 23, NUMBER 12 15 JUNE 1981

Theoretical study of the hydrogen-saturated ideal silicon vacancy

Warren E. Pickett
Naval Research Laboratory, Washington, D. C. 20375
(Received 12 November 1980)

The self-consistent pseudopotential method and supercell configuration are used to study the electronic structure of the hydrogen-saturated vacancy (HSV) in Si. A unified picture is obtained by comparing three systems: (i) bulk Si (no vacancy), (ii) the vacancy alone, and (iii) the HSV complex in which each Si dangling bond is compensated by H. The vacancy dangling-bond states are found to be removed from the gap and the H-H interactions do not interfere with the formation of a strong H–Si bond. The reappearance of the gap and the form of the charge density in the proximity of the HSV implies a stability which suggests this may be one of the strain-relieving configurations which occurs upon hydrogenation of amorphous silicon. These calculations also suggest a potentially observable acceptor state if a HSV-like defect can be created in crystalline silicon.

I. INTRODUCTION

The recent upsurge in interest in amorphous silicon arises primarily from two sources. The first involves the possible widespread technological application of these materials, particularly hydrogenated amorphous silicon (a-Si:H) in solar cells. The second impetus centers on answering fundamental theoretical questions about the nature of electronic states in disordered systems, with the existence of a gap and the structure in its proximity being of central importance.

The theoretical description of disordered systems is complicated greatly by a lack of knowledge of the atomic geometry. The problem of disorder on an atomic scale is exacerbated in a a-Si:H by the existence of voids and related large-scale inhomogeneities,[1] i.e., disorder on a macroscopic scale which is extremely difficult to model theoretically. Attempts to describe the effects of the lack of short-range order on the electronic spectrum of a-Si and a-Si:H have concentrated on valence force field (bond-stretching and -bending) effects or on low-symmetry H–Si or Si dangling-bond configuration. Each of these approaches focuses on specific features of the actual system of interest and together they have led to a rudimentary understanding of some of the observed phenomena.

One potentially important area which has seen very little theoretical attention is the careful description of H–Si bonding in a solid-state environment. Obviously low-symmetry configurations involving H–Si bonds will occur, and it is particularly in such low-symmetry situations that self-consistency is often found to be essential in a realistic description of the electronic structure. The present work was motivated by these considerations. As a first step toward an understanding of H–Si bonding in the solid state, the (by now standard) self-consistent pseudopotential method has been applied to the H-saturated Si vacancy. Although this is *not* a low-symmetry configuration, it provides (as will be shown) a basic example of the removal of dangling-bond gap states in a bulk environment, much like what has been found to occur at surfaces and is expected by hydrogenation of a-Si. The method that is used in this study guarantees that the bonding electrons react to a potential which is itself derived from the electronic charge density, unlike those used in previous work (discussed in Sec. IV).

In Sec. II the calculational details are reviewed briefly. Section II is devoted to an exposition of electronic structure of the H-saturated Si vacancy, and comparison to both the ideal vacancy and to crystalline silicon is presented. The local density of states is used extensively to provide an understanding of the "chemical bonding" of H and Si in an extended system. Comparison with previous work is presented in Sec. IV, as well as a brief discussion of the possible connection with experimental data. A summary is given in Sec. V.

II. METHOD OF CALCULATION

A. Self-consistent pseudopotential method

The self-consistent pseudopotential (SCP) method has been documented elsewhere[2] and has been used in numerous applications. In the present study local ionic pseudopotentials which have been utilized successfully in other applications[3,4] were chosen. The pseudopotentials were fit to the form

$$V_{\rm ion}(q) = -\frac{4\pi Ze^2}{\Omega q^2}\, a[\cos(bq) + c]\exp(-dq^4), \quad (1)$$

where Ω denotes the atomic volume and $a(1+c) = 1$ to yield the correct $q \to 0$ limit. The constants b, c, and d for Si and H are listed in Table I.

With the SCP method it is conventional to cal-

TABLE I. Ionic pseudopotential parameters (in a.u.) b, c, d in Eq. (1) for H and Si.

	Si^{4+}	H^{+}
b	0.7907	0.2800
c	−0.3520	−1.5380
d	−0.01807	−0.0070

culate the Hamiltonian matrix elements in a plane-wave basis, with a cutoff plane-wave energy E_1. To improve convergence of the eigenvalues, additional plane waves up to a cutoff E_2 are used in the Löwdin perturbation scheme. In this study $E_1 = 3$ Ry, $E_2 = 6$ Ry were found to give convergence of eigenvalues to about 0.1 eV, which is sufficient for the present purposes

The plane-wave expansion of the charge density and screening potential (for which the Hedin-Lundqvist[5] local density functional was used) was carried out to 37 stars (equal to 485 plane waves). In the early stages of self-consistency the four special k-point set was used in calculating the charge density. The final charge density was self-consistent on the regularly spaced ten-point set.

B. Supercell geometry

A cubic cell with edge length $a_0 = 10.2626$ a.u. and containing eight diamond-lattice sites is used as the unit cell in a superlattice configuration. Three distinct systems have been studied. As a control system, the band structure of crystalline Si was calculated with the use of the 8-atom unit cell. Next, one Si atom was removed and the self-consistent electronic response was recalculated, without allowing atomic relaxation. This configuration corresponds to a regular array of 12.5% ideal vacancies, but in some ways (which we discuss in Sec. III) the results are similar to those of isolated vacancy calculations. Although this supercell is small, interactions between vacancies are transmitted along bonding chains for which a neighboring vacancy is four sites away. Finally, the four dangling bonds per vacancy were "compensated" by H atoms placed symmetrically around the vacant site. The H–Si bond length was chosen to be 2.874 a.u. (= 65% of the Si–Si distance) in accordance with the regularities of the H-Si-Si_3 system discussed by Lucovsky.[6]

There are two features of this H-saturated vacancy (HSV) configuration which should be noted. First, it is evident that there will be interactions between HSV's in neighboring cells. This limitation is less serious than it seems initially, since there is rather little interest here in the *isolated* HSV. *In a*-Si:H *there will be nearby* H–Si *complexes which are nearly as well modeled by repeated* HSV's *as by any other specific configuration.* (The sharp structure in the density of states characteristic of crystalline systems of course will be spurious.) Secondly, there is the likelihood of H-H interactions at a given HSV. The H–H distance is 2.563 a.u. and the H-H interaction is appreciable but hard to quantify, although the local density of states which we calculate provides some indication of the nature of the H-H interactions.

C. Local densities of states

The wave functions and associated weights (see below) were calculated on the regular 35 k-point grid (vertices of 64 tetrahedra) in the irreducible Brillouin zone. The total and local densities of states (DOS) were calculated with the tetrahedron method of Lehmann and Taut,[7] in which both energies and weights are interpolated linearly within each tetrahedron.

For the weights we have used the fraction of charge of the state which lies within a sphere of radius R centered at various sites of interest. The chosen sites were (1) the vacant site, (2) the H site, (3) the H–Si bond center (denoted "H–Si bond"), (4) the nearest-neighbor Si to the vacant site ["Si(1)"], (5) the Si–Si bond center ("Si–Si bond"), and (6) the second-neighbor Si ["Si(2)"]. In each case R has been chosen to be $0.15a_0 = 1.539$ a.u., which is slightly more than half the H–Si bond length. Therefore the various spheres overlap considerably and the sum of their weights is meaningless. For the Si vacancy calculation the same notation is used although no H atom is actually present.

III. CALCULATIONAL RESULTS

A. Charge density

A contour plot of the self-consistent pseudo-charge-density of the HSV in the (110) plane is shown in Fig. 1. Both Si–Si and H–Si bonds lie in this plane. The Si–Si bonds are virtually identical to those calculated for the bulk (not shown) using the same potential. This result is encouraging as it indicates that interactions between charge-density disturbances from neighboring HSV's are rather unimportant.

The peak in charge corresponding to the H–Si bond is also evident in Fig. 1. The charge density in the bonding region is similar to that calculated for the H–Si bond at the Si(111) surface.[4,8] The large value of charge density at the vacant Si site, ~17 electrons per diamond-lattice unit cell, suggests significant interactions between the four H

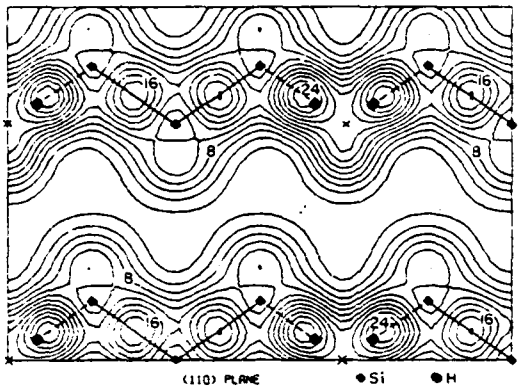

FIG. 1. Contour plot in the (110) plane of the pseudo-charge-density of the H-saturated Si vacancy. The units are electrons per diamond-lattice unit cell. Solid straight lines denote Si–Si bonding directions and dashed lines indicate H–Si bonds; crosses denote vacant Si sites. For clarity the abscissa and ordinate lengths are 1.5 times the corresponding supercell dimension.

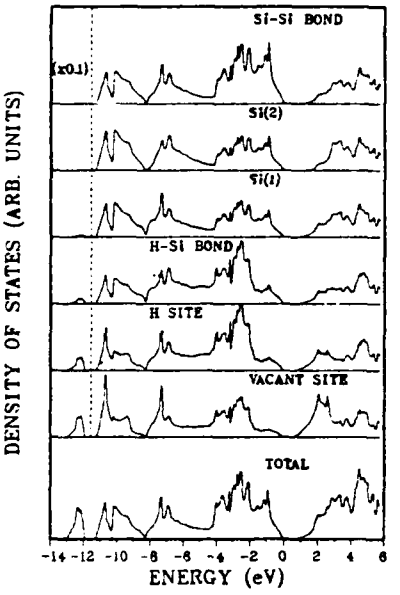

FIG. 3. Total and local density of states of the H-saturated vacancy, as defined in the text. Note that for the local densities of states the large peak at −12.5 eV has been scaled down by a factor of 10.

atoms surrounding the vacant site. However, apart from the immediate region of the H atoms the charge density is typical of Si, particularly the channel of nearly zero density running parallel to the bonding chains.

The charge density near the Si vacancy (not shown) was found to be very similar to those calculated for isolated ideal Si vacancy.[9] As an illustration of the charge-density deformation which results from (conceptually) placing H atoms so as to terminate the vacancy dangling bonds, the charge-density difference (HSV-vacancy) is shown in Fig. 2. This difference in density is altered from that arising from overlapping spherical H atom densities in two ways. First, there is the aforementioned interaction between H atoms, resulting in a small net flow of charge into the vacant site (centroid of the four proton sites). Secondly, and more noticeable in Fig. 2, there is a shifting of the pseudocharge maximum from the H site along the H–Si bonding direction. This is primarily a result of the dangling-bond charge, which is known in the vacancy[9] to "heal" by decreasing its magnitude in the (broken) bond position, being attracted back into the H–Si bond. The separation of the charge-density differences in Fig. 2 again is a testimony to the small interaction between charge disturbances even in the small supercell being used here.

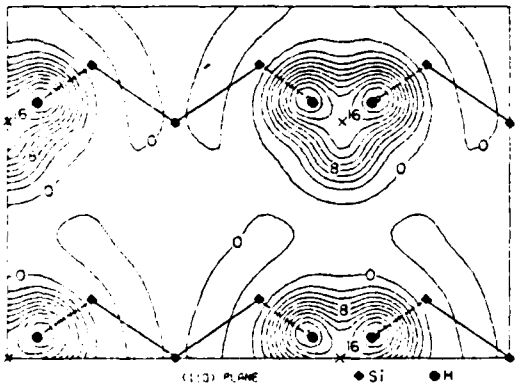

FIG. 2. Contour plot in the (110) plane of the charge-density difference between the H-saturated vacancy and the ideal Si vacancy. Notation is the same as in Fig. 1.

B. Density of states

The total density of states (DOS) at the HSV is shown at the bottom of Fig. 3. The overall structure is similar to that of crystalline Si, shown at the bottom of Fig. 4, calculated using identical k-point sampling and Brillouin-zone integration techniques as described in Sec. II C. Most significant is the result that terminating the vacancy dangling bonds with H removes from the gap the well known ideal vacancy gap states,[9] which in the present supercell fill in the gap as shown in Fig. 5. This is just what is expected in a chemical bonding picture if the H-H interactions within an HSV do not

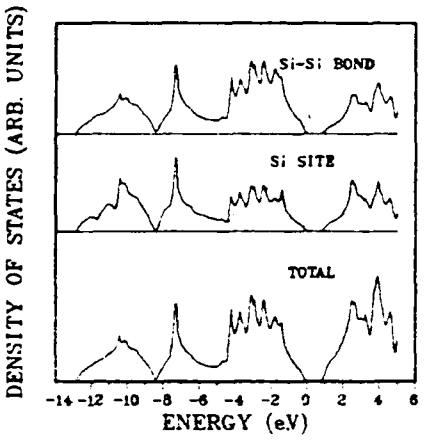

FIG. 4. Total and local density of states of crystalline Si.

cause too much disruption. The calculated gap for the superlattice of HSV's is 0.5 eV compared to the crystalline value of 0.9 eV (for this potential and for the convergence criteria that have been imposed). This 0.5-eV "gap" is discussed more fully below. The only *qualitative* difference between the HSV DOS and that of crystalline Si is the splitting off of a band in the lower-valence region $-13 \leq E \leq -12$ eV. Comparison to the DOS of crystalline Si in Fig. 4 suggests that in the case of an *isolated* HSV this state will occur as a resonance at the bottom of the valence bands.

Also shown in Fig. 3 are the local DOS's (LDOS's) as described in Sec. II C. For comparison, the corresponding LDOS's for the Si site and Si–Si bond in crystalline Si are pictured in Fig. 4. (The primary difference between these latter two very similar LDOS's is a larger density of bonding states within 4 eV of the gap in the Si–Si *bond* LDOS.) Figure 3 shows that the split-off bound state at ~ -12.5 eV is confined to the region of the four H atoms, i.e., the vacant site and the H positions. (Note that this huge LDOS peak has been divided by ten in Fig. 3.) The other energy region of interest, that is, where there is large variation in the LDOS within the supercell, is centered on the fundamental gap 0.0–0.5 eV. The LDOS immediately below the gap is primarily due to the Si–Si bonding regions, as in the crystal. The H–Si bond, H site, and vacant Si site show a progressively lower density of bonding states in the region -2 to 0 eV which indicates the electrons in the H–Si bond are bound more tightly than in the Si–Si bond. The states above the gap, on the other hand, are strongly H-related states, with the lowest unoccupied state at Γ being localized (apparently) and centered at the vacant site. This suggests, for the isolated HSV, a bound state near the top of the gap, which we discuss further below. In Fig. 5 the total and local DOS's for the vacancy superlattice are shown. The regions of states which are strongly affected by the vacancy are crosshatched for emphasis. No gap exists, the bound states in the gap of the isolated ideal Si vacancy are broadened by intervacancy interactions into bands more than 1 eV wide. (We note, however, that the charge-density disturbance due to the vacancy is well localized even for this small supercell.) These dangling-bond states lie primarily in the region -0.5 to 1 eV, although some extend down to -2 eV. In addition, the s state on the Si nearest the vacancy is repelled upward into the low DOS region at -9 eV by the effectively repulsive potential of the vacancy. These results correspond closely to the isolated vacancy results of Ref. 9, with the cross hatching at -9 eV in Fig. 5 corresponding to A_1 symmetry states, and cross hatching at 0 to 1 eV corresponding to the T_2 symmetry gap states, in this reference.

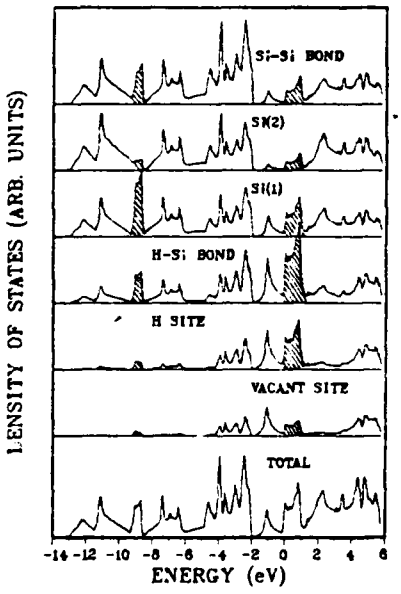

FIG. 5. Total and local density of states for the ideal Si vacancy (superlattice). Cross hatching is used to emphasize the segments of the partial densities of states which are strongly vacancy related. The energy zero denotes the top of the filled states.

C. H-related states

The similarity of the energy bands of a superlattice of HSV's ("Si_7H_4") to those of Si in the same

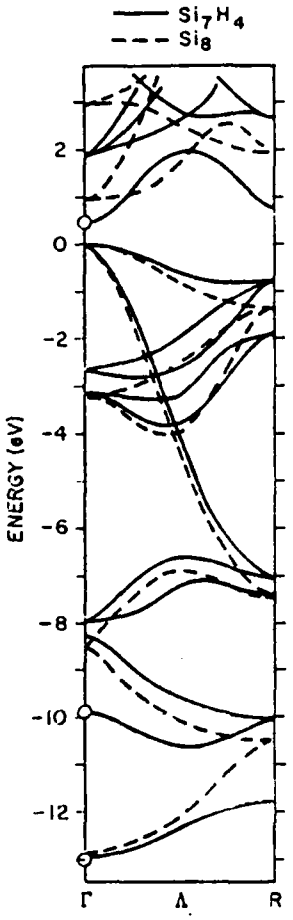

FIG. 6. Energy bands along the ⟨111⟩ direction of the superlattice of HSV's ("Si_7H_4") and of bulk silicon for the same unit cell ("Si_8"). Open circles at Γ indicate the hydrogen-related states which are discussed in the text and pictured in Fig. 7.

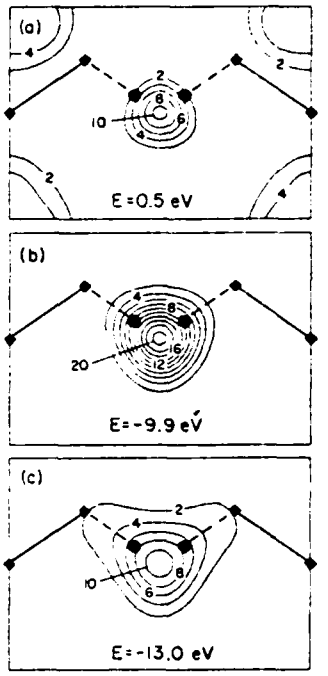

FIG. 7. Contour plots in the (110) plane of the three hydrogen-derived states at the zone center of the H-saturated Si vacancy superlattice. The charge density is normalized to one electron per superlattice unit cell.

unit cell ("Si_8") is evident in Fig. 6, where the bands are shown with the valence-band maxima aligned. From this figure it is possible to identify the bulk Si states which are strongly perturbed by the HSV complex. In essence, this makes use of the fact that the tetrahedral arrangement of four hydrogen atoms in the HSV is isoelectronic with Si and, in fact, it is not too dissimilar in many of its effects on the overall spectrum. For this comparison it is expedient to focus on states at Γ, rather than at other positions in the Brillouin zone, where many characteristics of Bloch states are sensitive to supercell size and geometry. The strongly perturbed, and therefore H-related, states at Γ occur both below and above the lower gap at − 12 to − 11 eV in Fig. 3, and at the bottom of the conduction band at 0.5 eV. Contour plots in the (110) plane of the charge densities of these states are shown in Fig. 7. The two lower states [Figs. 7(b) and 7(c)] are derived from a symmetric combination of the four H 1s orbitals, with the splitting arising from interaction with the Si s states which lie in the same energy range. Lower-symmetry combinations of the H 1s orbitals bond with the Si sp^3 orbitals throughout the range − 8 to 0 eV.

The lowest "conduction-band" state at 0.5 eV also is derived from a symmetric combination of H orbitals (presumably 2s and 2p). The small charge density of this state in both the H–Si and Si–Si bonding regions indicates a nonbonding (rather than antibonding) tendency toward the Si sp^3 orbitals. This behavior suggests that this state corresponds to a bound state in the gap for the isolated HSV. The supercell used in this calculation is far too small to get any reasonable estimate of the energy of such a state, that is, whether it is a deep or a shallow acceptor, if indeed it lies within the gap. Either type could be consistent with the charge density in Fig. 7(a): (1) the state is deep and very localized, in which case the interstitial charge density would be due to supercell-induced mixing with the conduction-band states (which have large densities in the interstices), or (2) the state is shallow and weakly localized, in

which case the conduction-band mixing and interstitial charge density is an integral component of the state. Qualitatively, the large density within the tetrahedron of H atoms tends to support the deep acceptor point of view.

IV. DISCUSSION

A. Relation to previous work

Using an extended Hückel method, Choo and Tong[10] investigated an HSV in Ge. Their system consisted of a 47-atom crystalline cluster with surface dangling bonds compensated with H atoms to remove them from the gap region. When the central Ge was replaced with four H atoms a hydrogen-related acceptor state (with 40% of the charge on the four H atoms) appeared in the upper part of the gap, much as appears to be the case in the present study.

Recently Economou and Papaconstantopoulos[11] have studied the electronic structure of a *random* array of HSV's in Si using a tight-binding coherent-potential-approximation method. Aside from the different method of calculation, their work differs from the present work in essentially two ways. First, they considered a *random* array of 5% HSV's compared to the *periodic* array of 12.5% HSV's studied here. Secondly, the H-H interaction within a given HSV was taken to be the same as in the SiH_4 molecule. Their H LDOS near the fundamental gap is very similar to the "H-site" curve of Fig. 3, with a strong H component in states immediately above the gap and a comparatively small H component in bonding states just below the gap. The first H LDOS peak below the gap occurs somewhat lower (−6 to 5 eV) than in the present study (−4 to −2 eV), and the splitoff (by the H-H interaction) state at the bottom of the valence band is broadened, but in other respects the H and Si LDOS's are similar.

There are several other calculations[12] in the literature which include the basic H-Si-Si_3 configuration. However, the similarity of these systems to the HSV is insufficient to warrant a detailed comparison with the present study.

B. Relationship to experimental systems

The basic unit in the HSV studied here is the bonded H–Si pair, which is expected to occur in *a*-Si:H, no doubt in several different types of complexes. Moreover, the HSV is one of the simplest configurations which exhibits hydrogen clustering, a phenomenon which has been observed[13] in *a*-Si:H. Unfortunately, the presently available experimental results provide only very indirect information on atomic configurations. The LDOS's of Fig. 3 bear some resemblance to photoemission data[14] on unannealed *a*-Si:H, which show H-related peaks at 6 and 11 eV binding energy. The calculated peaks at 7 and 12.5 eV, which will shift if the HSV is allowed to relax, may be related to the observed states. However, it is naive to expect much quantitative correspondence between the present study and any of the variety of experimental samples of *a*-Si:H. In particular, the calculated gap of 0.5 eV and the precise location of peaks are sensitive to the supercell size and, therefore, the calculated gap bears no clear relationship to the (much wider) experimental gap which plays a central role in device performance.

Nevertheless, the strong H–Si bond and the restoration of the gap suggest that the (relaxed) HSV may be a stable local configuration in spite of the H-H interaction. Thus the HSV-type complex could be one of many strain-relieving configurations to occur upon hydrogenation of *a*-Si.

Finally, it should be noted that, if indeed an HSV-related acceptor state does occur in the crystal (which should be resolvable on a strictly theoretical basis with more precise calculations[9]), it should be detectable in defected[15] Si or Ge.

Note added in proof. A recent self-consistent Green's-function study of the *isolated* HSV (D.P. DiVincenzo, J. Bernholc, M. H. Brodsky, N. O. Lipari, and S. T. Pantelides, in Proceedings of the Topical Conference on Tetrahedrally Bonded Amorphous Semiconductors, Carefree, Arizona, 1981, in press) found no states in the silicon energy gap.

ACKNOWLEDGMENTS

The author is indebted to D. A. Papaconstantopoulos for encouragement and for useful discussions in the course of this work, and to L. L. Boyer, B. M. Klein, and D. J. Nagel for comments on the manuscript. This work was supported in part by the U. S. Department of Energy.

[1] P. D'Antonio and J. H. Konnert, Phys. Rev. Lett. 43, 1161 (1979); T. A. Postol, C. M. Falco, R. T. Kampwirth, I. K. Schuller, and W. B. Yelon, *ibid.* 45, 648 (1980); A. J. Leadbetter, A. A. M. Rashid, R. M. Richardson, A. F. Wright, and J. C. Knights, Solid State Commun. 33, 973 (1980).

[2] J. R. Chelikowsky and M. L. Cohen, Phys. Rev. B 13, 826 (1976).

[3]W. E. Pickett, M. L. Cohen, and C. Kittel, Phys. Rev. B 20, 5050 (1979).
[4]K. M. Ho, M. L. Cohen, and M. Schlüter, Phys. Rev. B 15, 3888 (1977).
[5]L. Hedin and B. I. Lundqvist, J. Phys. C 4, 2064 (1971).
[6]G. Lucovsky, Solid State Commun. 29, 571 (1979).
[7]G. Lehmann and M. Taut, Phys. Status Solidi B 54, 469 (1972).
[8]J. A. Appelbaum and D. R. Hamann, Phys. Rev. Lett. 34, 806 (1975).
[9]G. A. Baraff and M. Schlüter, Phys. Rev. B 19, 4965 (1979); J. Bernholc, N. O. Lipari, and S. T. Pantelides, *ibid.* 21, 3545 (1980).
[10]F. C. Choo and B. Y. Tong, Solid State Commun. 25, 385 (1978).
[11]E. N. Economou and D. A. Papaconstantopoulos, Phys. Rev. B 23, 2042 (1981); in Proceedings of the Topical Conference on Tetrahedrally Bonded Amorphous Semiconductors, Carefree, Arizona, 1981 (in press).
[12]W. Y. Ching, D. J. Lam, and C. C. Lin, Phys. Rev. Lett. 42, 805 (1979); J. D. Joannopoulos, J. Non-Cryst. Solids 32, 241 (1979); D. C. Allan and J. D. Joannopoulos, Phys. Rev. Lett. 44, 43 (1980); K. H. Johnson, H. J. Kolari, J. P. de Neufville, and D. L. Morel, Phys. Rev. B 21, 643 (1980); W. Y. Ching, D. J. Lam, and C. C. Lin, *ibid.* 21, 2378 (1980).
[13]W. E. Carlos and P. C. Taylor, Phys. Rev. Lett. 45, 358 (1980).
[14]B. von Roedern, L. Ley, and M. Cardona, Phys. Rev. Lett. 39, 1576 (1977); B. von Roedern, L. Ley, M. Cardona, and F. W. Smith, Philos. Mag. B 40, 433 (1979).
[15]Infrared absorption data on H-implanted crystalline Si and references to related literature are given by H. J. Stein, Phys. Rev. Lett. 43, 1030 (1979).

PHYSICAL REVIEW B VOLUME 26, NUMBER 10 15 NOVEMBER 1982

Symmetric relaxation of the hydrogen-saturated silicon vacancy

Warren E. Pickett
Condensed Matter Physics Branch, Naval Research Laboratory, Washington, D.C. 20375
(Received 9 June 1982)

With the use of the self-consistent pseudopotential method, the Hellman-Feynman theorem is applied to study the symmetric relaxation in the hydrogen-saturated vacancy (HSV) which has been used previously to model the electronic properties of amorphous silicon hydride. The hydrogen and nearest-neighbor silicon atoms are found to relax outward by 0.46 and 0.35 a.u., respectively. The primary effect of this relaxation, which is driven by the large H-H interactions in the ideal HSV, is to *restore* the depleted local H density of states just below the band gap. It is suggested that geometries other than those considered here may lead to more stable configurations.

I. INTRODUCTION

Recently several investigators have used the hydrogen-saturated vacancy (HSV) in Si to model the electronic structure and transport properties of hydrogenated amorphous silicon (a-SiH$_x$). A tight-binding coherent potential approximation (CPA) treatment[1] on a random 5% "alloy" of HSV's in a silicon lattice displayed a valence-band spectrum very similar to that of a-SiH$_x$ as well as reproducing the experimentally observed widening of the gap when the H content is increased. The self-consistent electronic structure of the HSV itself has been studied from both the supercell[2] and the isolated-defect[3] approaches. Both of these studies found the density of states (DOS) immediately below the gap to be strongly depleted around the H sites, and the former study (Ref. 2, hereafter referred to as I) also found a DOS *increase* around the H sites for conduction states immediately above the gap.

The depletion of conduction-band states near the gap by H has been suggested[3,4] as the cause of the low hole mobility in a-SiH$_x$, and dc transport calculations[5] on the CPA model[1] have borne out this qualitative picture. More recently, a calculation[6] of the absorption coefficient (i.e., ac conductivity) based on the CPA model has suggested an interpretation of the difference between the "optical gap" and the "DOS gap" in a-SiH$_x$. Thus it seems that the HSV has provided a reliable basis for understanding several of the crucial properties of a-SiH$_x$.

The interpretation discussed above has all been based on the electronic structure of the *ideal* HSV. However, in I it was emphasized that the large repulsion between H atoms in the ideal HSV was likely to lead to substantial atomic relaxation in this defect, and a preliminary study of the magnitude of the relaxation has been reported.[7] In this paper we allow the symmetric breathing relaxation of the HSV and find substantial rearrangement of the H local DOS both above and below the gap which must be reconciled with the data on a-SiH$_x$ if the HSV is to remain a viable model for this system.

The plan of the paper is as follows. In Sec. II the numerical procedure which is used to calculate the forces on the atoms is presented. The numerical results and their interpretation are given in Sec. III. The last section is devoted to a discussion of the implications of these results for our current understanding of the electronic properties of a-SiH$_x$.

II. NUMERICAL TECHNIQUES

The self-consistent pseudopotential (SCP) method has been described in detail elsewhere.[7] The Si and H local pseudopotentials, Hedin-Lundqvist exchange-correlation potential, supercell size corresponding to eight Si atoms, and calculation of local DOS (LDOS) are as described in I. The novel feature of the present work is the calculation of forces on atoms using the Hellman-Feynman (HF) theorem.[8] Formal aspects of the HF theorem in density-functional theory have been discussed elsewhere.[9] However, since this study may be the first of its kind for a model of a localized defect in a

bulk solid, and since technical aspects of the calculation of HF forces have not been presented in much detail elsewhere, selected details of the present calculations will be presented in this section.

A. Hellman-Feynman force calculations

For a given atomic configuration $\{\vec{R}_j\}$, the force $\vec{F}_j$ on an ion at $\vec{R}_j$ is given by

$$\vec{F}_j = \vec{F}_j^{\text{ion}} + \vec{F}_j^{e}, \tag{1}$$

where $\vec{F}_j^{\text{ion}}$ is the direct Coulomb contribution from all other ions,[9] which can be calculated using an Ewald technique,[10] and $\vec{F}_j^{e}$ is the electronic contribution which takes the classical form

$$\vec{F}_j^{e} = \int d^3r\, \rho(r) \vec{\nabla} v_j(r - R_j) \tag{2}$$

in terms of the local ionic pseudopotential v_j. The charge density ρ should be the "exact" charge density, i.e., that which satisfies the local-density-functional equations. An approximate charge density, which might lead to a reasonable total energy $E_{\text{tot}}\{\vec{R}_i\}$ (which is variational in ρ) and thereby to reasonable forces from the numerical derivative $\Delta E_{\text{tot}}/\Delta \vec{R}_j$, can lead to widly uncontrolled results for $\vec{F}_j$ if the HF expression is applied directly. An example is the Gordon-Kim[11] procedure for deriving the forces between two closed-shell ions from a total charge density approximated by the sum of two spherical ionic densities. Direct application of the HF theorem to this approximate charge density leads to nearly vanishing forces for ionic separations of interest, resulting solely from the exponential tail of one ionic charge overlapping the *nucleus* of the other ion, whereas the Gordon-Kim procedure of calculating E_{tot} in an *intermediate* step is known to be quite reliable.

Physically, the HF force $\vec{F}_j^{e}$ originates from the distortion (dipolar with respect to $\vec{R}_j$) of the valence charge density (away from that of overlapping spherical atomic densities) due to bonding. In practice, the calculated (and therefore approximate) charge density must be (1) converged with respect to $\vec{k}$-point sampling, (2) self-consistent, and (3) represented sufficiently generally to allow the important bonding-charge distortions. A plane-wave representation, either of the total (valence pseudo-) charge density ρ (as done here) or of the distortions of ρ due to bonding, seems to be a particularly satisfactory representation as it is not fixed to particular atomic positions.

For the HSV, $\vec{F}_j^{e}$ was calculated from the expression

$$\vec{F}_j^{e} = i \sum_{G < \vec{G}} \vec{G} v_j(|\vec{G}|) \rho(\vec{G}) e^{-i\vec{G}\cdot\vec{R}_j}, \tag{3}$$

where $v_j(G)$ and $\rho(\vec{G})$ are Fourier coefficients of v_j and ρ. The summation limit $\vec{G}$ must be extended until convergence is obtained. Figure 1 shows the convergence of $\vec{F}^{e}$ for both H and Si as $\vec{G}$ is increased. The important contributions to $\vec{F}^{e}$ arise from wavelengths $(2\pi/G) > a_0/4$, where $a_0 = 10.263$ a.u. is the Si lattice constant. For all results quoted here the cutoff was taken as $\vec{G}^2 = 27$ $(2\pi/a_0)^2 = 10$ Ry.

Accurate values of $\vec{F}_j^{e}$ require a charge density which is more accurate than is necessary for simply determining a self-consistent potential or the total energy. This in turn requires more precise eigenvectors of the Hamiltonian matrix $H_{\vec{G}\,\vec{G}'}$. A common procedure[7] in the SCP method for obtaining eigenvalues efficiently is to construct $H_{\vec{G}\,\vec{G}'}$ matrix elements up to a large cutoff $G_2^2 = E_2$ and use the Lowdin procedure[12] to fold down the eigenvalue problem to a smaller one corresponding to $G_1^2 = E_1$. For the present calculations the Lowdin unfolding procedure[12] for subsequently obtaining the eigenvector components up to $G = G_2$ has also been employed. These procedures, which are reminiscent of second-order perturbation theory in the matrix elements $H_{\vec{G}\,\vec{G}'}$ for $E_1 < G^2$, $G'^2 \le E_2$, produce eigenvectors of sufficient accuracy for the present purposes. The cutoffs $E_1 = 4.5$ Ry, $E_2 = 8$ Ry corre-

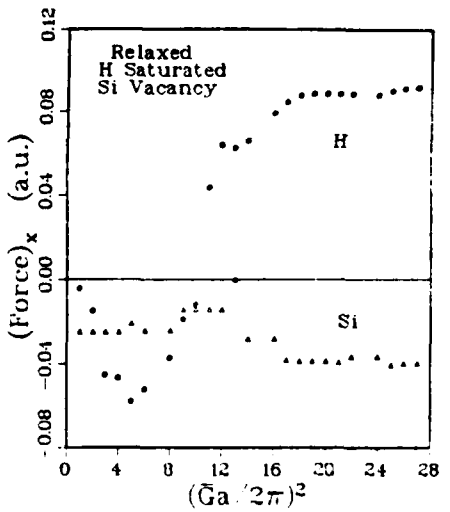

FIG. 1. x component of the electronic contribution to the force, in hartrees/bohr, on H and nearest-neighbor Si atoms, illustrating convergence vs $\vec{G}$-space cutoff $\vec{G}$. Results are for configuration 1.

spond to plane-wave basis sets of approximately 175 and 400 plane waves, respectively, and provide only slightly less accurate solutions to the 400×400 secular equation at substantially less cost than by direct methods.

In Table I examples of the changes in the calculated forces due to large-G components of the wave function are displayed. For this convergence check, the single special $\vec{k}$ point[13] was used to approximate the charge density for the ideal configuration, and the Lowdin unfolding procedure was applied to give initially 300 and then 400 plane-wave coefficients of the wave functions. The calculated forces on the H and Si atoms increased in magnitude by 35% and 6%, respectively, while the total energy per atom changed only from -5.5028 to -5.5058 Ry.

The set of four special $\vec{k}$ points[13] for the simple cubic lattice has proven adequate for the HSV supercell for determining ρ. One special point is clearly insufficient, while results almost identical to those from the four-special-point mesh were obtained using the 10- and 35-point regular meshes and the 20-special-point set.

B. Geometry

The HSV supercell is a cube corresponding to the crystalline Si cubic cell of edge length a_0 and containing eight Si sites. For the HSV the Si atom at the origin is replaced by hydrogens at (u,u,u) and equivalent positions tetrahedrally placed around the origin. For the *ideal* HSV, u was chosen[2] as $0.0883a_0$, corresponding to a H—Si bond length of Si_3-SiH suggested by Lucovsky.[14] Only symmetric "breathing-mode" relaxations, i.e., atoms relaxing radially from the center of the defect only, of the HSV have been considered. Thus only u and the

TABLE I. Comparison of the x component of the calculated electronic forces (in arbitrary units) on H and Si atoms when 300 or 400 plane-wave coefficients are included in the plane-wave expansion. Contributions from each star of reciprocal-lattice vectors as well as the total are given. Owing to the symmetric placement of the Si atom [at $(a_0/4,a_0/4,a_0/4)$] within the unit cell, several stars G give vanishing contributions to the force independently of $\rho(\vec{G})$.

	H		Si	
$\left\lvert\frac{a}{2\pi}\right\rvert\vec{G}$	300	400	300	400
100	−1.57	−1.60	−9.54	−9.70
110	−3.52	−3.56		
111	−8.78	−8.78		
200	−1.21	−1.23		
210	−4.69	−4.76	1.64	1.66
211	−1.49	−1.48	−0.59	−0.61
220	2.85	3.13		
221	1.61	1.71	1.71	1.75
310	0.32	0.31		
311	11.86	12.66		
222	4.52	4.68		
320	−0.56	−0.63	2.68	3.03
321	0.69	0.77	−4.68	−5.26
400	2.52	2.91		
322	1.42	1.58	−1.54	−1.73
330	0.39	0.44	−0.33	−0.43
331	0.19	0.18		
420	−0.01	−0.02		
421	−0.01	−0.01	−0.05	−0.07
332	0.06	0.07	0.61	0.69
422	−0.04	−0.05		
430	0.21	0.27	−0.58	−0.75
431	0.19	0.24	0.25	0.38
333	0.06	0.07		
Total	5.01	6.90	−10.42	−11.04

coordinate v of the neighboring Si atom at (v,v,v) and symmetric positions are allowed to vary ($v=0.25a_0$ for the ideal HSV). Changes in unit-cell volume have not been considered.

III. RESULTS

A. Relaxation of the HSV

In addition to the ideal HSV geometry, three relaxed geometries have been studied. Their coordinates and the calculated atomic forces are presented in Table II. Configuration 3 was determined from the previous configurations (0,1,2) by fitting forces determined from the harmonic potential-energy expression, valid for small enough displacements,

$$V(u,v)=Au+Bv+Cu^2+Dv^2+Euv\ , \qquad (3)$$

to the six calculated forces, and then determining the equilibrium values of u and v. After calculating the forces for configuration 3 (Table II), forces derived from expression (3) were least-squares-fitted twice, to the calculated forces for all four configurations, and separately to configurations 1, 2, and 3 (those nearest equilibrium). From these two potential functions the equilibrium values u_0 and v_0 and their uncertainties (arising from which fit one chooses to use) were found and are given in Table II.

The results of the geometrical relaxation can be summarized as follows. The H atoms relax outward by $\sqrt{3}\,|u_0-u(0)|=0.46$ a.u. [$u(0)=u$ for configuration 0] while the neighboring Si atoms relax outward by 0.35 a.u., resulting in a 7% decrease of the H—Si bond length. This relaxation rotates the Si—Si bond by 4.5° and compresses it by 2.5%. The ideal and relaxed geometries in the (110) plane are shown in Fig. 2. In terms of $\bar{u}=u-u_0$,

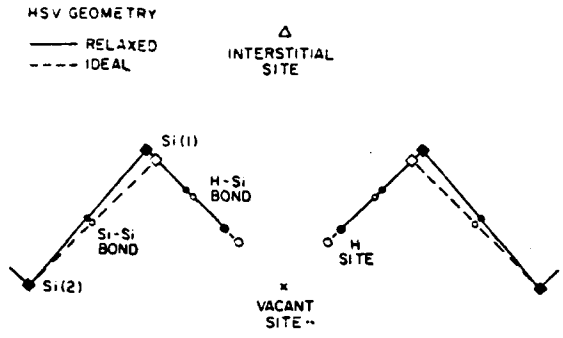

FIG. 2. Schematic geometry of the HSV relaxation in the (110) plane of the supercell. Dashed lines represent the configuration before relaxation.

$\bar{v}=v-v_0$, the potential energy V for small displacements can be written

$$V(\bar{u},\bar{v})=a\bar{u}^2+b\bar{v}^2+c\bar{u}\,\bar{v}\ . \qquad (4)$$

From this expression the energy ΔE gained by relaxation is found to be about 1 eV/supercell, i.e., per HSV defect. Direct calculation of ΔE (discussed more fully below) between configurations 0 and 3 is 1.1 eV.

B. Changes in eigenstates and LDOS

As expected, this rather large atomic relaxation leads to significant changes in the hydrogen-related states and LDOS. In Fig. 3 the supercell band structure along Γ-R is shown for both the ideal and relaxed HSV. The states of particular interest in following the effect of relaxation are numbered 1 through 6, and the charges of each of these states within spheres distributed throughout the cell are given in Table III. States 1—3 lie in the lower valence bands and before relaxation each is strongly

TABLE II. x components of H,u and Si,v positions (in units of the lattice constant 10.263 a.u.), and the x components of ionic, electronic, and total forces on H and Si atoms (hartree/bohr). Equilibrium positions are calculated by fitting to quadratic potentials as described in the text; uncertainties (in parentheses) are due to the two separate fits to the calculated forces and *do not include* uncertainties in the calculated forces.

			H			Si		
Configuration	u	v	F_x^{ion}	F_x^{e}	F_x^{tot}	F_x^{ion}	F_x^{e}	F_x^{tot}
0	0.0883	0.2500	−0.019	0.038	0.019	0.060	−0.041	0.019
1	0.0960	0.2500	−0.090	0.091	−0.001	0.080	−0.040	0.040
2	0.1000	0.2560	−0.108	0.115	0.007	0.036	−0.014	0.022
3	0.1203	0.2730	−0.213	0.202	−0.011	−0.049	0.052	0.003
Equilibrium	0.1142(3)	0.2696(1)	−0.179	0.179[a]	0.0	−0.040	0.040[a]	0.0

[a]Calculated from equilibrium condition $F_x^{tot}=0$.

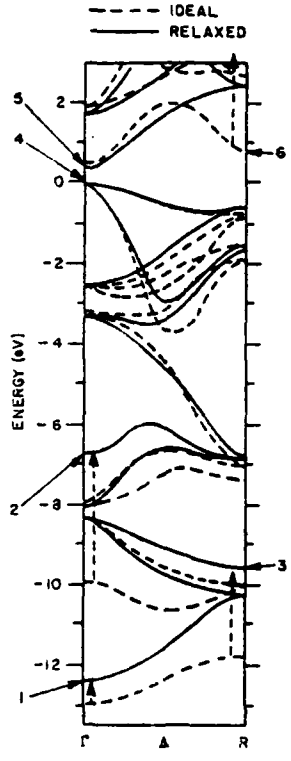

FIG. 3. Supercell band structure along the Γ-R direction for configuration 0 (ideal) and configuration 3 (near equilibrium). Dotted arrows indicate states which are affected strongly by the relaxation. Numbers label states discussed in text and referred to in Table III.

localized near the H atoms. The outward relaxation of the H atoms decreases the overlap of the attractive H pseudopotentials in this region. As a result these states rise in energy and lower their amplitude near the H atoms, although state 2 (and to a lesser extent state 3) remains strongly H related.

States 4—6 lie near the gap and therefore are crucial in determining low-excitation-energy properties. State 4 is the uppermost valence band whose eigenvalue is used to fix the energy zero in Figs. 3 and 4. [With respect to the average potential $V_{\rm tot}(\vec{G}=\vec{0})$, the energy of state 4 moved downward by 0.5 eV during relaxation.] From Table III it can be seen that for this state the charge near H nearly doubles during relaxation. Conversely, the charge on the lower-conduction-band state 5 decreases dramatically near and between the H atoms during relaxation, although its eigenvalue changes very little. Finally, state 6, the low-conduction-band state at R in the ideal HSV, is raised by nearly 3 eV by the relaxation although its strong H-related character is not changed dramatically (Table III). Both states 5 and 6 have large amplitudes in the interstitial regions of the cell.

The LDOS's for the spheres along the bonding chain pictured in Fig. 2 are given in Fig. 4 along with the total DOS. The only notable change in the total DOS occurs at the bottom of the valence bands, where the strongly H-related peak at -13 to -12 eV found in I for the ideal HSV is found to merge with the low Si valence states during relaxa-

TABLE III. Relative charges within each of the equal-volume spheres at the positions indicated in Fig. 2 for the six states designated in Fig. 3. Both ideal (configuration 0, in parentheses) and near equilibrium (configuration 3) values are given, with normalization such that a uniform state will have a value 1.00 within each sphere. Also given below is the total charge (in electrons) within each sphere and the ratio "charge (relaxed)/charge (ideal)."

State number	Vacant site	H	H—Si bond	Si(1)	Si—Si bond	Si(2)	Interstitial
1	0.44	1.13	1.53	1.61	2.15	1.74	0.61
	(7.90)	(5.29)	(2.72)	(1.66)	(1.06)	(1.06)	(0.14)
2	6.27	7.92	4.60	0.73	0.50	0.60	0.82
	(13.15)	(7.35)	(1.55)	(0.54)	(1.68)	(1.15)	(0.26)
3	1.49	3.06	3.20	2.45	1.75	0.38	1.15
	(17.46)	(11.00)	(4.25)	(1.29)	(0.05)	(0.25)	(0.05)
4	0.66	2.86	2.20	1.36	2.75	1.21	0.05
	(0.83)	(1.50)	(1.52)	(1.21)	(1.40)	(2.74)	(0.07)
5	1.98	1.10	0.31	0.63	0.89	1.37	8.22
	(5.27)	(2.18)	(0.90)	(0.77)	(0.09)	(0.54)	(4.99)
6	8.64	2.96	1.61	1.80	1.12	0.15	4.59
	(8.58)	(3.61)	(2.13)	(2.34)	(0.18)	(0.71)	(1.57)
Total charge	0.84	2.35	2.21	1.39	1.34	2.03	0.32
	(2.10)	(2.12)	(1.90)	(1.51)	(1.79)	(1.47)	(0.20)
Ratio	0.40	1.11	1.17	0.92	0.75	1.38	1.63

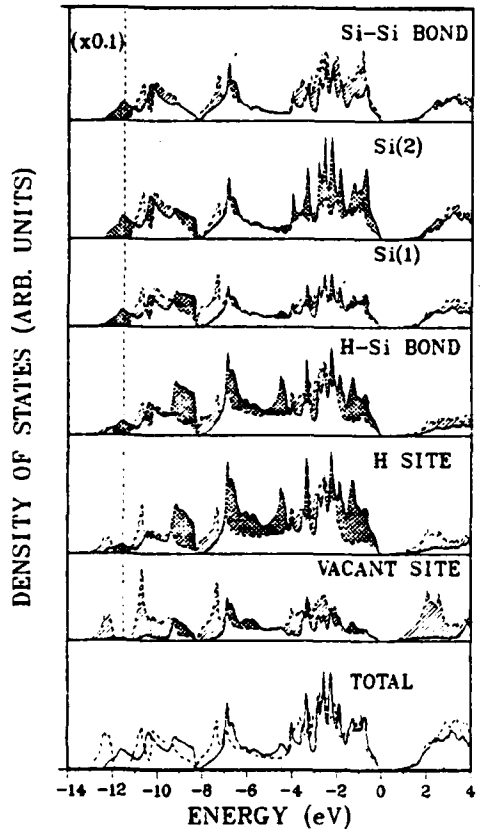

FIG. 4. Total and local densities of states in the spherical regions pictured in Fig. 2. In the LDOS curves the dashed peak below −12 eV has been divided by ten. All LDOS are plotted on the same scale. States move from the single- to the double-cross-hatched regions during relaxation.

tion. Accordingly, the vacant-site and H-site LDOS's show a general decrease in the −13- to −9-eV region.

There is a large *increase* in the LDOS just below the gap at the H site, H−Si bond, and the second-neighbor Si ["Si(2)"], of which the latter may be a "supercell effect" which indicates that for these energies the charge perturbation extends to larger distances. Conversely, near the bottom of the conduction bands there is a strong *decrease* in the LDOS at the vacant site, H site, and H−Si bond, together with a significant increase near Si(2) which again may be a supercell effect.

It should be noted that little can be learned about the energetics of the relaxation solely from the DOS, i.e., from the sum over occupied states of the eigenvalues. It is found that the change in eigenvalue [relative to $V_{\text{Hartree}}(\vec{G}=\vec{0})=0$] sum between configurations 3 and 0 is −7.70 eV, while the change in the Coulomb double-counting correction[9] is a similar contribution of −7.24 eV. The Ewald and exchange-correlation correction energy differences are 13.10 and 0.72 eV, giving the final energy change (gain) from relaxation of −1.12 eV. Thus the eigenvalue sum contribution has the same sign as the total energy difference in this case, but other contributions compete in importance with the eigenvalue sum.

C. Charge density

The overall appearance of the charge density of the relaxed HSV in the (110) plane is similar to that of the ideal HSV in I and is not shown. The difference plot in Fig. 5 of ρ(configuration 3)$-\rho$(ideal) indicates that the charge distortion accompanying atomic relaxation is dominated by a removal of charge from between the tetrahedron of H atoms and the addition of charge to Si−H bonding region. This rearrangement of charge can be accounted for qualitatively by the rigid motion of atomiclike H and Si charge densities. In addition, there is an increase in charge in the H−Si backbonding position (more than 1 a.u. from the Si nucleus) which is consistent with this rigid-atom picture. The increase in charge in the Si−Si bond likewise can be ascribed to the 2.5% compression of this bond; its asymmetric form, however, suggests a distortion of the bond charge due to bond rotation. The atomic relaxation also results in a decrease of the already small charge density in the interstitial region.

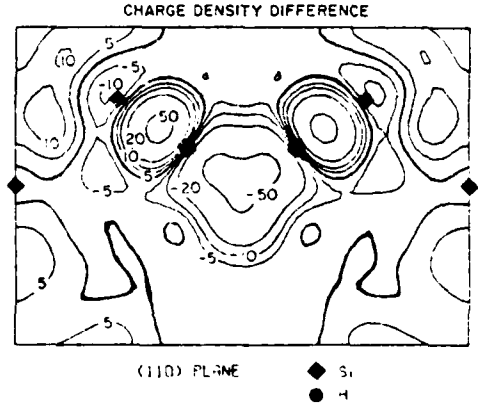

FIG. 5. Plot in the (110) plane of the difference in charge density between configuration 3 and configuration 0; i.e., "relaxed" minus "ideal." Contours are drawn at 0 (heavy contour), ±5, ±10, ±20, and ±50 electrons/cell.

IV. DISCUSSION

The preceding section has described the symmetric, constant volume relaxation of H and neighboring Si atoms in the HSV. The restriction to constant volume has compressed the H—Si and Si—Si bonds by 7% and 2.5% compared to their "equilibrium" values, indicating the "relaxed" HSV as described here is under pressure. The compressibility of crystalline silicon and the Si—Si bond compression (corresponding to $\Delta V/V=7.5\%$) implies a local pressure of the order of 75 kbar. A full relaxation of the HSV (within the breathing-mode constraint assumed here) would require minimizing the energy with respect to lattice constant, then again allowing internal atomic relaxation, and iterating this procedure to convergence. It is not clear that the result of such a calculation would justify the expense, so "full relaxation" in this sense has not been attempted.

As a first approximation the "fully relaxed" HSV (in the sense described above) can be approximated by the present relaxed atomic configuration, but with lattice constant expanded by 2.5% to restore the Si—Si bond to its length in crystalline silicon. This leaves the H—Si bond compressed by 4.5% by the H-H interactions.

One important property which can be sensitive to the variation of lattice constant and to internal stresses is the vibrational frequency of the system. From the potential-energy expression (4) and atomic masses the breathing-mode frequencies are found to be 3300 and 425 cm^{-1} for "optic" and "acoustic" modes, respectively. [These modes however are not normal modes of the present supercell lattice since the Si(2) atoms are fixed.] The high-frequency H-Si stretching mode is 50% above the 2100-cm^{-1} band assigned to H-Si stretching modes[14–16] in a-SiH_x. Volume relaxation would lower the calculated frequency, perhaps drastically, considering the large but canceling electronic and ionic forces on H (Table II) at equilibrium.

Experience in electronic structure calculations indicates, however, that the qualitative features of the electronic structure of the HSV should not vary significantly with a 2.5% increase in lattice constant. Thus the changes in the LDOS near the gap should be taken seriously and their implications given consideration.

Brodsky[4] has suggested a "quantum-well model" for a-SiH_x in which it is assumed that H—Si bonds deplete the valence-band DOS's near the gap and result in localization of the wave functions within 0.6 eV of the valence-band edge. Support for this model arose from the isolated HSV calculations of DiVincenzo *et al.*[3] (and also from I), and the model could explain qualitatively certain optical and transport processes. On the contrary, the present study shows that most of the H—Si bonding states are restored to the region $-0.6<E<0$ eV by symmetric relaxation.

The CPA HSV alloy model of Papaconstantopoulos and Economou[1] (PE) also indicates a strong depletion of valence-band states just below the gap. Moreover, this model explains in *a quantitative manner* a number of properties of a-SiH_x: (1) removal of states from, and the widening of, the gap upon hydrogenation,[1] (2) existence of Si—H antibonding resonance states[1,5] just *above* the gap, (3) the absorption coefficient[6] in the range $2<h\nu\leq 3$ eV, and (4) the position of H-related bonding states in the valence band.[1] From the "H-site" and "H—Si bond" LDOS in Fig. 4 it is clear that *symmetric breathing relaxation of the HSV removes precisely those features of the H-related LDOS in the CPA model which are responsible for giving an interpretation of properties (1)—(3) above.* Property (4)—the position of H-related photoemission peaks—is less sensitive to the relaxation calculated here, with relaxation causing peaks to shift away somewhat from those measured by von Roedern *et al.*[17] but more toward agreement with those found by Smith and Strongin.[18]

As a consequence, it appears that the ideal HSV provides a good model of a local defect upon which an alloy model of a-SiH_x can be built, while our relaxed HSV fails. This result, in itself, implies no contradiction, as PE have emphasized that it is the local H-Si chemical environment rather than the geometrical arrangement of the cluster of four H atoms which is the determining factor in their model.

This result may however be interpreted as suggesting only that the present model of relaxed HSV does not actually occur, but rather is dynamically unstable towards a lower-symmetry, lower-energy configuration. The present study guarantees only that the relaxed configuration is stable with respect to breathing-type distortions with full tetrahedral symmetry, and that it is not Jahn-Teller unstable toward a lower-symmetry configuration. However, the restricted minimum-energy configuration found here may well be a saddle point in the full configuration space of atomic distortions.

In such a case the H (and Si) atoms are dynamically unstable with respect to motion perpendicular

to the (111) H—Si bonding directions. The fully relaxed configuration could be a low-symmetry one which allows lengthening of the compressed H—Si and Si—Si bonds toward more typical lengths as well as the avoidance of strong H-H interactions, at the cost of relatively low-energy distortions of H—Si—Si and Si—Si—Si bond angles. Avoiding the compression of the H—Si bond should leave the H LDOS depleted in the upper valence-band region, similar to that of the ideal HSV in I, and therefore retain the single feature (the local H-Si chemical environment discussed by PE) most essential to modeling *a*-SiH_x.

Assuming a complete loss of symmetry, the configuration space consists of the coordinates of each of the four H and four Si atoms, a total of 24 variables. The present approach of calculating *forces* rather than energies provides the only reasonable approach to finding the lowest-energy configuration in such a case. However, the loss of symmetry leads to a large increase in computational effort (from $\vec{k}$-point sampling), and nothing is known at present about the number of configurational iterations to be expected to reach equilibrium in such a large parameter space. Nevertheless restricted relaxations along these lines may be studied in the near future.

ACKNOWLEDGMENTS

I have benefitted from numerous discussions with D. A. Papaconstantopoulos, E. N. Economou, B. M. Klein, L. L. Boyer, and C. S. Wang on various aspects of this work and from comments on the manuscript. Useful computer codes were made available by J. Ihm and B. Chakraborty. The technical assistance of A. Koppenhaver is gratefully acknowledged. This work was supported in part by the Solar Energy Research Institute through an interagency agreement between the Naval Research Laboratory and the Department of Energy, and by the Office of Naval Research under Contract No. N00014-79-WR-90028.

[1]D. A. Papaconstantopoulos and E. N. Economou, Phys. Rev. B 24, 7233 (1981).
[2]W. E. Pickett, Phys. Rev. B 23, 6603 (1981).
[3]D. P. DiVincenzo, J. Bernholc, M. H. Brodsky, N. O. Lipari, and S. T. Pantelides, in *Tetrahedrally Bonded Amorphous Semiconductors (Carefree, Arizona)*, A Topical Conference on Tetrahedrally Bonded Amorphous Semiconductors, AIP Conf. Proc. No. 73, edited by R. A. Street, D. K. Biegelsen, and J. C. Knights (AIP, New York, 1981), p. 156.
[4]M. H. Brodsky, Solid State Commun. 36, 55 (1980).
[5]W. E. Pickett, D. A. Papaconstantopoulos, and E. N. Economou, J. Phys. (Paris) Colloq. C4 42, 769 (1981).
[6]W. E. Pickett, D. A. Papaconstantopoulos, and E. N. Economou (unpublished).
[7]J. R. Chelikowsky and M. L. Cohen, Phys. Rev. B 13, 826 (1976).
[8]W. Pauli, *Handbuch der Physik*, 2nd ed. (Springer, Berlin, 1933), Vol. 24, p. 162; H. Hellman, *Einfuhrung in die Quantenchemie* (Deuticke, Leipzig, 1937); R. P. Feynman, Phys. Rev. 56, 340 (1939).
[9]J. Ihm, A. Zunger, and M. L. Cohen, J. Phys. C 12, 4409 (1979).
[10]Codes for calculating F_j^{ion} were kindly provided by J. Ihm.
[11]R. G. Gordon and Y. S. Kim, J. Chem. Phys. 56, 3122 (1972).
[12]P. O. Lowdin, J. Chem. Phys. 19, 1396 (1951).
[13]D. J. Chadi and M. L. Cohen, Phys. Rev. B 8, 5747 (1973).
[14]G. Lucovsky, Solid State Commun. 29, 571 (1979).
[15]W. Paul, Solid State Commun. 34, 283 (1980).
[16]P. John, I. M. Odeh, and M. J. K. Thomas, Solid State Commun. 41, 341 (1982), and references therein.
[17]B. von Roedern, L. Ley, and M. Cardona, Phys. Rev. Lett. 39, 1576 (1977); B. von Roedern, L. Ley, M. Cardona, and F. W. Smith, Philos. Mag. B 40, 433 (1970).
[18]R. J. Smith and M. Strongin, Phys. Rev. B 24, 5863 (1981).

JOURNAL DE PHYSIQUE

Colloque C4, supplément au n°10, Tome 42, octobre 1981 page C4-769

CALCULATIONS OF TRANSPORT PROPERTIES IN a-Si:H

W.E. Pickett, D.A. Papaconstantopoulos and E.N. Economou

Naval Research Laboratory, Washington, DC 20375, U.S.A.

Abstract.- We have used the coherent potential approximation to calculate the d.c. conductivity for a model of hydrogenated amorphous silicon. The results show that the mobility of electrons is greater than that of holes. This appears to be related to the strong hydrogen component of the density of states just above the gap.

The incorporation of hydrogen into amorphous Si has been found to change its electronic structure and transport properties drastically. The density of states in the band gap is reduced by several orders of magnitude (1), thereby allowing the "adjustment", by doping (2) with impurities, of the Fermi level E_F which is otherwise pinned near the center of the gap in a-Si. Spectral features related to hydrogenation, such as the removal of states (1) from the gap, the widening of the optical gap (1,3), and the alteration of both the valence (4) and conduction densities of states, have been studied by a variety of theoretical methods (5-8).

The model proposed by two of the authors (6,7) accounts for the data mentioned above as well as showing substantial agreement (7) with the optical absorption data of Cody et al (2). In this paper we begin a theoretical study of the transport properties of a-Si:H by calculating the d.c. conductivity for this model system.

The model consists of an effective lattice whose sites have a probability c of being vacant and probability 1-c of being occupied by a Si atom. This Si-vacancy alloy provides a model which exhibits many of the properties (6,7) of a-Si. In addition, hydrogen atoms (one, two, three, or four) are incorporated around the vacant site such as to bond with neighboring Si dangling bonds, and the resulting spectral properties reproduce many trends evident in the experimental data on hydrogenation of a-Si. The model is based on a Slater-Koster (SK) Hamiltonian fit (8) to the pseudopotential band structure of Si, and the Coherent Potential Approximation (CPA) is invoked to treat the disorder. The calculational details have been given elsewhere (6,7).

In the present work we treat only the fully hydrogenated case of four hydrogens per vacant Si site. The resulting system shows a very low density of states in the band gap, similar to data on a-Si:H. To evaluate the conductivity σ we begin with the zero frequency Kubo-Greenwood formula

$$\sigma = \frac{2e^2\pi}{\pi^2\Omega m^2} \int dE \left(-\frac{\partial f}{\partial E}\right) \mathrm{Tr}\langle p_x \mathrm{Im}G(E+i\delta) p_x \mathrm{Im}G(E+i\delta)\rangle. \qquad (1)$$

where $\langle \ldots \rangle$ denotes the configuration average and f is the Fermi function. The evaluation of this expression in a manner consistent

with the CPA has been discussed in detail elsewhere (9). By ignoring the vertex corrections arising from correlations in intermediate scatterings, the Green's functions G can be averaged separately, resulting in the effective medium function $\bar{G}$. The trace operator Tr in Eq. (1) includes a sum over the Brillouin zone as well as a matrix trace over the basis states, which we have taken as the Bloch sum of s- and p-orbitals which provide the representation for the SK Hamiltonian (8) of silicon. In this basis the momentum (p_x) matrix elements are given by

$$(p_x/m)_{ij} = \hbar^{-1} [H(k+\delta k_x)-H(k)]_{ij}/\delta k_x \qquad (2)$$

which we have evaluated numerically by using a finite wavevector displacement δk_x. If a transformation is made to band states which diagonalize H and give eigenvalues E_k, the diagonal elements of p_x/m become the band velocity $dE_k/d(\hbar k)$. However, preliminary evaluation of σ retaining only band-diagonal components of p_x/m has shown that the full matrix nature of this operator must be retained. As opposed to previous CPA evaluations (10) of σ which relied on single band models, we emphasize that the present calculation retains the full multiband character of our model of a-Si:H.

The zone integration of our expression for $\sigma(E)$,

$$\sigma(E) = \frac{2e^2\hbar}{\pi^2\Omega m^2} \sum_k \sum_{ijmn} p_{x,ij}(\mathrm{Im}\bar{G}_{jm})p_{x,mn}(\mathrm{Im}\bar{G}_{ni}) \qquad (3)$$

was done by an analytic tetrahedron approach (11). The irreducible zone (1/48th) was divided into 4000 equal volume tetrahedra (comprising 916 distinct vertices), with the integrand being assumed linear within each tetrahedron. The integration within each tetrahedron can be evaluated analytically, and the result is summed over all 4000 tetrahedra. The same mesh was used to solve for the CPA Green's function $\bar{G}$ and the related density of states N(E). At zero temperature the thermal redistribution $(-\partial f/\partial E)$ reduces to a δ-function located at E_F, and Eq. (1) reduces to Eq. (3).

The results for N(E) and $\sigma(E)$ near the gap region are shown in Fig. 1. We find that states very near the top of the valence band at $E \lesssim -0.5$ eV) are only poorly conducting, as the initial increase in $\sigma(E)$ for negative energies occurs below that of N(E). At the top of the gap, however, both $\sigma(E)$ and N(E) show the same "onset" at ~ 0.85 eV. (The energy zero has been set at the bottom of the gap of the reference crystalline Si system (8).)

The comparison of the contribution of electron and hole states to conductivity can be made if we define

$$\sigma(E) = \text{const.} \times \langle p_x^2(E)\rangle N^2(E) \qquad (4)$$

which is suggested by the relation $N(E) \propto \mathrm{Im}\bar{G}(E+i\delta)$. The mean square matrix element $\langle p_x^2(E)\rangle$, which describes everything except density of states effects, is 5 to 15 times larger for electron states than for hole states. This difference reflects the character of the states which are involved: hole states derived from bonding combinations of Si-Si and Si-H orbitals, and electron states derived

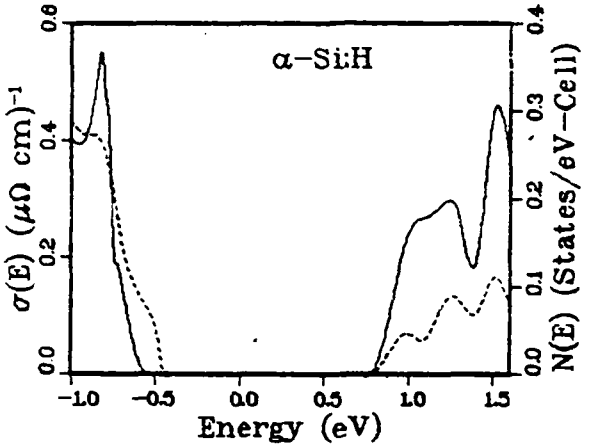

Fig. 1 The zero temperature conductivity σ(E) (full line) and density of states N(E) (dashed line) near the gap region for the present model of fully hydrogenated amorphous silicon.

from anti-bonding combinations of these orbitals. Both Si-H combinations are pulled down in energy relative to their Si-Si counterparts, and this is reflected in the ratio $N_H(E)/N_t(E)$ of H local density of states N_H to the total N_t being three times larger for electron states than for hole states (~ 7% to 2.5%).

The finite temperature conductivity (ignoring thermal lattice disorder) can be calculated from the relation

$$\sigma(T) = \int dE \left(- \frac{\partial f(E-E_F)}{\partial E} \right) \sigma(E). \qquad (5)$$

The results are shown in Fig. 2 for various values of E_F within the gap, corresponding physically to different doping levels. The calculated values of log σ vs. 1/T reproduce the approximately linear behavior found in intrinsic and doped samples of a-Si:H (2,12).

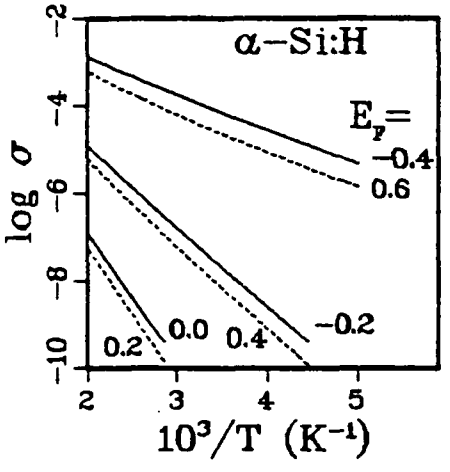

Fig. 2 Logarithm of $\sigma(\mu\Omega\ cm)^{-1}$ vs inverse temperature for various placements of E_F, corresponding to different doping levels. Solid lines denote values of E_F in the lower half of the gap (-0.4, -0.2, 0.0 eV), while dashed lines are used for values of E_F in the upper part of the gap (0.2, 0.4, 0.6 e V).

This work was supported in part by the Solar Energy Research Institute via an interagency agreement between the US Naval Research Laboratory and the US Department of Energy.

References

1. Moustakas T.D., Anderson D.A., and Paul W., Solid State Commun. 23 (1977) 155.
2. Spear W.E. and LeComber P.G., Solid State Commun. 17 (1975) 1193; Carlson D.E. and Wronski C.R. Appl. Phys. Lett. 28 (1976) 671; Spear W.E., Adv. Phys. 26 (1977) 811.
3. Moustakas T.D., Wronski C.R., and Morel D.L., J. Non-Cryst. Solids 35-36 (1980) 719; Cody G.D., Wronski C.R., Abeles B., Stephens R.B., and Brooks B., Solar Cells, 2 (1980) 227.
4. von Roedern B., Ley L., and Cardona M., Phys. Rev. Lett. 39 (1977) 1576; von Roedern B., Ley L., Cardona M.,and Smith F.W., Phil. Mag. B40 (1979) 433.
5. Ching W.Y., Lam D.J., and Lin C.C., Phys. Rev. Lett. 42 (1979) 805; Allan D.C. and Joannopoulos J.D., Phys. Rev. Lett. 44 (1980) 43; Johnson K.J., Kolari H.J., deNeufville J.P., and Morel D.L., Phys Rev. B21 (1980) 643; Pickett W.E., Phys. Rev. B23 (1981, in press); DiVincenzo D.P., Bernholc J., Brodsky M.H., Lipari N.O., and Pantelides S.T., AIP Proc. Tetrahedrally Bonded Amorphous Semiconductors Conf. (1981, in press).
6. Economou E.N. and Papaconstantopoulos D.A., Phys. Rev. B23 (1981) 2042.
7. Papaconstantopoulos D.A. and Economou E.N., AIP Proc., Tetrahedrally Bonded Amorphous Semiconductors Conf. (1981, in press).
8. Papaconstantopoulos D.A. and Economou E.N., Phys. Rev. B22 (1980) 2901.
9. Velicky B., Phys. Rev. 184 (1969) 614; Chen A. B., Weisz G., and Sher A., Phys. Rev. B5 (1972), 2987.
10. Morita T., Horiguchi T., and Chen C.C., J. Phys. Soc. Japan 38 (1975) 981; Taranko E., Taranko R., Wysokinski K.I., and Pilat M., Z. Physik B39 (1980) 187.
11. Note that this integration is not confined to an energy surface in the Brillouin zone as would be the case for a crystalline system.
12. Anderson D.A., Moustakas T.D., and Paul W., Proc. of the 7th Int. Conf. on Amorphous and Liquid Semiconductors (1977), ed. by Spear W.E. (CICL University of Edinburgh) 467.

P8

Theoretical Study of Optical Absorption in Hydrogenated Amorphous Silicon

W.E. Pickett
Condensed Matter Physics Branch
Naval Research Laboratory, Washington, DC 20375

D.A. Papaconstantopoulos
Metal Physics Branch
Naval Research Laboratory, Washington, DC 20375

and

E.N. Economou
Exxon Research and Engineering Company
Linden, NJ 07036
and
Department of Physics, University of Crete
Heraklion, Crete, Greece

We present the first application of the coherent-potential-approximation in the evaluation of optical absorption $\alpha(E)$ of a-SiH_x using a realistic multi-band model. The optical gap is larger than the calculated density of states gap and the theoretical $\alpha(E)$ agrees well with experimental data. These results suggest that $\alpha(E)$ is determined primarily by the local H-Si configuration and short range order, but that it is insensitive to the particular long range order, which is not included in our model.

PACS. Nos. 72.80.Ng, 71.25.Mg, 78.40.Fy

Submitted to Physical Review Letters

In spite of several recent developments in the theoretical understanding of the electronic spectrum of a-SiH_x, a gap remains in the interpretation of measured quantities[1-3] such as the optical absorption coefficient α, photoconductivity, photoluminescence, etc. These properties depend not only on the electronic density of states (DOS), N(E), but also upon transition matrix elements involving the eigenfunctions of the system. Since realistic matrix elements are much more difficult to obtain theoretically than is N(E), the usual approach is to assume that the matrix elements are constant, i.e. energy-independent. With this assumption $\alpha(\omega)$ is proportional to the convoluted DOS (CDOS)

$$\alpha(\omega) \sim \omega^{-1} \int_{E_F-\hbar\omega}^{E_F} N_v(E)N_c(E+\hbar\omega)dE \qquad (1)$$

(v,c denote valence, conduction band) and the resulting optical gap E_g^{opt} coincides with the DOS gap E_g^{DOS}. In this paper we show that both the magnitude of α and the measured[1,2] E_g^{opt} of fully hydrogenated a-SiH_x are reproduced by our calculations if we remove the assumption of constant matrix elements, and a better understanding of the optical process is thereby obtained.

In the present work we calculate $\alpha(\omega)$ within a recently developed multiband model[4,5] of a-SiH_x. These calculations are the first application of the coherent-potential-approximation (CPA) in the evaluation of optical properties of a real material using a realistic multiband system; previous calculations[6] of the optical conductivity have been limited to simple single or double band models. The

significant aspects of our work include: (i) without adjustable parameters we obtain good agreement with experiment[1] for $\alpha(\omega)$, both in energy dependence and absolute magnitude, and (ii) we find that $E_g^{opt} > E_g^{DOS}$ is due primarily to remanent conservation of the magnitude of the wavevector resulting from short-range order.

The optical absorption coefficient is given in terms of the optical conductivity $\sigma(\omega)$ and index of refraction $n(\omega)$ by

$$\alpha(\omega) = 4\pi \mathrm{Re}\,\sigma(\omega)/cn(\omega). \tag{2}$$

where c is the speed of light. The weak ω-dependence of n has been measured[1] and is included in the calculations below. For $\sigma(\omega)$ we use the general expression[7]

$$\mathrm{Re}\sigma(\omega) = \frac{2e^2}{\pi\Omega m^2\omega} \sum_{\vec{k}} \int_{E_F-\hbar\omega}^{E_F} dE\ \mathrm{Tr}\langle \tilde{p}_x \mathrm{Im}\tilde{G}(\vec{k},E+i0)\tilde{p}_x \mathrm{Im}\tilde{G}(\vec{k},E+\hbar\omega+i0)\rangle \quad , \tag{3}$$

$$\simeq \frac{2e^2}{\pi\Omega m^2\omega} \sum_{\vec{k}} \int_{E_F-\hbar\omega}^{E_F} dE\ \mathrm{Tr}\left\{\tilde{p}_x \langle \mathrm{Im}\tilde{G}(\vec{k},E+i0)\rangle \tilde{p}_x \langle \mathrm{Im}\tilde{G}(\vec{k},E+\hbar\omega+i0)\rangle\right\},$$

where Ω is the normalization volume, p_x is the x-component of the momentum operator and G is the Green's function of the system. The brackets $\langle \ldots. \rangle$ indicate an ensemble average over the disorder and $\tilde{A}$ denotes that A is an 8x8 matrix. For G we use CPA results for a highly successful model a-SiH_x system discussed elsewhere.[4] The model consists of a tight-binding description of 20 at.% H bonded to 5% Si vacancies in random positions on a Si lattice. The second

approximate relation (3) results from ignoring vertex corrections[8] to the exact expression, and allows the evaluation of $Re\sigma$ directly from the CPA Green's function $\langle G \rangle$. The momentum matrix is given by

$$\tilde{p}_x = \frac{d\tilde{H}(\vec{k})}{dk_x} , \tag{4}$$

where $\tilde{H}$ is the virtual crystal tight-binding Hamiltonian.[4]

The results for $Re\sigma(\omega=0,E_F)$ have been presented previously[5] as a function of E_F. There it was found that contributions from off-diagonal matrix elements of $\tilde{p}_x$ and $\langle \tilde{G} \rangle$ were negligible (typically ~2%), consistent with an "intraband" picture of the d.c. conductivity. In crystals absorption at finite frequency occurs due only to interband transitions, but disorder admits the possibility of "intraband" transitions. Whereas it will be seen that the $\vec{k}$-dependence of the matrix elements is necessary to understand the energy gaps, the full matrix summations in the trace in Eq. (3) are necessary to obtain the correct magnitude of α.

Our result for $\alpha(\omega)$, calculated from Eqs. (2-4) at T=0 (no thermal disorder) with no adjustable parameters is compared in Fig. 1 (as the dashed line) in the form $(\alpha E)^{1/2}$ vs E ($E=\hbar\omega$) with the experimental data of Cody *et al.*[1] (symbols) and with the CDOS expression of Eq. (1) (dotted line) corresponding to energy-independent, non-momentum conserving matrix elements of $\tilde{p}_x$. In the range $2.1 \leq E \leq 3.0$ eV, $(\alpha E)^{1/2}$ is in excellent agreement with the data apart from an overall factor of 1.5. In the region $1.6 \leq E \leq 2.1$ eV the calculation leads to higher absorption (relative to the higher energy region) than is found for the sample shown in Fig. 1. This could

be due to the lack of full atomic disorder or to the absence of off-diagonal disorder, either of which would require a more sophisticated CPA model.

Another possibility, which we now address, is that the approximation of Eq. (3) of neglecting vertex corrections is breaking down in this region. Examination of contributions to $\alpha(\omega)$ for $\hbar\omega < 2eV$ from various regions of $\vec{k}$-space shows that this absorption is due entirely to transitions for which either $(\vec{k},E)$ or $(\vec{k},E+\hbar\omega)$ is rather far from a broadened "band" of a-SiH$_x$. In terms of the spectral density S given by

$$S(\vec{k},E) = -\pi^{-1}\mathrm{Tr}\tilde{G}(\vec{k},E+i0), \tag{5}$$

either initial or final state of the transition lies where S is small. The CPA, however, is designed primarily to provide average, macroscopic properties of the system, and it may be overestimating $S(\vec{k},E)$ in regions far away from bands which, for example, contribute little to N(E). In a region where the influence of a single band m with energy $E_{\vec{k}m}$ is dominant, $S(\vec{k},E)$ assumes the form

$$S(\vec{k},E) \approx \frac{1}{\pi} \frac{|\mathrm{Im}\Sigma_m(E)|}{(E-E_{\vec{k}m})^2+[\mathrm{Im}\Sigma_m(E)]^2}, \tag{6}$$

since for the tight-binding CPA we find the self-energy $\Sigma_m(\vec{k},E)$ in the band representation is nearly $\vec{k}$-independent. Therefore $S(\vec{k},E)$ is Lorentzian in $E_{\vec{k}m}$ at fixed E. Observation of first principles muffin-tin CPA spectral functions[9] however suggests a much faster than Lorentzian fall-off of $S(\vec{k},E)$; i.e. $|\mathrm{Im}\Sigma_m(\vec{k},E)|$ should <u>decrease</u> as $\vec{k}$ leaves the vicinity of band m.

Following this line of reasoning we modified the CPA self-energy to conform to this more physical behavior by defining a k-dependent on-site self-energy $\hat{\Sigma}$ by[10]

$$\mathrm{Im}\hat{\Sigma}_{s,p}(\vec{k},E) = c_{s,p}\ \frac{\Gamma^2}{(E-E_{\vec{k}n})^2+\Gamma^2}\ \ \mathrm{Im}\Sigma_{s,p}(E) \tag{7}$$

$$\Gamma = c\ \left|\mathrm{Im}\Sigma_s(E)+ 3\mathrm{Im}\Sigma_p(E)\right|\ /4, \tag{8}$$

where $E_{\vec{k}n}$ is the eigenvalue at $\vec{k}$ nearest to E. The real part of Σ is relatively less important in the calculation and was left unchanged. The constants c_s and c_p were determined iteratively by the requirement that the derived "modified CPA" (MCPA) DOS N_s, N_p differ by less than 10% from the CPA values. The value c=0.2 was used, but with this self-consistency constraint on N_s and N_p the results are weakly dependent on the choice of c.

The effect upon $S(\vec{k},E)$ of this modification is shown in Fig. 2 for $\vec{k}$ along the Δ direction and for two energies, -0.8 eV and 1.1 eV, which contribute to absorption at $\hbar\omega$ = 1.9 eV. S peaks near the eigenvalues of the underlying crystalline Hamiltonian. Far from a peak, S in the MCPA is typically reduced by an order of magnitude, which in turn reduces the low frequency absorption. By constructing this more physical form for $\langle\mathrm{Im}\tilde{G}\rangle$ by our MCPA procedure, we obtain corrections to α which must be included in the vertex corrections neglected in Eq. (3). The result is shown in Fig. 1 as the full line. The energy dependence of $(\alpha E)^{1/2}$ calculated from the MCPA is slightly steeper at higher energy than the experimental values of Cody <u>et al</u>., but the behavior below 2 eV is much improved over the CPA results.

Comparison of the calculated value of $(\alpha E)^{1/2}$ to that arising from a simple CDOS[4] demonstrates that $E_g^{opt} > E_g^{DOS}$ (Fig. 1). Linear extrapolation of $(\alpha E)^{1/2}$ to zero from the linear high frequency region leads to a value $E_g^{opt} \approx 1.8$ eV (CPA) or 2.1 eV (MCPA), whereas $E_g^{DOS} = 1.4$ eV from the CDOS. Cody *et al.*[1] have shown that E_g^{opt} varies from 1.5 to 2.0 eV with increasing hydrogen content. It is encouraging that our model, which contains 20% H, gives an optical gap of the order of 2 eV, in excellent agreement with data[1] on samples with similiar H content. By making the replacement $\tilde{p}_x \longrightarrow$ diagonal constant in Eq. (3) we obtain a similiar frequency dependence, indicating the widening of the optical gap is due primarily to $\vec{k}$-space correlations of the electron and hole in the excitation process rather than an explicit energy dependence of $\tilde{p}_x$. Physically this remanent $\vec{k}$ conservation is due to the short-range order in a-SiH$_x$. Note that our value $E_g^{opt} \approx 2$ eV is much smaller than that for crystalline Si (~3 eV) in spite of the widening of the gap[4] due to lowering of the valence bands upon incorporation of H. All of the absorption below 3 eV arises from the disorder in the model, and the close agreement with experiment indicates both that the underlying "crystallinity" of our model is not a serious defect and that knowledge of the long range disorder in a-SiH$_x$ is not essential for describing α.

We performed two additional calculations which illustrated other features of our model. First, we reduced the density of fully hydrogenated vacancies from 5% to 2.5%. This introduced two competing effects; the decrease of the H/Si ratio reduced E_g^{DOS}, but since the

disorder was also severely reduced, E_g^{opt} actually widened somewhat, demonstrating the approach to the crystalline Si limit $E_g^{opt} \approx 3$ eV. The net effect was to reduce $(\alpha E)^{1/2}$ by a factor of two below E = 2.6 eV. Secondly, we replaced 1/4 of the H atoms in the original calculation by dangling bonds. This caused a dramatic increase of $(\alpha E)^{1/2}$ below 2 eV due to both the increased disorder and dangling bond gap states, and resulted in a much smaller E_g^{opt}. Although this result follows the trend in the data when the H content is reduced, it should not be expected to agree numerically with the experimental E_g^{opt}-versus-H-content line[1] because the dangling bonds have not been allowed to reconstruct. "Fully hydrogenated" a-SiH_x does not reconstruct significantly because all potential dangling bonds have bonded with hydrogen. Therefore our model, when fully hydrogenated, corresponds semiquantitatively to fully hydrogenated samples (as long as localized band tail and gap states are not crucial), but it does not have the flexibility to model situations with reduced H content to the same accuracy.

To summarize, we have presented here realistic microscopic calculations of the absorption coefficient of a model for a-SiH_x. The calculated absorption coefficient, obtained without adjustable parameters, is within a factor of two of the experimental value, which is itself sample dependent. Considered alongside the other successes[4] of the model, this agreement indicates that knowledge of the precise atomic positions are not necessary for the understanding of many properties of a-SiH_x for which band tail or gap states are not intimately involved.

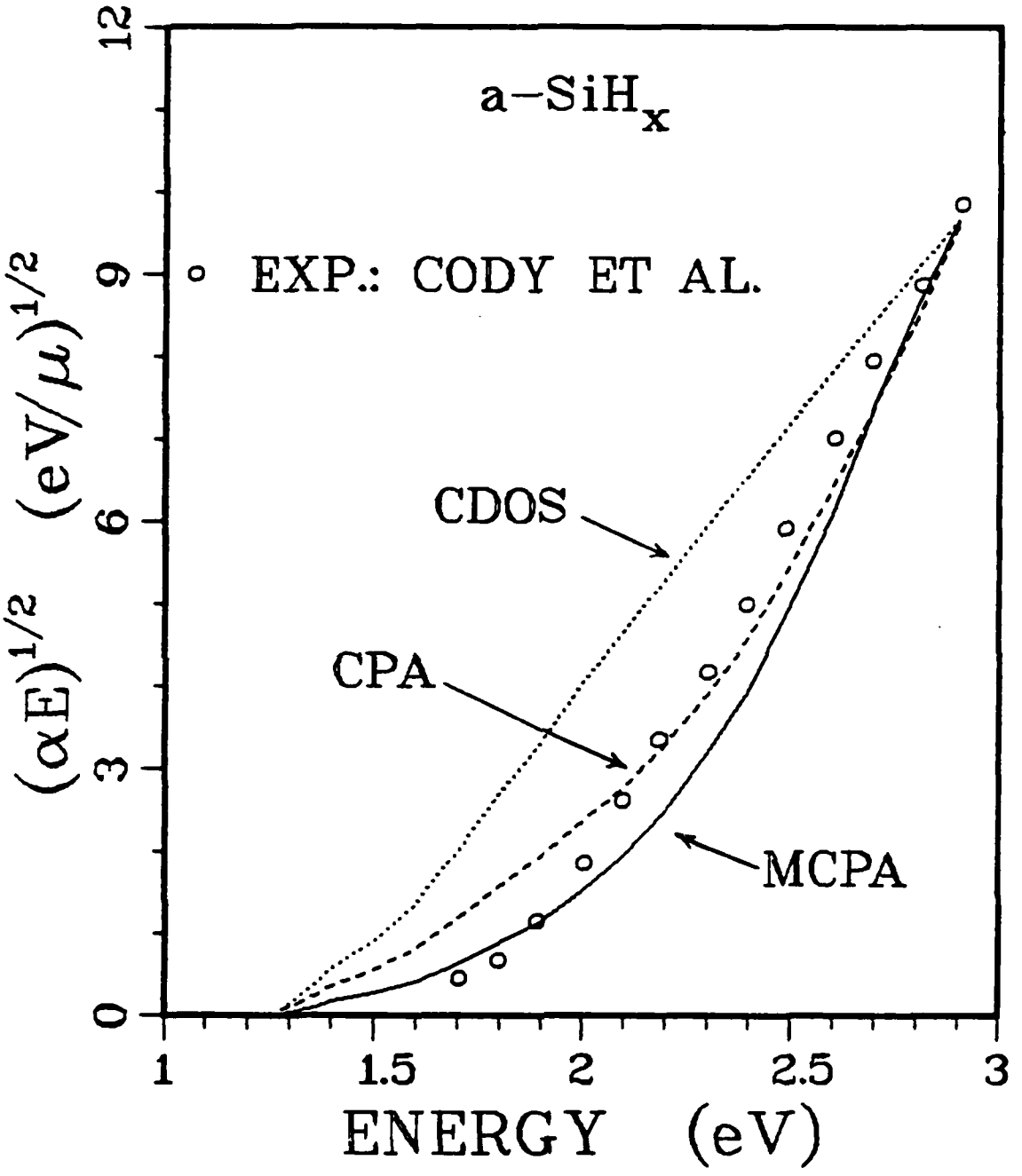

Fig. 1 Comparison of calculated absorption coefficient α with measured value (data points) of Cody *et al.*, Ref. 1, plotted as $(\alpha E)^{1/2}$ vs E. The CPA and MCPA results were multiplied by 1.5 and 2.4, respectively, to normalize to the experimental data at 2.9 eV.

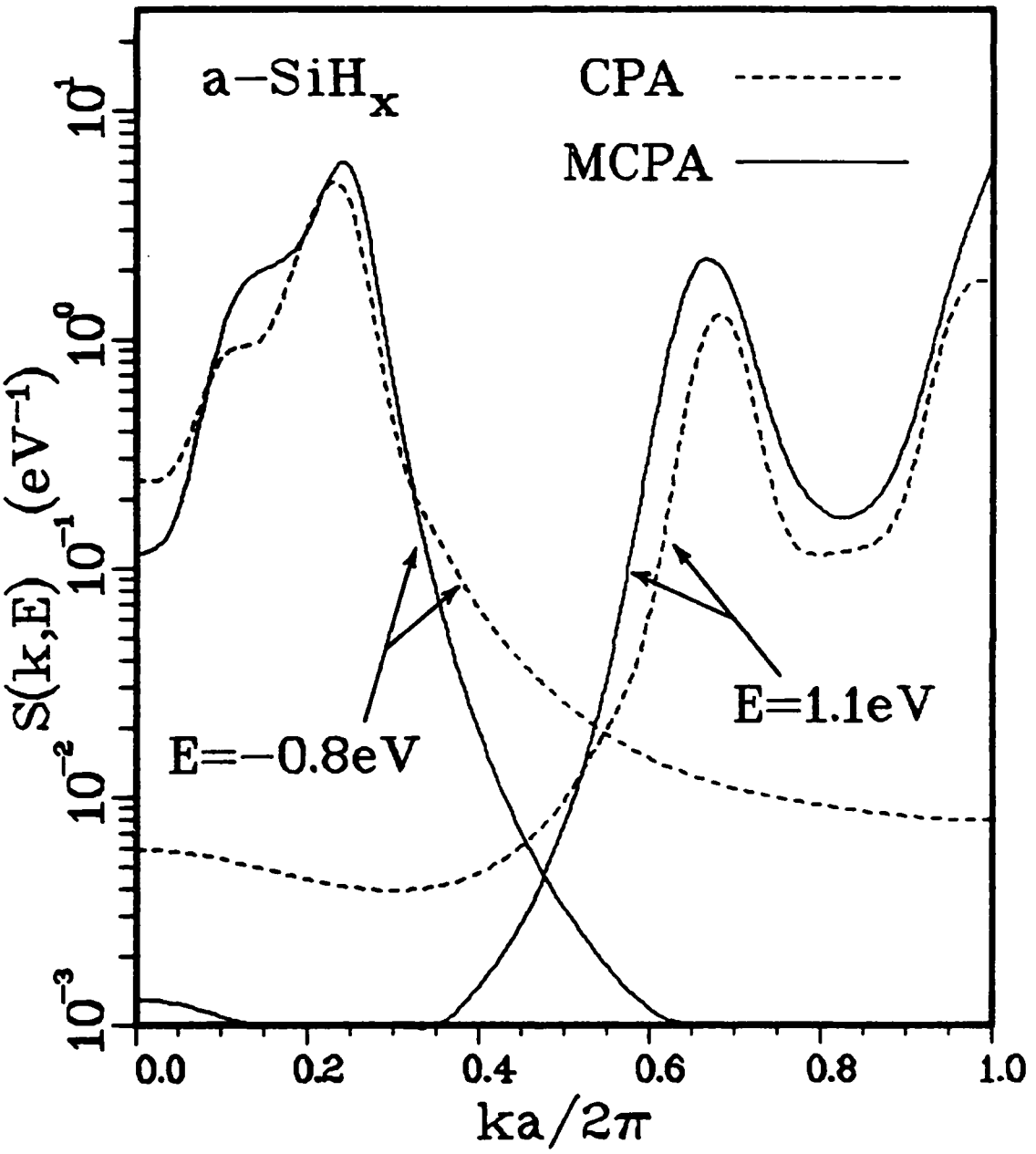

Fig. 2 Semilog plot of CPA and MCPA spectral densities $S(\vec{k},E)$ at E = -0.8 eV and E = 1.1 eV for $\vec{k} \parallel (100)$. The MCPA value is roughly one order of magnitude smaller than the CPA value far from the peaks.

References

1. G.D. Cody, C.R. Wronski, B. Abeles, R.B. Stephens, and B. Brooks, Solar Cells 2, 227 (1980).
2. E.C. Freeman and W. Paul, Phys. Rev. B20, 716 (1979).
3. T.D. Moustakas, J. Elec. Mater. 8, 39 (1979); W. Paul, T.D. Moustakas, D.A. Anderson, and E.C. Freeman, Proc. 7th Int. Conf. on Amorphous and Liquid Semiconductors, ed. W.E. Spear (CICL Univ. of Edinburgh, 1977), p. 467; P. Viktorovitch, G. Moddel, J. Blake and W. Paul, J. Appl. Phys. 52, 6203 (1981).
4. E.N. Economou and D.A. Papaconstantopoulos, Phys. Rev. B23, 2042 (1981); D.A. Papaconstantopoulos and E.N. Economou, in Tetrahedrally Bonded Amorphous Semiconductors, edited by R.A. Street, D.K. Biegelsen, and J.C. Knights, (AIP Conf. Proc. No. 73, New York, 1981), p. 130; D.A. Papaconstantopoulos and E.N. Economou, Phys. Rev. B24, 7233 (1981).
5. W.E. Pickett, D.A. Papaconstantopoulos, and E.N. Economou, J. Phys. (Paris) Colloq. 42, C4-769 (1981).
6. E. Taranko, R. Taranko, K.I. Wysokinski, and M. Pilat, Z. Physik B39, 187 (1980); S. Abe and Y. Toyozawa, J. Phys. Soc. Japan 50, 2185 (1981).
7. R. Kubo, J. Phys. Soc. Japan 12, 570 (1957); D.A. Greenwood, Proc. Roy. Soc. (London) 71, 585 (1958).
8. B. Velický, Phys. Rev. 184, 614 (1969).
9. B.L. Gyorffy, R. Jordan, D.R. Lloyd, C.M. Quinn, N.V. Richardson, G.M. Stocks, and W.M. Temmerman, Transition Metals, 1977, eds. M.J.G. Lee, J.M. Perz, and E. Fawcett (Inst. of Phys. Conf. Ser. No. 39, London, 1978), 248; J.S. Faulkner and G.M. Stocks, Phys. Rev. B21, 3222 (1980).
10. In the region $|E_{\vec{k}n}-E| < \Gamma$ the use of Eq. (7) occasionally resulted in a lower spectral density. In those cases we set $\mathrm{Im}\hat{\Sigma} = \mathrm{Im}\Sigma$.

We are grateful to L.L. Boyer for assistance with Brillouin zone integration schemes, to T.D. Moustakas for conversations and comments on the manuscript, and to W.H. Butler and J.S. Faulkner for discussions on muffin-tin CPA spectral densities. This work was supported in part by the Solar Energy Research Institute via an interagency agreement between the US Naval Research Laboratory and the US Department of Energy, and by the Office of Naval Research, Contract No. N00014-79-WR-N0028.


ATE
LME